FOREWORD

This report was prepared by The Boeing Company under USAF Contract AF 33(616)-7815. This contract was initiated under Project No. 7381, "Materials Application," Task No. 738102, "Materials Preproduction Processes." The work was administered under the direction of the Directorate of Materials and Processes, Deputy for Technology, Aeronautical Systems Division, Wright-Patterson Air Force Base, Ohio. Mr. L. N. Hjelm was the project engineer.

This report covers work performed from 1 February 1961 through February 1962.

ABSTRACT

Thoria and magnesia bodies were developed for use in metal-ceramic composites. Good thermal shock resistance was imparted to these bodies through control of particle size distribution. Magnesia was sintered at 2200°F and thoria at 2800°F.

Plasma and oxyacetylene torch tests developed to evaluate these materials and similar zirconia composites showed that magnesia and zirconia can be used to 4600°F and thoria to 5400°F. The order of decreasing emittances for the pure bodies is: (1) zirconia, (2) magnesia, and (3) thoria. The addition of chrome oxide to the magnesia body increased its apparent emittance to that of zirconia—0.8 at 4000°F. Magnesia produced lower weight composites than either of the other ceramics. Zirconia and magnesia show a steady decrease in strength to 3200°F, at which point an increase occurs.

A magnesia foam backing was developed for use with composites to reduce heat transfer to the substructure with a minimum gain in overall weight.

Platinum and Inconel honeycomb were selected for use as a metal reinforcement for these bodies to produce material systems suitable for use in high heat flux applications such as the nose cap of a glide re-entry vehicle. Leading-edge configuration samples prepared from magnesia with Inconel honeycomb reinforcements were fabricated.

This technical documentary report has been reviewed and approved.

W. P. Conrardy

W. P. CONRARDY
Chief, Materials Engineering Branch
Materials Applications Division
AF Materials Laboratory

CONTENTS

ILLUSTRATIONS

TABLES

I. INTRODUCTION

The high heat flux and oxidizing environment encountered in many aerospace applications exceeds the capabilities of conventional unprotected refractory metals. For example, at the nose cap of a glide re-entry vehicle, temperatures are expected to approach 5000°F; this will necessitate the use of refractory materials such as tungsten, graphite, and ceramics. The use of tungsten and other refractory metals requires suitable protective coatings to prevent damage from oxidation. This problem is also encountered with graphite, borides, nitrides, and carbides. In addition, many of these materials decompose at temperatures well below their melting points. The use of stable oxides such as magnesia, thoria, and zirconia avoids the problem of oxidation and decomposition. However, it introduces new problems because these ceramics are susceptible to thermal and mechanical shock.

Cermets were investigated during World War II for use in turbojet engines. Initial results were promising, and it was felt that further development would lead to useful materials. Since then, cermets have been produced for use as friction materials and, recently, metals containing small percentages of ceramic additives have been developed. The latter cannot be classed as a true cermet since the properties of the composite material are basically those of the metal matrix. However, development work on cermets has not yet produced the desired materials combining the better properties of metals and ceramics.

The use of metal wire reinforcement in ceramics has also been investigated. Attempts at the University of California were made to prestress ceramic wing sections through the use of pretensioned wires. These efforts had limited success because of difficulties in applying the load uniformly to the brittle ceramic structure. Tinklepaugh (46) investigated the use of metal fibers despersed in a hot-pressed ceramic body. In most of these samples, the unequal thermal expansion of the metal wire and the ceramic fractured the ceramic during cooling. However, certain composite structures prepared in this manner showed better thermal shock resistance than the unreinforced ceramic.

The combination of metal and ceramic phases has also been accomplished by using a ceramic body in which is imbedded a metal honeycomb. Considerable success has been achieved in this manner. Both ballistic missile nose cones and rocket engine parts have been successfully fabricated and tested using material systems of this type. The metal reinforcement serves primarily to control thermal shock properties by preventing the propagation of cracks through the ceramic phase and providing some flexibility to the overall structure.

A zirconia-based composite, representative of the current state-of-the-art in this area, was selected as the starting point for the present program. The work done in developing improved metal-ceramic composites and evaluating their physical properties is described in this report.

Manuscript released by the authors August 1962 for publication as an RTD Technical Documentary Report.

II. SUMMARY

This program was conducted with the following objectives:

1. The development of metal-ceramic composite materials suitable for high-temperature structural applications such as nose caps and leading edges for re-entry vehicles.
2. The determination of selected physical properties of metal-ceramic composites.
3. The establishment of subscale screening tests for evaluating these materials.
4. The fabrication of small samples and relatively large shapes for delivery to the program monitor for evaluation.
5. The establishment of test procedures for evaluating relatively large shapes.

A literature survey of the current state-of-the-art was conducted as the first step toward those objectives. This survey showed that, of the many approaches tried in the development of metal reinforced ceramic structures, the use of a metal honeycomb had produced the most promising results. Therefore, metal honeycomb reinforcement was selected for this program.

On the basis of the information gathered in the literature survey, zirconia, magnesia, hafnia, thoria, and beryllia were considered to be promising materials for use as the ceramic phase. Magnesia and thoria were selected for initial development since hafnia is not available in suitable grades; beryllia requires special processing facilities; and zirconia is being investigated under a separate program. Magnesia was particularly attractive due to its high melting point, low density, and ready availability; therefore, the experimental portion of the program was initiated using magnesia as the basic material. Evaluation of magnesia compositions developed showed that, through careful selection of particle size distributions, bodies could be prepared that possessed excellent thermal shock properties and a density approximately half that of comparable zirconia compositions. Attempts to prepare these bodies using chemical binders were unsuccessful. Sintering aids were also investigated. They did not appreciably improve the magnesia composition, and a temperature of 2200°F was required to adequately sinter either the pure magnesia bodies or the bodies containing sintering aids.

Although magnesia bodies are more refractory than zirconia bodies, their use in radiative cooled structures is handicapped by a low emittance. To offset this, the use of additivies to increase emittance was investigated and chrome oxide was found to be satisfactory. The addition of chrome oxide to the magnesia body increased its emittance from an initial value of 0.3 to a value of 0.8 at 4000°F.

The investigation of thoria was less exhaustive than that of magnesia. This was due to the high sintering temperatures required to produce thermal-shock-resistant

bodies and the need for special facilities to protect personnel from the radioactive thoria. Sulfuric acid, as a binder for thoria, was investigated, but it was found that, as with magnesia, the benefits achieved through the use of additives were questionable. A pure thoria body with good thermal shock resistance was developed by presintering the raw material and controlling particle size distribution.

Testing of these material systems consisted primarily of comparing them with a previously developed zirconia body. Hot-gas tests were conducted both with plasma torches and oxygen-acetylene torches. Results of these tests showed the magnesia and thoria bodies to be equivalent to the zirconia body in thermal shock resistance, while the magnesia body was lighter and the thoria body was more refractory. Inconel and platinum were selected for use as honeycomb reinforcement in these ceramic bodies. Platinum is the better of the two, but its high cost made it desirable to investigate less expensive materials. Superalloys such as Rene'41 were considered, but a tendency to embrittle during sintering of the composite body made the use of Inconel preferable. Some problems were encountered with Inconel in sintering but the use of an inert atmosphere sintering cycle has eliminated them.

Sample magnesia leading edges were fabricated.

III. LITERATURE SURVEY

Fiber-Based Composites — Fiber-reinforced materials have been investigated as a means of combining ceramics and metals to obtain the best properties of each. Work has been conducted both with ceramic fibers being used as a reinforcement for metals and with metal fibers being used to reinforce ceramics. Composites have been investigated where fibers are used for other purposes than strengthening composites, such as providing a protective surface of molten material and as a source of gas for film cooling. The following section summarizes some of the results obtained with fiber composites.

Considerable work has been reported by Tinklepaugh (46) on the development of metal fiber-reinforced ceramics. Numerous material systems were evaluated by this group to develop thermally stable composites in which both components carried an appreciable portion of the imposed loads. Of the various fabrication methods that were tried, they found hot-pressing to provide the best results. The samples were fabricated in graphite dies by conventional techniques. Some difficulties were encountered due to the carburization of the metal reinforcements, but this was overcome by a ceramic wash coating of the dies prior to fabrication of the samples.

In the early stages of the program, the composites were found to possess microcracks. The authors attributed this to the difference in expansion of the ceramic matrix and the fiber reinforcements. From their analysis of the results they concluded that it would be desirable to use a form of composite in which the ceramic possessed a lower thermal expansion than the metal fibers. To accomplish this, an alumina-kaolin body was developed that possessed the desired thermal expansion characteristics and it was then combined with molybdenum fibers. Composites prepared with these materials were successfully fabricated in a crack-free condition. Tests on these bodies confirmed theories that composites could be prepared in which the mechanical stresses were distributed between the matrix and the fibers. These composite bodies showed better thermal shock resistance than the unreinforced ceramic body. Failure under tension did not occur until the metal fibers were either ruptured or pulled free of the matrix. Conclusions reached by Tinklepaugh at the completion of the program are as follows.

1. A metal fiber may be successfully incorporated into a ceramic body to provide a reinforcement and to reduce thermal shock problems.
2. It is essential that the metal fiber be expansion-matched to the ceramic body to provide a crack-free structure.
3. Based on theoretical considerations, a hafnia-based system with tungsten metal reinforcements should be feasible.
4. The degree of porosity in the ceramic body and the presence of a coating on the metal fibers are the determining factors in the oxidation rate of the fiber reinforcements.

5. The most suitable means of fabricating these composites is hot pressing.

A program similar to that above was carried out by Baskin, et al. (2,3). The samples were fabricated in graphite dies at 1500°C and 2500 psi. Little difficulty was encountered with oxidation of the metal fibers. Attempts to use steel fibers were unsuccessful because the metal fibers softened sufficiently to be extruded from the composite. Tests with niobium fiber indicated that this material carburized in the pressing operation.

Numerous samples were made of thoria reinforced with molybdenum fibers. The fibers did not oxidize in the pressing operation but microcracks occurred in the thoria. Thermal shock tests, conducted by heating the samples to 1000°C followed by a quench in mercury, showed the reinforced samples to be superior to unreinforced thoria in thermal shock resistance.

The Young's modulus and modulus of rupture of the composites were found to increase with temperature to a maximum at 650°C. This behavior is reversed from that of pure thoria. In tests to determine the optimum fiber content, 20 percent was found to be the maximum amount that could be satisfactorily added. As the amount of fiber was increased from 2-1/2 to 10 percent, the strength of the composites decreased. Above 10 percent, the trend was reversed.

Other tests showed the fibers to be completely oxidized by exposure to air for an hour at 1000°C. Baskin concluded that molybdenum reinforced thoria composites must be used in an inert atmosphere or a suitable oxidation protective coating must be developed. The thermal expansion of the composites was lower than expected, and was attributed to the closing of the microcracks present from the fabrication process.

Bradstreet (8) reported on the effects of metal-fiber reinforcements on strength and thermal shock resistance. He found that when samples were fabricated by hot pressing, the thermal expansion ratio of the two materials played a major role in determining the effect of the inclusions. Where the metal fibers had a higher rate of thermal expansion than the ceramic, as in the case with molybdenum-zircon composites, the metal fibers place the ceramic under compression during the cooling period and increase the tensile strength of the composite over that of the unreinforced ceramic material. Within reasonable limits the effect of the reinforcement is enhanced by increases in the differential thermal expansion of the two materials. For materials where the differential thermal expansion of the two materials is essentially zero, the metal fibers have no appreciable effect on the elastic modulus of the ceramic. However, tests show that the metal reinforcement appreciably increases the thermal shock resistance. Composites containing a metal-fiber reinforcement of lower thermal expansion than the ceramic matrix showed the structure to be weakened by the addition of metal fibers. The conclusions were based on a mullite body containing 10 percent molybdenum fibers.

A mathematical analysis of the stress distribution in metal-fiber-reinforced ceramic composite materials at elevated temperatures was conducted by Stowell

and Tien-Shih Liu (43). The authors found that, based on the assumption that the materials were viscoelastic at the temperatures under consideration, the stresses in the fibers furthest from the neutral axis decreased with time. This is due to creep, and at the end of a finite time an equilibrium was reached with a stress concentration in these fibers that was less than the initial value. Therefore, on a body subjected to continued deformation, the stresses would gradually be transferred to the ceramic. The referenced report contains tabulated data for metals and mixed oxides melting above 3000°F.

Considerable interest has been shown in "whiskers" for use as high-strength fibers. Hoffman (18) reports tensile strengths for whiskers to be considerably above that achieved with the materials in the normal form. Some whisker compositions are listed below with reported tensile strength values:

*Carbon	150,000,000 psi
Sapphire	74,000,000 psi
Iron	29,000,000 psi

*One value only obtained

These extreme strengths greatly expand the potential application of fiber-reinforced materials. Preliminary calculations show that, when allowances are made for binders, a conservative estimate gives weight reductions of five to one in tensile loaded members by the use of fiber composites instead of the massive material.

The application of high-strength metal and nonmetal fibers has been limited by the lack of well developed techniques for producing fibers. Methods studied are chemical reduction, electrolytic deposition, vapor deposition, and drawing in the manner of conventional fibers. Estimates of the cost of structural materials made from these products place them at $200.00 per pound. While these costs may seem excessive, a comparison based on the weight penalties incurred in airborne structures shows that they may be used profitably in certain applications.

Morden (30) described composites prepared from metal-fiber felts. The fibers are felted by suspending them in a liquid medium in a porous container. Vacuum is applied to the container and the liquid drawn off through the fibers. Ceramic slip may then be introduced and the composite sintered.

A different approach to composite structures has been taken by Raynes (34). In his experiments ceramic fibers have been incorporated into a metal matrix. Fabrication of these materials was accomplished through extrusion. The author did not feel that either hot pressing or slip casting were suitable for his application due to expenditures required for capital equipment. Also, the temperatures and pressures required in hot pressing limited the shapes and sizes to which the process could be applied.

The general fabrication technique employed by Raynes consisted of combining alumina fibers with a metal-ceramic brazing mix. The mix formed a coating on

the fibers that improved bonding between the metal and the ceramic phases. The coated fibers were then combined with the required ratio of metal powder and extruded to produce sintering blanks. After sintering, the blanks were then cold worked to improve strength properties. It was found desirable in the cold working operation to move the metal perpendicular to the axis of the fibers. Rolling billets parallel to the fiber axis caused the fibers to break.

Present results have not shown an improvement in tensile strength for the composites over conventional metals. However, Raynes feels that improvement in metal-to-ceramic bonding will increase the transfer of stresses to the fibers.

Ceramic fibers incorporated into a metal matrix have also been found to accomplish effects other than strengthening. It has been reported that the inclusion of ceramic fibers may act as a means of inhibiting grain growth and as a termination point for any cracks that may develop. At least one refractory metal composite has been developed in which the fiber inclusion is utilized to supply a source of material for a combination of transpiration cooling and a protective gas film for use in rocket nozzles. Additional information on these materials is not available for proprietary reasons.

Generally, high-temperature, fiber-reinforced ceramic composite structures may be said to have considerable potential for future applications, but improved fabrication techniques and fiber materials will be required before they can become a reality as load-bearing members in structural applications.

Prestressed Ceramic Structures — Reinforced concrete was probably the first commercially successful metal-ceramic composite. As a logical outgrowth of this procedure, prestressed concrete was developed. This enabled designers to transfer tensile stresses into compressive stresses in the concrete. As a result, it became possible to fabricate precast concrete structures with much longer unsupported roof spans than those previously feasible.

Shanley, et al. (41), attempted to apply these principles to aircraft structures. A model alumina wing section was chosen for experimental studies. The method used to fabricate the test parts consisted of slip casting the desired shape in sections and assembling them spanwise. The completed structure was then prestressed compressively by passing steel cables through the wing in a spanwise direction. All of the specimens prepared in this manner failed in the stressing operation. Attempts to eliminate this through modifications in the means of applying the prestress load were partially successful. It appears that in future work it would be desirable to use rigid end-plates for application of the prestress load to prevent the development of localized stresses. Another factor that the authors felt should be investigated was the nature of the gasketing material between adjacent ceramic sections. The properties of this material, to a large extent, govern the successful transmission of load through adjacent sections. The development of ceramic "wires" would also be desirable for lessening thermal expansion and creep problems for high-temperature operations.

In a concurrent effort, Shanley and co-workers investigated the effect of cellulating ceramics to increase strength-to-weight ratios. An interesting characteristics of these materials is that when their porosity is directional and parallel to the applied load, an increase in strength is observed.

More recently, Bell and Arnquist (6) studied the feasibility of prestressing ceramics as a means of increasing their strength for structural applications. From their calculations the authors estimated that approximately 50 to 80 percent metal would be required in composite bodies to achieve appreciable tensile strengths. They also felt that below 2000°F the superiority of the metals in tension was such that the benefits of a composite in this range are doubtful, and found that above 2000°F metal additions to the ceramic weakened the structure.

Bell and Arnquist concluded that to develop usable prestressed high-temperature composites, metals (such as whiskers) with extremely high tensile strengths would be required. At the present state-of-the-art, the amount of metal required in the composite structure approaches coated metals and the author indicated that a coated metal structure would be a more practical way of achieving the desired end.

While prestressing did not appear practical to Bell and Arnquist, the use of ceramic cores in metal structures to increase stiffness was felt to be feasible. They suggested that foamed-in-place ceramics would accomplish this purpose.

From the work that has been reported, it does not appear that the prestressed structures prepared in the manner of conventional prestressed concrete are feasible with currently available materials. Two other methods of prestressing ceramics have been investigated. The first of these is the "jacketing of the ceramic." This is done by flame spraying a metal of the desired properties onto a preformed ceramic. Compressive stress is applied to the ceramic as the metal cools. This method is applicable only to structures where the thermal gradient in the ceramic is sufficient to prevent a loss of strength in the metal. This process has been successfully applied to rocket nozzle inserts.

Warshaw (48) reported on another means of producing prestressed ceramic bodies. This consisted of slip casting a ceramic body with low firing shrinkage onto the outer surface of a ceramic body with high firing shrinkage. During firing, the differential shrinkage between the two ceramic bodies produced compressive stresses in the outer layer. Consequently, when samples prepared in this manner were tensile tested, an appreciable gain in strength was reported since the surface compressive stresses had to be overcome before failure occurred. When these samples were subjected to high temperatures, the prestress was relieved by viscous flow of the ceramic.

Multilayer Composites — Multilayer composites have received some study, with the majority of the programs in this area being conducted using flame spray techniques. Flame spray fabrication is particularly well suited to this type of composite because of the ease with which the compositions of the various strata can be controlled.

Flame sprayed multilayer structures have been reported by Aves (1) and Long (26). These coatings were prepared by spraying alternate layers of metal and ceramic on a metal substrate. Molybdenum-alumina and tungsten-zirconia were tried. Under testing, the coatings failed due to delamination. The most probable cause of this delamination was oxidation of the metal layers.

Similar multilayer structures have been fabricated (49) using alternate layers of nickel and zirconia. Test results on this system were encouraging for short duration exposures. Under these conditions, nickel oxide, which was formed, served to flux the zirconia forming a viscous melt that sealed cracks as they formed during testing. Under prolonged exposure at high temperatures, the nickel oxide fluxed the zirconia sufficiently to destroy its refractory properties.

Little data has been reported on the physical properties of multilayer materials. Francis and Tinklepaugh (14) have compared measured with calculated values of thermal conductivity. Measured thermal conductivities parallel to the planes of the structure were 12 percent greater than the calculated values and those perpendicular to the planes were 10 percent less than calculated. The calculated values were then corrected for the effect of the interfaces, and the disagreement for calculated and measured values was reduced to the 2 to 3 percent range.

A variation on the multilayer flame spray structure is the utilization of the multilayer coating as an intermediate step in the fabrication process. The layers of materials are sprayed onto a mandrel in the desired ratio. This "coating" is then stripped from the substrate and crushed. The material thus obtained consists of laminated particles which can be fabricated into shapes by conventional powder metal techniques. Structures prepared in this manner reduce the anisotrophic properties normally encountered with multilayer structures.

Giles, Shevlin, and Everhart (15) investigated laminar structures prepared by hot pressing. The material investigated was a nickel-titanium carbide multilayer composite. Sandwiches consisting of alternate layers of 0.034-inch nickel and titanium carbide sheets were hot pressed at 2480°F and 500 psi. The interlayer bonding of these structures was reported as good. It was found that extremely close control has to be maintained over the temperature cycle. Insufficient temperature prevented the formation of a reliable bond, while any appreciable excess caused the nickel layer to flow out of the system. Structural property data is not yet available for this composite.

The problems encountered in the fabrication of multilayer composites are similar to those of other metal-ceramic compositions. Differential thermal expansion, oxidation of the metal, and bonding between the metal and the ceramic phase all need to be investigated further before systems can be prepared to yield the required reliability. None of the literature surveyed gave a successful solution to these problems.

Miscellaneous Metal-Ceramic Composites — Several other approaches to the development of composite materials have been tried with varying degrees of

success. Blocker, Levy, Locke, and Leggett (7, 23, 25) have reported on composite structures prepared by trowelling a chemically bonded ceramic coating onto a metal substrate. Several materials have been investigated as a bonding agent for the ceramic. Of these, the most successful has been a combination of monofluorophosphoric acid and dihydrogen phosphate. The ratio of these compounds can be varied to control the setting rate. Compositions have been developed that can be cured at room temperatures, while other compositions require curing at elevated temperatures. Optimum porosity of the ceramic phase was found to lie in the 20 to 40 percent range for the composites. To obtain a firm bond to the substrate, metal strips formed in a sine wave are welded to the metal backing. A chemically bonded zirconia layer is then trowelled in place over the corrugated metal backing. The metal is protected from the acid and oxidation by a plasma sprayed coating of chromium and barium silicate frit or a pack-cementation process. These composites are operable at 4200°F in a ramjet exhaust and a 1/4-inch thickness produces a thermal drop of 2000°F.

Similar chemically bonded coatings were developed by Eubanks and Moore (12) for protection of airframes. The bond was formed by monoaluminum phosphate and cured at 400°F. Thin coatings showed good adherence to cleaned sandblasted aluminum and, being based on inorganic bonded alumina, are operable at temperatures in excess of that for organic bonded coatings. Attempts to prepare heavy coatings from these compositions using a metal reinforcement were unsuccessful due to cracks formed during curing.

Ceramic honeycomb sandwich structures have been studied for use in high-temperature components. Radomes are a typical application for these systems where, in addition to the high-temperature requirements, certain electrical requirements preclude the use of metal reinforcements. Pearl (32) describes a procedure that has been used to fabricate a test nose cone 10 inches in diameter, 12 inches high with a 1/2-inch wall thickness. A ceramic honeycomb core is formed from an alumina-silica paper which is formed into the desired cell structure. This core is then impregnated with an alumina slip and the skins are bonded into the core. The completed unit is dried and fired to form a unified structure. The primary limitation on this type of fabrication is the availability of fibers that can be formed into a suitable paper. As more materials become available in fiber forms, other applications may be developed for such structures.

Composites prepared by infiltration of a ceramic structure have been the subject of several investigations. Bradstreet (8) has listed the general requirements for an impregnated ceramic coating that will be protected by the vaporization of the impregnant.

1. The substrate or supporting material should have a thermal conductivity higher than that of the impregnated coating.
2. The coating should be as insulative and refractory as possible.
3. The impregnant should vaporize without melting at a temperature only slightly below the melting point of the ceramic.

4. The pores in the ceramic should be small, continuous, and evenly dispersed.

These specifications will, to some extent, apply to any impregnated structure for high-temperature use. While the first three may be compromised to a large extent, the pore size and distribution are important to successful impregnation.

Composites based on ceramic foams with various impregnants are an attractive possibility for high-temperature, lightweight insulating structures.

Strauss (44) has tested refractory foams impregnated with organic materials and bonded to a metal or plastic substructure. The impregnant imparts an appreciable degree of thermal shock resistance, and materials prepared in this manner have been successfully tested at hot-face temperatures of 4000°F. Comparison with silicon carbide foams using a zirconia impregnant shows the organic impregnant to have reduced back-face temperatures appreciably.

Several other materials have been considered as possible impregnants. Lithium and its compounds have been suggested as possibilities, but information on results of this approach is lacking.

Porous magnesium-oxide bodies have been successfully impregnated with Teflon in a similar fashion. Tests on the resultant composite structure have shown the thermal properties to be enhanced in short-duration exposures at extreme temperatures. The data obtained on these materials is not complete, but indications are that the impregnant reduced the rate of temperature rise on the hot face by ablative cooling. This effect reduced the thermal gradients in the sample, causing a more uniform "heat up" with reduced thermal stresses.

A composite system that has had considerable success is the ceramic-filled metal honeycomb. This type of structure is not a reinforced composite in the conventional sense, but the metal component provides a means of increasing thermal shock resistance.

Burnett (9) has reported that, in addition to the oxide filled structures, nitrides and carbides have been successfully fabricated into similar structures. Also, the problems of fabricating refractory-metal honeycomb structures have been solved, permitting the development of composite structures for use at higher temperatures than was previously possible.

A unique system reported by Roller (40) is the oxide coated cermet, which is produced by conventional powder metallurgy techniques. A beryllium oxide-molybdenum composition is pressed and sintered in hydrogen to achieve suitable core strengths. This compact is then machined, as required, to the desired shape, followed by a second sintering in a controlled oxidizing atmosphere. This treatment results in oxidation and volatilization of the surface molybdenum, leaving behind a dense ceramic surface coating. The resulting structure is a coated composite possessing a graduated structure from pure ceramic to the base composition. These materials have withstood prolonged exposures in oxyacetylene test facilities.

Only a few composites have been described as possible rocket nozzles. These are generally thin tungsten shells backed by a refractory support. Tungsten liners with a graphite support have been described by Long (26). A tungsten sheet is spun into the desired form and the graphite support is then bonded to the tungsten by controlled carbide formation from various metals applied at the interface.

Similar structures have been prepared by the author (49) from plasma formed tungsten liners, with the backup material being chemically bonded zirconia. Attempts to use slip cast silica as a backup for tungsten liners have been unsuccessful due to the low melting point of the silica.

Boeing-Developed Composites — Current projects in composite structures within this contractor's organization have been reviewed to determine their applicability to the present program.

The sulfuric-acid bonded zirconia compositions reported in WADD TR 60-491 have been further investigated with a view towards optimization of their properties. These investigations have shown the basic approach to be sound, and considerable improvement has been made in erosion and thermal shock resistance.

Various types and particle sizes of material have been evaluated in the basic zirconia composition. The use of bubble zirconia to reduce density and thermal conductivity has been moderately successful. Selected size fractions are used in the same manner as in the conventional composition to obtain a thermal shock resistant body. However, composites prepared from this material are limited to short-duration applications because of shrinkage of the spheres upon prolonged exposure at high temperatures.

An investigation of wire reinforcements for composites was also conducted. Samples were prepared containing tantalum, molybdenum, tungsten, and Rene' 41 wires imbedded in a zirconia matrix and exposed to an oxyacetylene torch. The sample hot-face temperature was maintained at 4300°F. The zirconia was found to provide negligible protection for the metal wire under these conditions and the tantalum, molybdenum, tungsten, and Rene' 41 wire reinforcements were oxidized. In addition, molybdenum and HS-25 reacted with the zirconia. Platinum wire was found to be unaffected by the test conditions except for melting in the immediate vicinity of the surface. In spite of its high cost, platinum is considered to be one of the most promising materials for future work.

Metal honeycomb reinforcements have been evaluated as part of the continued development effort on this material. These reinforcements serve primarily to control thermal shock and to limit subsequent crack growth, and large samples have been prepared from this system for evaluation. These structures are basically chemically bonded zirconia incorporating a noble metal honeycomb. Excellent thermal shock resistance for operation at 4200°F is obtained by selecting the proper honeycomb cell size.

Preliminary work on thoria based systems has shown that composites, similar to those prepared from zirconia, can be fabricated. Development of this material into metal-ceramic systems will require metal honeycombs of a more refractory nature than platinum in order to achieve the maximum temperature capabilities. Tungsten would be particularly attractive for this if suitable protection from oxidation could be obtained.

Work conducted on alumina based composites for applications at lower temperatures has produced a phosphate-bonded alumina matrix reinforced with alumina fibers. It has a density of only 2.8 grams/cc and fair thermal shock resistance. Molybdenum wire reinforcements were also investigated for incorporation into these alumina composites. The best results were obtained with 0.002-inch-diameter wires 1/4-inch long. These were found to increase thermal shock resistance to the point where samples could withstand three quench cycles from 2600°F to water.

Alumina with metal honeycomb reinforcements has been evaluated. The best system studied is a partially crushed honeycomb structure in which the honeycomb is bonded to the desired backing material and partially filled with a fibrous insulating material. The remainder of the structure is then filled with an alumina-binder mix which is pressed into place and cured at 800°F. A 1/2-inch-thick composite of this material has been found to produce a temperature gradient of 1400°F when the hot-face temperature is 3000°F. The required thickness and alumina-to-fiber ratio are determined by the temperature requirements of the load bearing substructure. Superalloy honeycomb materials have proven to be satisfactory for service conditions up to 3000°F. Although some melting occurs at the surface, this has not proven to be detrimental. Tests are now in progress to determine the depth of heat penetration. From this data it will be possible to establish the minimum amount of metal that can be used.

Work with these materials has shown that ceramic retention is considerably improved by partially crushing the honeycomb. To accomplish this, the honeycomb is filled with a removable matrix material to prevent buckling of the honeycomb. The filled honeycomb is then compressed and the filler is removed. The crushed metal honeycomb is used in the normal manner. This method permits the close control on the amount and type of crushing of the honeycomb.

In the area of ceramic fibers for reinforced composites, two fiber fabrication methods are being investigated — preparation from colloidal sols and conversion from the metal. Fibers prepared from sols as described in ASD TR 61-420, have been made in sizable quantities. The present program is directed towards their use in a ceramic filamentized radome. At present, fibers with $1\text{-}5 \times 10^{-6}$ $inch^2$ cross section up to 8 inches in length can be prepared. Dielectric measurements show these materials to be suitable for use in radome construction.

Another material composite that shows promise is a Boeing-developed graphite base material. It is a graphitic material containing carbides, borides, and

silicides of refractory metal that oxidize to form an oxide coating protective to 3000°F. Since it is self-forming and self-healing, any cracks or other damage that may occur in the coating are automatically healed. The problems encountered with conventional coated materials, where a coating flaw may cause destruction of the base material, are thus eliminated. The Boeing-developed material can be used in an oxidizing atmosphere to 2800°F without deterioration of the substrate. The graphite composite has a flexural strength of approximately 7500 psi at room temperature as compared with 4000 psi for ATJ graphite under the same conditions and maintains its strength above 3500°F. This composite is being evaluated for use in applications where oxidation prevents the use of conventional graphites.

IV. PHYSICAL AND MECHANICAL PROPERTY DETERMINATIONS

Introduction — The general approach to material evaluation in the present program has been to select relatively simple tests which would permit rapid and inexpensive screening of a large number of material systems. The previously developed zirconia based metal-ceramic composite was selected as a reference material. A considerable amount of data on this material system was available, thereby enabling correlation of these tests with possible end-use applications. Minimum performance requirements for new metal-ceramic composites were established by determining the behavior of the reference material under the screening test conditions. Also, by knowing the capabilities and properties of the reinforced zirconia body the results of the screening tests could be correlated with data from more sophisticated large-component tests.

An objective of the test program was to measure the physical properties of the metal-ceramic composite. The majority of these tests were conducted on the unreinforced ceramic body because of the following factors.

1) Tests on reinforced samples would not be representative of the composite structure due to the small specimen size as compared with the size of the reinforcement system.

2) The steady-state conditions required in furnace-heated tests introduce effects on the reinforcing metal that do not apply to the transient conditions of end-use applications.

3) The physical properties of the metal reinforcements are well known in comparison to the available information on the ceramic phase. If sufficient data could be obtained for the ceramic phase, the properties of the composite could be predicted from calculations.

4) The ceramic phase is the predominant phase and its properties will establish the limits of composite performance in areas such as emittance, maximum usable temperature, density, etc.

The following section of this report describes the test procedures used in this program.

Modulus of Rupture — The induction-heated, modulus-of-rupture test facility (Figure 1) is capable of operation to approximately 4200°F. The samples are tested in an argon atmosphere using a conventional three-point, dead-weight loading system. A detailed description of this equipment is given by Stejskal (42).

The 1/2 by 1/2 by 2-3/4-inch samples were broken on a 2-inch span. Four samples of each composition tested were broken at room temperature and two samples were broken at each of the following temperatures: 2800°F, 3200°F, and 3600°F. The modulus of rupture was calculated from the following equation:

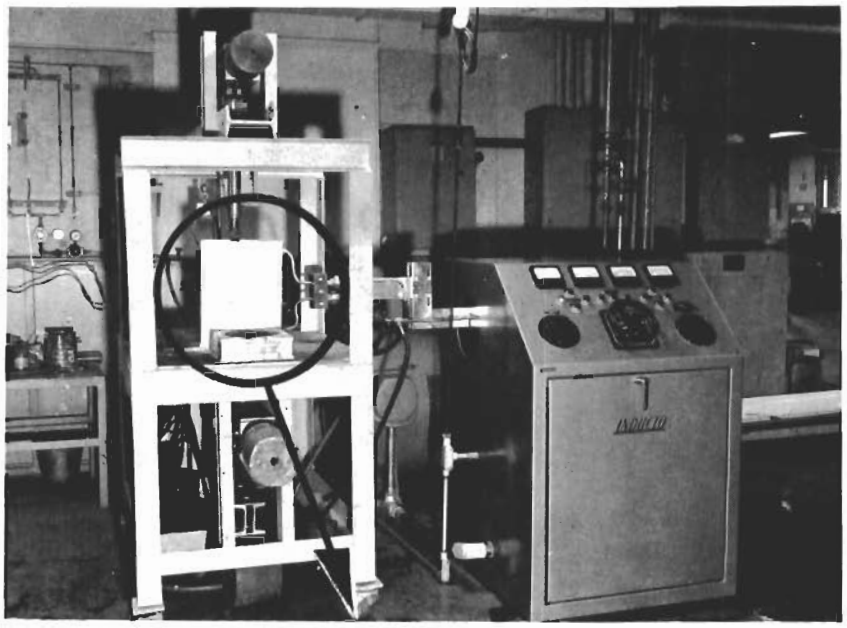

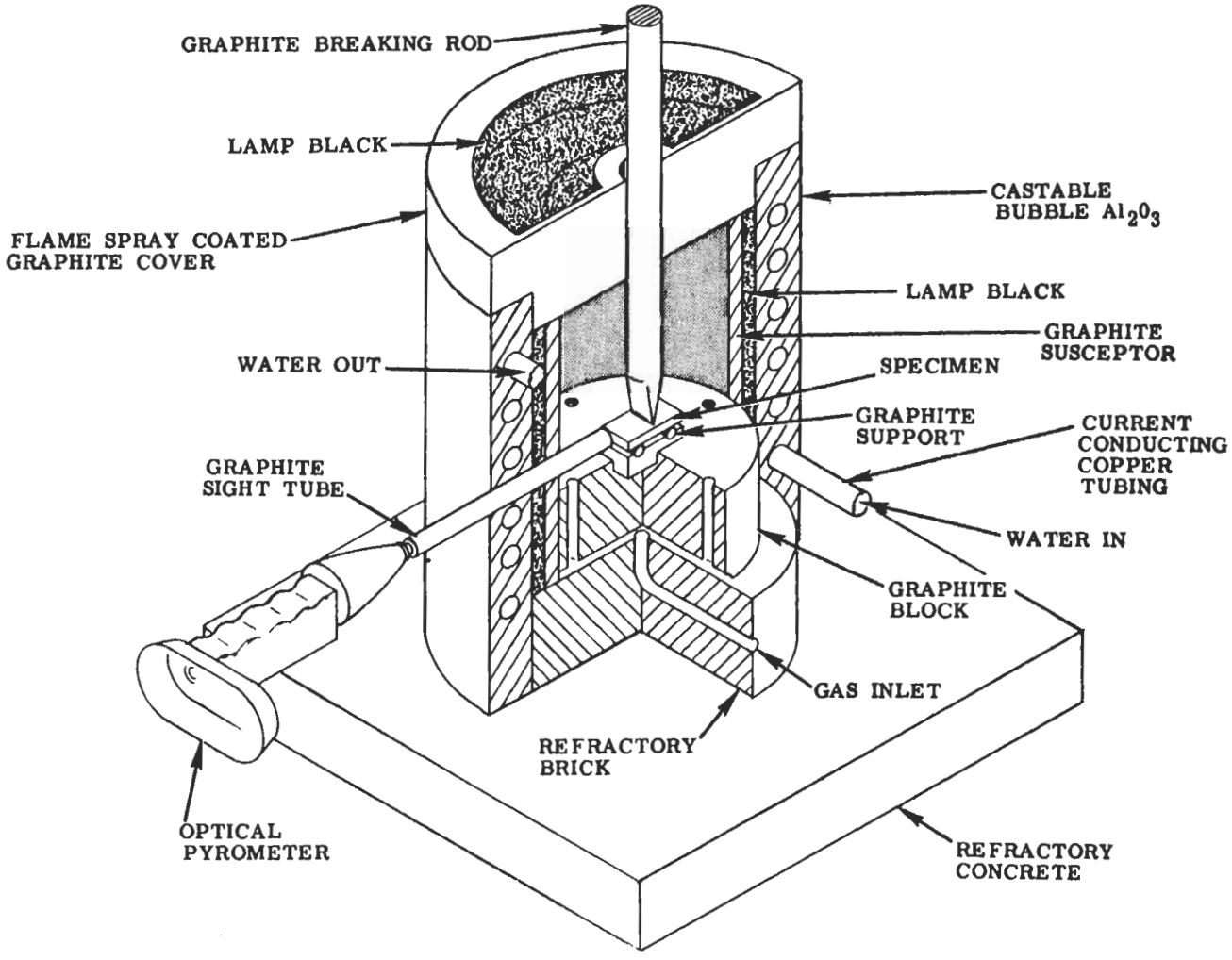

FIGURE 1 HIGH TEMPERATURE MODULUS OF RUPTURE APPARATUS

$$M = \frac{3PL}{2bd^2}$$

where: M = Modulus of Rupture
P = Load
L = Span
b = Breadth of Sample
d = Depth of Sample

Test temperatures were limited to 3600°F. Oxidation of the graphite sight tube prevented accurate sample temperature determination above 3600°F. Modulus of rupture data for three magnesia compositions are shown in Figure 2.

Thermal Expansion Measurements — The thermal expansion of the materials developed in this program was measured using a Boeing designed facility (Figure 3). This equipment will operate from room temperature to 1800°F. Thermal expansion of the sample is measured by a previously calibrated quartz rod that transfers the linear thermal expansion of the sample to the movable core of a microtransformer. Thermal expansion versus temperature is continuously monitored by an "X-Y" recorder with temperature appearing on the "X" axis and thermal expansion on the "Y" axis. This equipment is accurate to ±1 percent.

Determinations of Relative Emittances — The method used in this program to determine the relative emittance of the various material systems was selected to provide a quick, simple emittance test. Calibration of this procedure relies on an emittance curve established for zirconia under a separate program.

In this test, a disk of each composition, 2 inches in diameter and 1/4 inch thick, was subjected to a measured heat flux on the plasma torch and the steady-state surface temperature observed. Since the sample was encased in insulating material, the heat loss was assumed to be primarily radiative. On this basis, the following equation may be applied.

$$\epsilon = \frac{q}{\sigma T^4} \qquad (1)$$

where: ϵ = Emittance
q = Heat Flux, Btu/ft^2-sec
σ = Stefan-Boltzman Constant, 4.75×10^{-12} Btu/ft^2-sec °R^4
T = Equilibrium Temperature

Since the value of q is not known, calculation of the absolute value of ϵ is not feasible. For the case where q is held constant, Equation (1) may be rearranged to:

$$\epsilon T^4 = \frac{q}{\sigma} = C \qquad (2)$$

or

$$\epsilon = \frac{C}{T^4} \qquad (3)$$

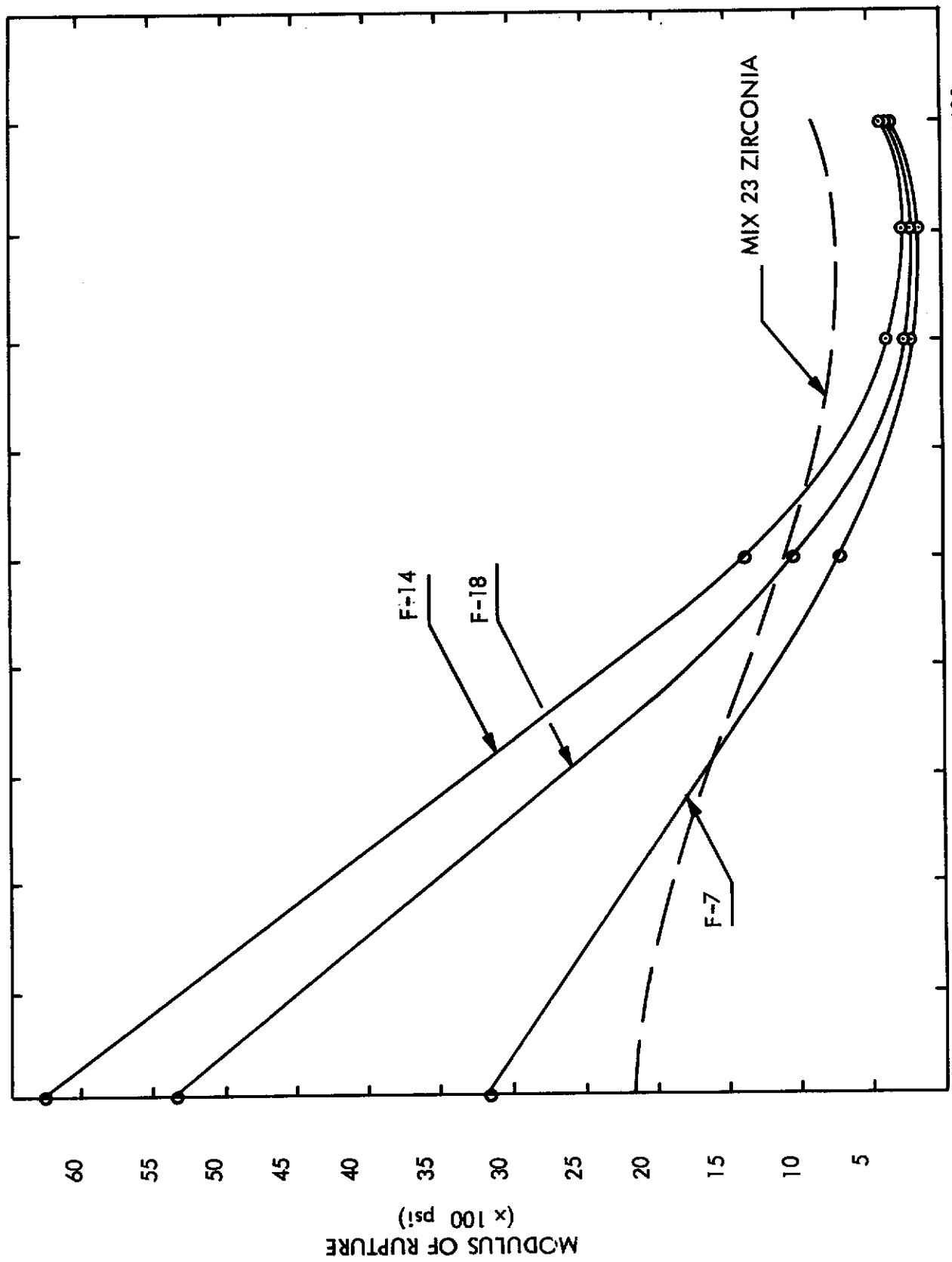

Figure 2 MODULUS OF RUPTURE FOR THREE MAGNESIA COMPOSITIONS AT ELEVATED TEMPERATURES

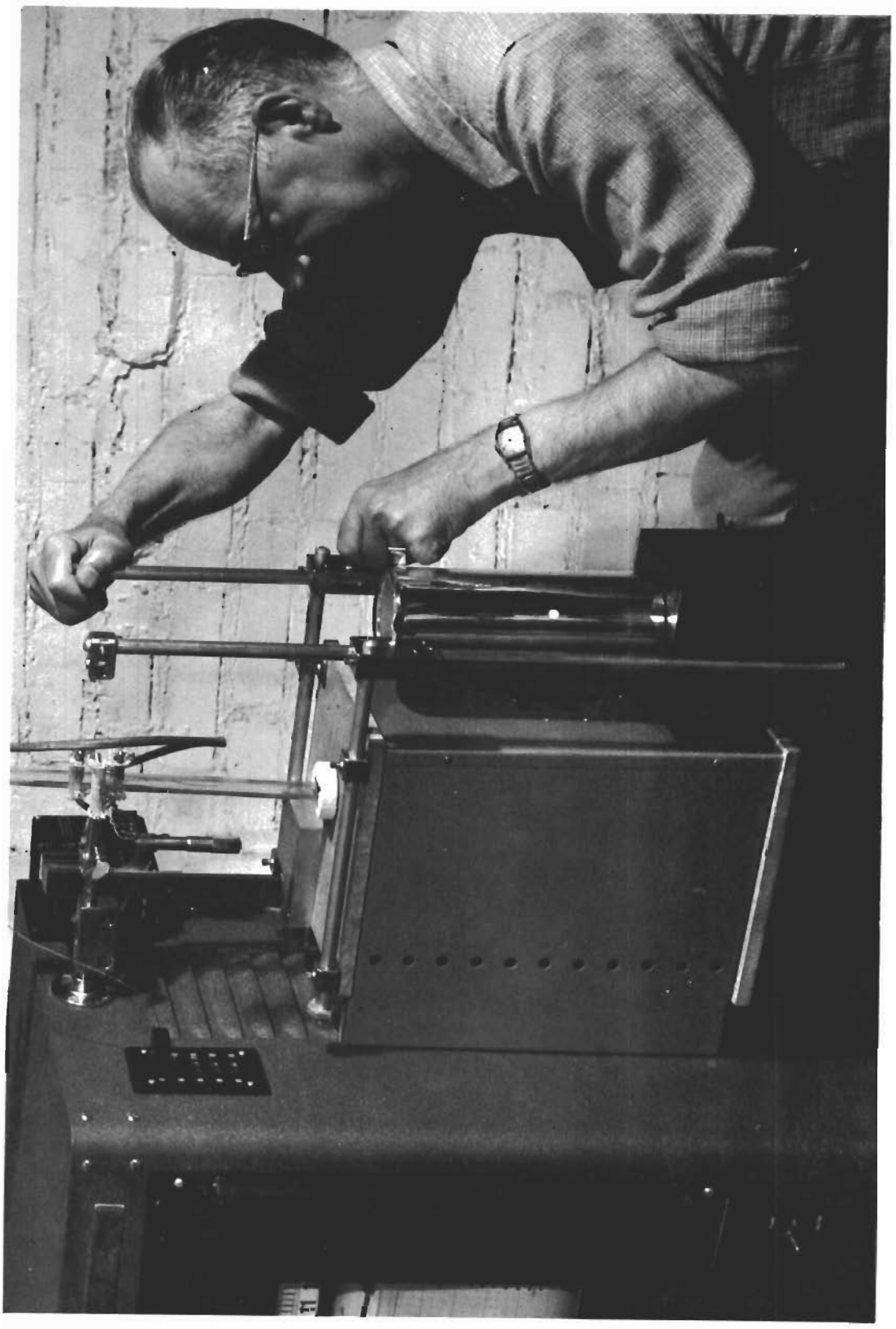

FIGURE 3 THERMAL EXPANSION TEST APPARATUS (1800°F MAX)

When the heat flux is held constant, emittance of various samples can be compared. For example: given that two materials (1 and 2) subjected to the same heat flux have apparent temperatures, T_1 and T_2, then the equations which enable comparison of emittance without knowledge of absolute values can be established:

$$\epsilon_1 T_1^4 = C \tag{4}$$

$$\epsilon_2 T_2^4 = C \tag{5}$$

$$\epsilon_1 T^4 = \epsilon_2 T_2^4 \tag{6}$$

and

$$\frac{\epsilon_1}{\epsilon_2} = \frac{T_2^4}{T_1^4} \tag{7}$$

If the emittance of one of the materials (material 2) is known, Equation (7) may be arranged to:

$$\epsilon_1 = \epsilon_2 \frac{T_2^4}{T_1^4} \tag{8}$$

and the apparent emittance (ϵ_1) can be calculated.

For the low temperature range (1800°F-2800°F), emittances were determined on the Boeing facility shown in Figure 4. This method is designed for use on transparent as well as opaque materials, and simultaneously measures both emittance and apparent transmittance. An induction heated furnace is used to produce an isothermal specimen. The specimen and its support, which incorporates a 3:1 depth-to-diameter reference blackbody, rotate inside the induction heated furnace. The rotating blackbody is sighted through a water cooled tube inserted in the side of the furnace. Since the blackbody rotates with the specimen and is heated to approximately the same temperature, it can be easily and accurately related to the blackbody temperature of the specimen. In addition, it provides continuous radiometer calibrations for use in the calculation of emittance and apparent transmittance when a thermocouple is installed at the base of the rotating blackbody.

Emission from and transmission through the rotating specimen is measured through the water-cooled sight tube mounted on an eccentric at the top of the furnace. The sight tube may be located in either of two positions. It is shown at the inner position in the sketch, where the radiometer sees the energy radiated from the specimen plus the energy transmitted through the specimen. Since the

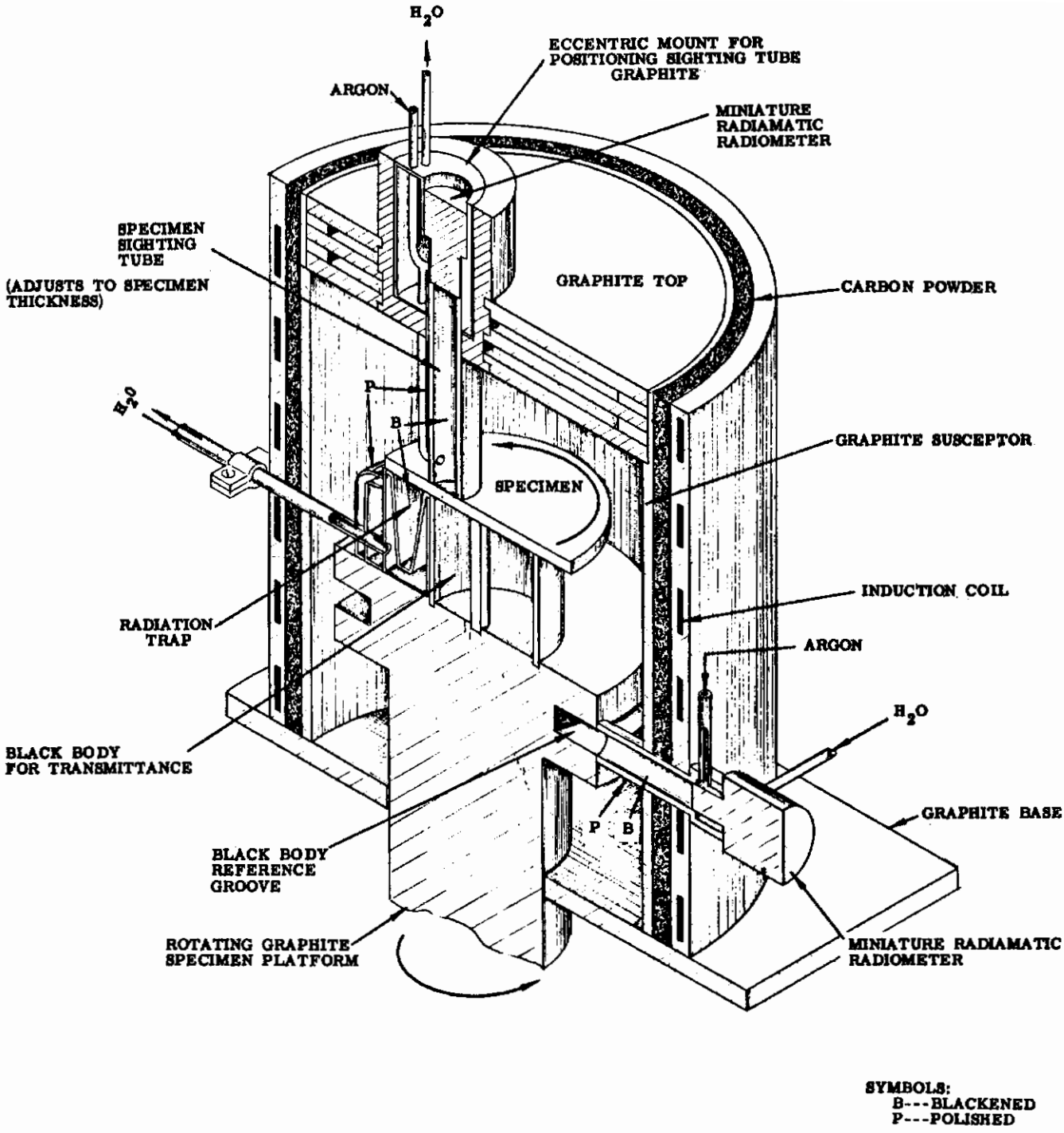

FIGURE 4 THERMAL RADIATION TEST FACILITY

effective opening is the area under the sight tube, the source of the transmitted energy is a 3:1 blackbody at the same temperature as the reference blackbody. At the outer position, the radiometer sees only energy emitted from the specimen. The radiation trap blocks transmittance through the specimen and prevents reflection upward of energy emitted in the downward direction.

About 4 hours are required to obtain equilibrium throughout the furnace, at which time readings are recorded with calibrated Brown Instrument Company Model RL-2 Miniature Radiamatic Radiometers which cover the wavelengths 0.2 to 9.6 microns. The samples tested in this program were disks, 3 inches in diameter by 1/2 inch thick.

Determination of Foam Compressive Strength — The compressive strength of the magnesia foam was measured by a penetration test. This method was selected to provide a quick comparison of relative sample strength.

Blocks of foam, 2 by 2 by 2 inches were placed on the lower platen of a Tinius-Olsen Universal Tester. A 1-inch diameter steel rod was attached to the upper platen with the longitudinal axis normal to the sample. Pressure was applied to the foam sample by the steel rod until failure occurred. The load (in psi) required to produce failure was recorded as the compressive strength of the sample.

Impact Strength — The impact strength was determined using a National Forge Impact Tester employing the Izod test method. In this test, the specimen is held as a vertical cantilever beam and broken by a blow delivered by a swinging weight at a fixed distance from the edge of the specimen clamp. A set point indicator, activated by the swinging weight, indicates the loss of kinetic energy.

Chemical Resistance — The magnesium-oxide body was tested for resistance to common acids and bases. Specimens were boiled in concentrated and dilute solutions of the following reagents: sulfuric acid, hydrochloric acid, phosphoric acid, nitric acid, ammonium hydroxide, and sodium hydroxide. The length, width, thickness, and weight of each specimen was measured before and after an 8-hour boiling cycle.

Component Compatibility — Three properties were measured prior to design of sample leading edges:

1) Chemical compatibility between the reinforcing metal and the ceramic phase;

2) Thermal expansion compatibility between the ceramic foam and the mounting stud;

3) Strength of the mounting stud assembly.

The test procedures used are described below:

To establish the chemical stability of the reinforcing metal in contact with the ceramic phase, disks, 3 inches in diameter, were pressed with wire imbedded in the ceramic matrix. These samples were sintered in the same manner as the normal composite structure. After sintering, the samples were sectioned and examined microscopically for evidence of reaction between the ceramic and the metal phase.

Samples were prepared, as shown in Figure 5, to test the thermal expansion of the mounting stud attachment concept. These samples were then mounted in the single oxyacetylene torch facility with the sample end opposite the mounting stud exposed to the torch flame. The torch was then advanced until cracking of the foam occurred. The temperatures of the sample surface and at the head of the stud were recorded. After testing, the samples were examined visually to determine the mode of failure (Fig. 5A).

A set of samples to determine the strength of the mounting stud-foam bond differed from those previously prepared in that an aluminum block was cemented to the end of the sample opposite the mounting stud. The aluminum block and the stud were then grasped by the tensile jaws of a Tinius-Olsen Universal Tester and the force required to pull the stud from the foam measured.

Hot Gas Testing — Oxyacetylene and plasma torches were chosen as the most practical way of determining the material system's ability to withstand high temperatures and thermal shock. To ensure reproducibility, the test facilities were calibrated with the cold wall calorimeter described below.

1) Cold Wall Calorimeter — The calorimeter used in this program was developed for calibration of plasma torches by the Composite Materials Working Group under the sponsorship of ASD and NASA. The design of this equipment is shown in Figure 6.

In use, the calorimeter is inserted into the hot gas stream. By monitoring the water flow and its temperature rise, the amount of heat transferred to the calorimeter may be calculated as shown in the following equation:

$$Q = \frac{(\Delta T)\,(W)\,(H_c)}{A}$$

where: Q = Heat Flux
ΔT = Rise in Temperature of the Cooling Water
W = Flow Rate of Water
H_c = Heat Capacity of the Water
A = Area of the Calorimeter

In the present program, English units were used to give the results in Btu/ft^2-sec.

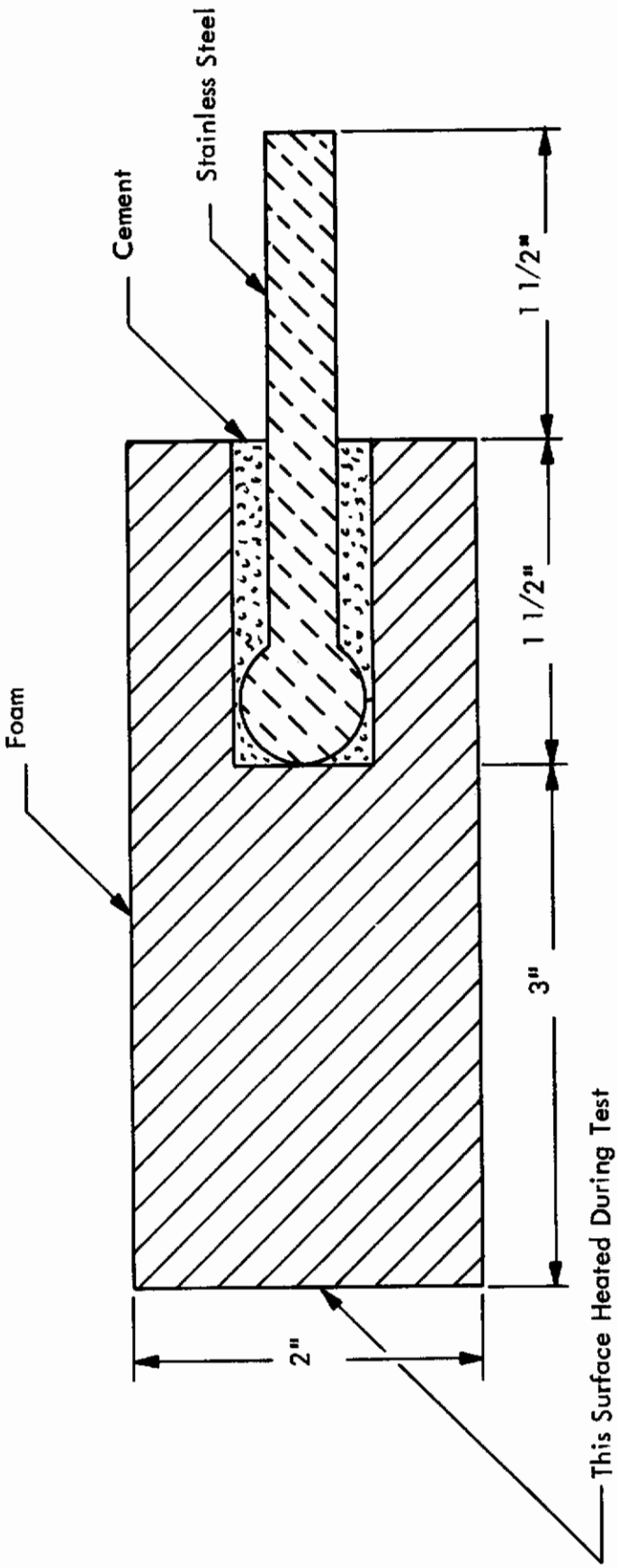

FIGURE 5. STUD ATTACHMENT TEST SPECIMEN

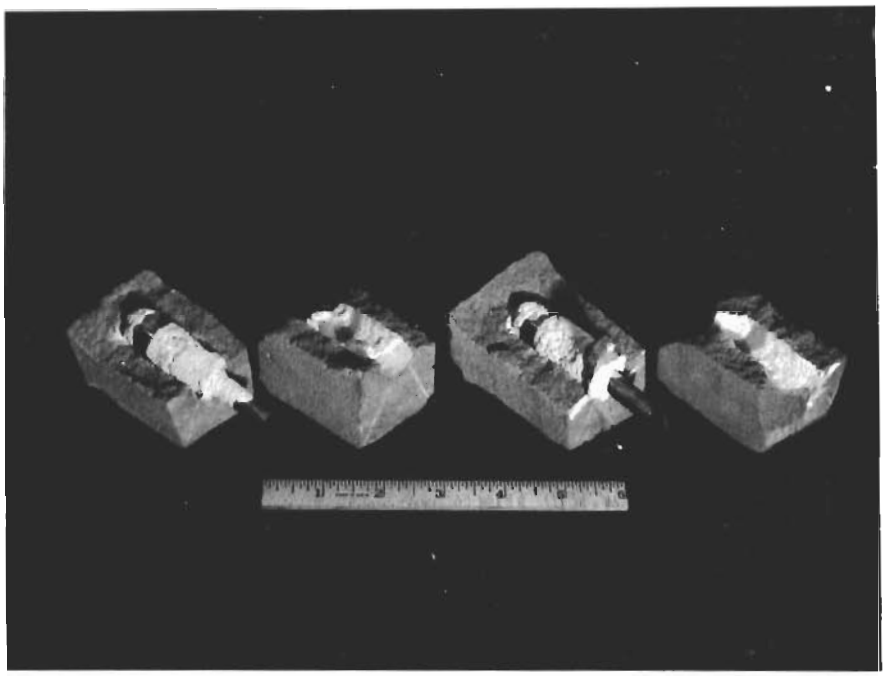

FIGURE 5A MAGNESIA FOAM BLOCKS CONTAINING MOUNTING STUDS AFTER TESTING

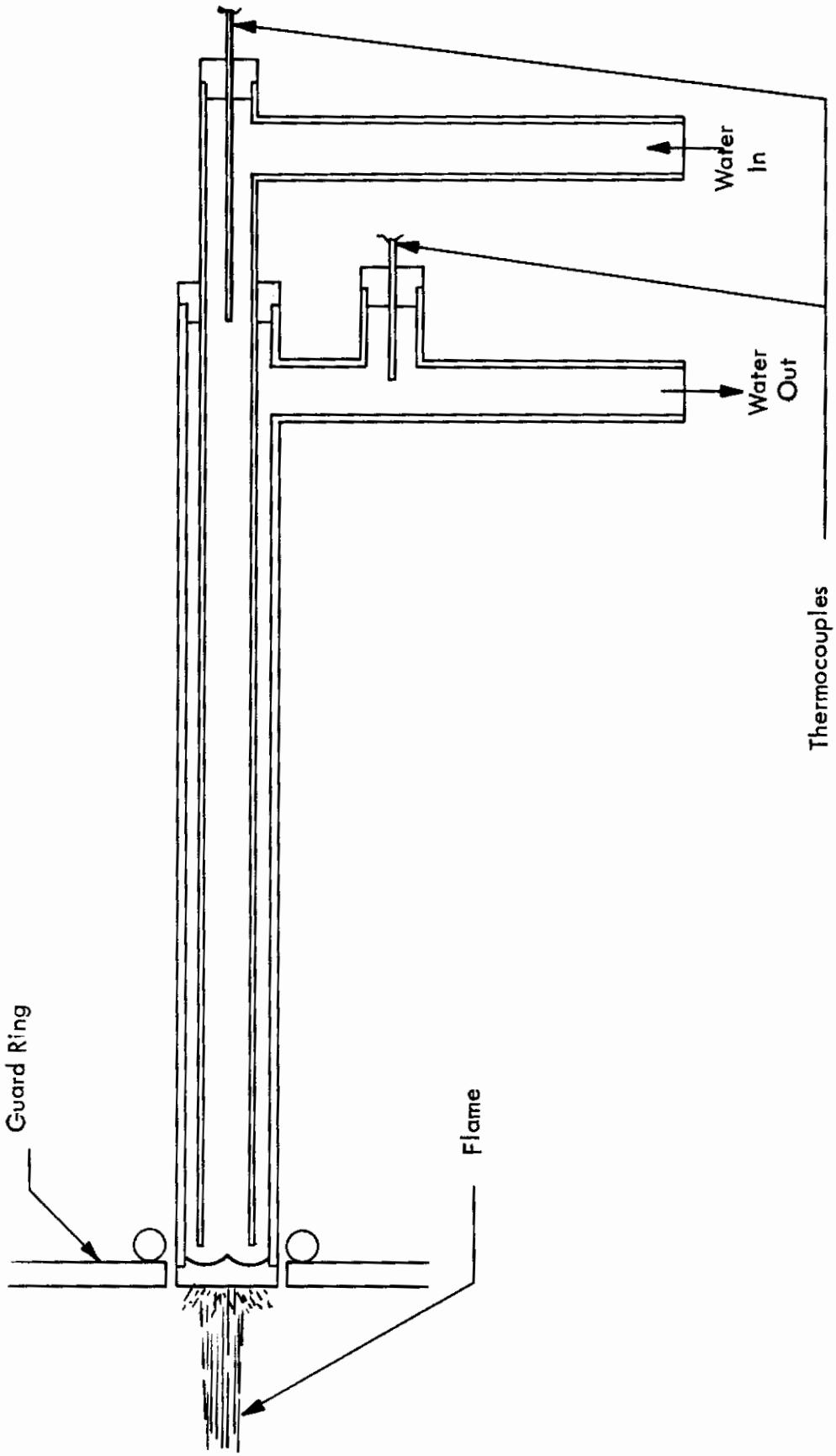

FIGURE 6 CALORIMETER FOR CALIBRATION OF OXYACETYLENE AND PLASMA TORCHES

The heat flux obtained by this method is the heat transferred to a cold wall. To apply this data to ceramic samples, it is necessary to correct for factors such as reflectance and surface temperature. In the present program, the cold-wall heat flux was used to compare data obtained from one test facility with that obtained from another and as a check on the reproducibility of the test conditions.

Figure 7 shows the surface temperature versus cold-wall heat flux of a magnesia sample tested with an oxyacetylene torch and a magnesia sample tested with a plasma torch. The results show that the data obtained on one test facility may be reliably compared with that obtained on another by calibrating both facilities with the calorimeter. This applies only where both facilities have comparatively low velocity flames and the mechanism of heat transfer is essentially the same.

The single oxyacetylene torch used in this program was calibrated with the cold-wall calorimeter described above. The results of this procedure are shown in Figure 8. The maximum cold-wall heat flux that can be obtained with this torch is 325 Btu/ft^2-sec at 1 inch. Bringing the sample closer to the torch leads to torch failure due to the reflected heat, which causes the burner to backflash.

A similar curve is shown in Figure 9 for the plasma torch. The maximum heat flux that can be obtained with this equipment is considerably higher, with the highest measured value being 1000 Btu/ft^2-sec at 1 inch.

An attempt was made to calibrate the large triple-torch test facility. The cooling water in the guard ring surrounding the calorimeter was unable to absorb the combined heat output of the three torches. Rather than redesign the guard ring to permit calibration of this torch, the effective heat flux was assumed to be the same at equivalent sample surface temperatures for both the single and the triple oxyacetylene torches on the basis of the data reported in Figure 7.

2) Single Oxyacetylene Torch Test Facility — The majority of the material screening in this program was conducted on the single oxyacetylene torch facility shown in Figure 10. The standard sample used was a 2-inch disk, 3/8-inch thick. This sample was supported by a refractory backing (magnesia for the thoria and magnesia samples, zirconia for the zirconia samples) selected for nonreactivity with the materials being tested.

This test is particularly useful for establishing comparative thermal shock resistance of materials up to approximately 4300°F since the low flame velocity prevents masking of thermal shock effects by erosion. The gradual slope of the heat flux versus distance curve makes control of heating rates relatively simple. The standard thermal shock test consisted of advancing the torch at a sufficient rate to produce the surface temperature profile shown in Figure 12. For comparison, a typical glide re-entry vehicle, nose-cap heating rate is also shown in Figure 11. The nose-cap heating rate is considerably less severe below 1500°F than the present test procedure. The more severe heating rate was selected as

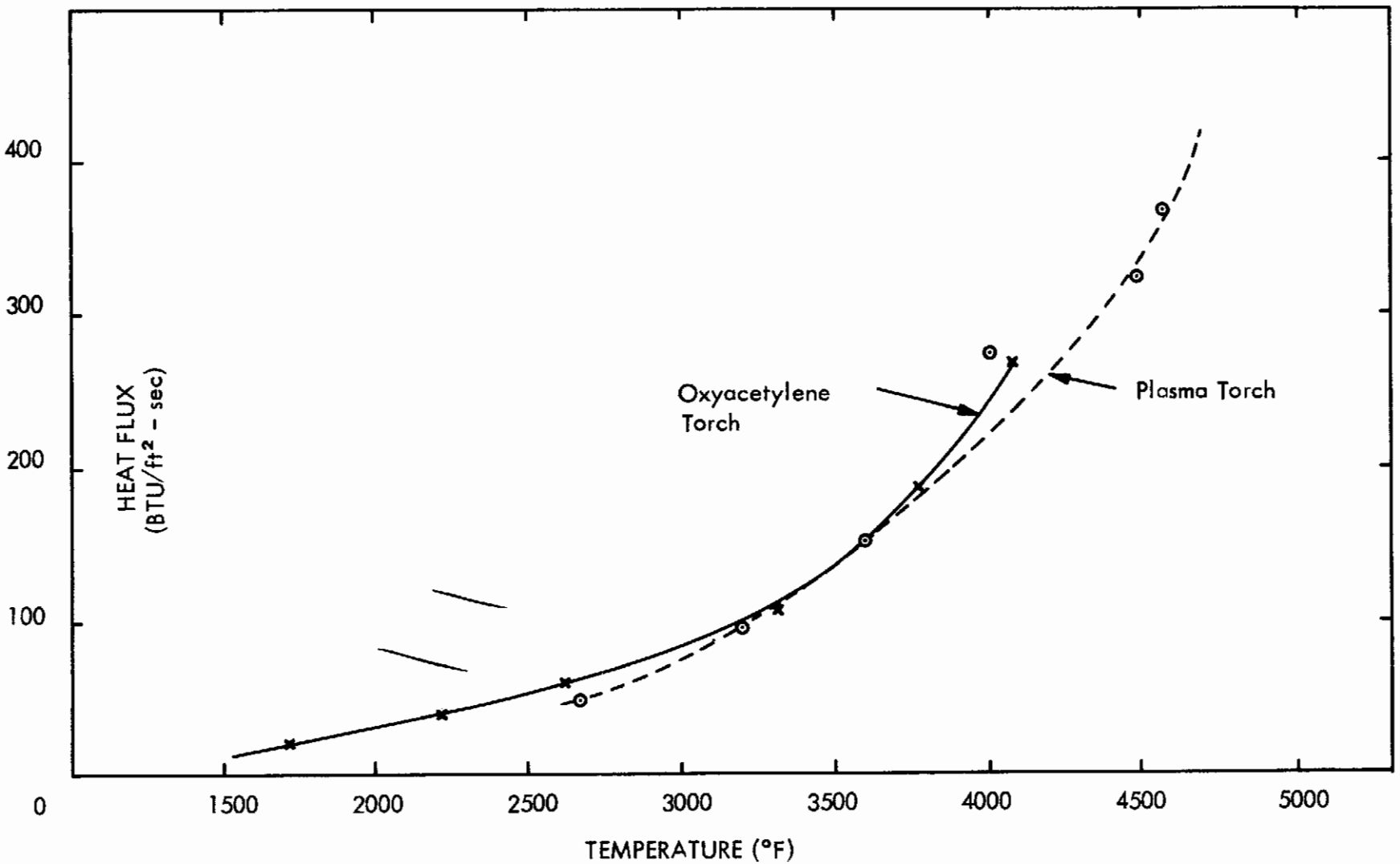

FIGURE 7. COMPARISON OF SURFACE TEMPERATURES OBSERVED FOR MAGNESIA BODIES TESTED ON OXYACETYLENE AND PLASMA TORCHES AT EQUIVALENT HEAT FLUXES

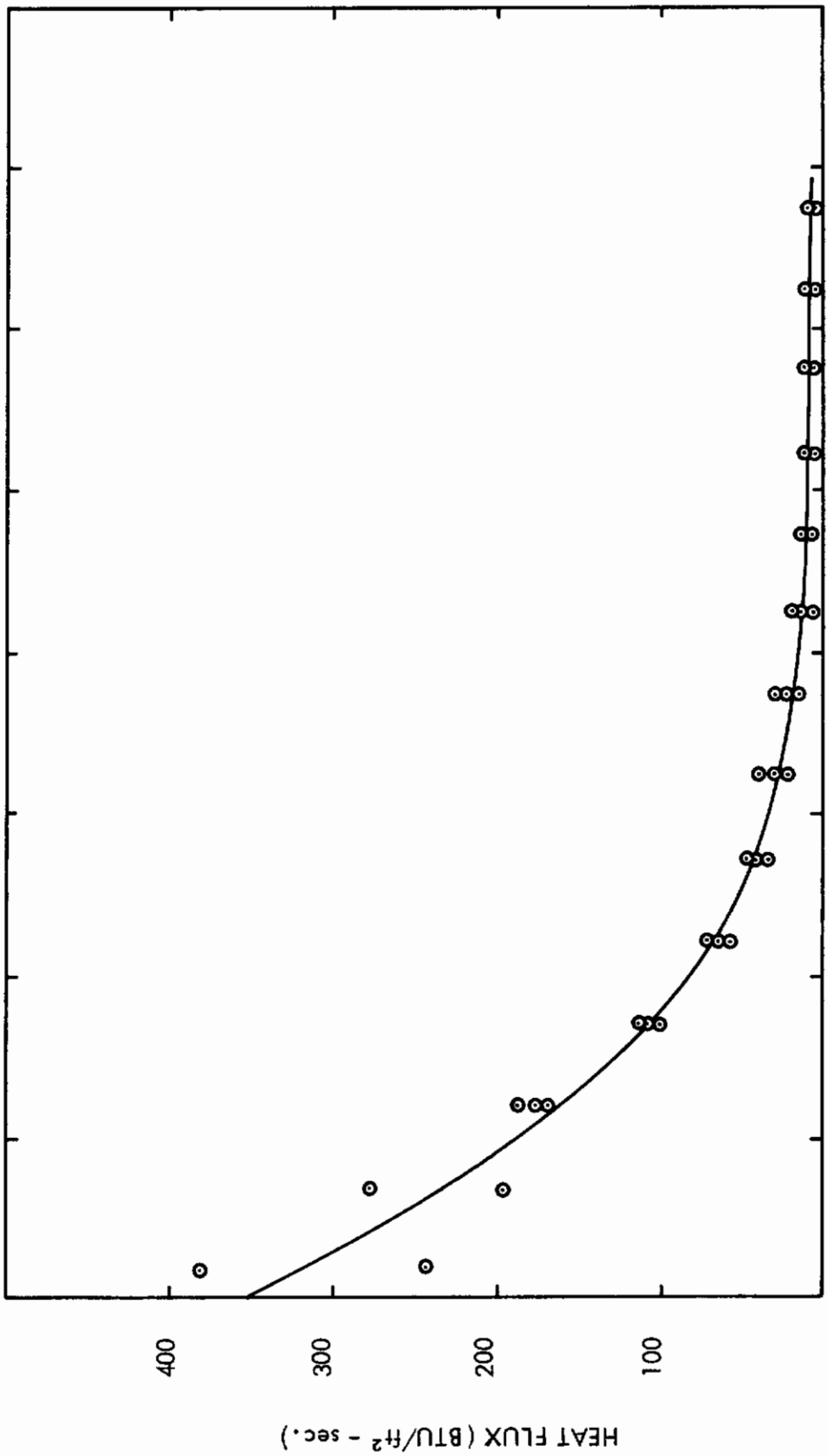

FIGURE 8. HEAT FLUX VS DISTANCE FROM NOZZLE FOR SINGLE OXYACETYLENE TORCH

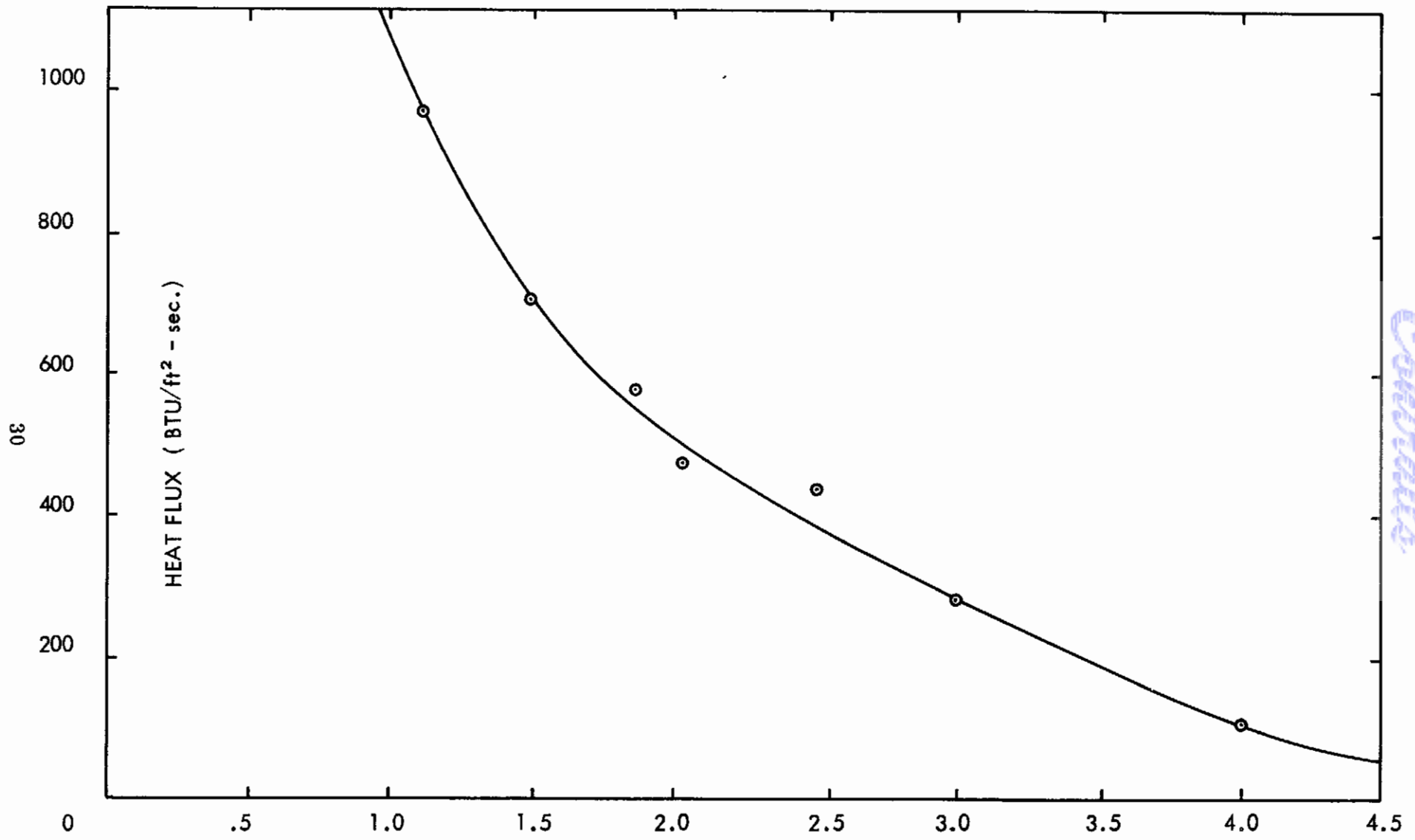

FIGURE 9. HEAT FLUX VS DISTANCE FROM NOZZLE FOR PLASMA TORCH

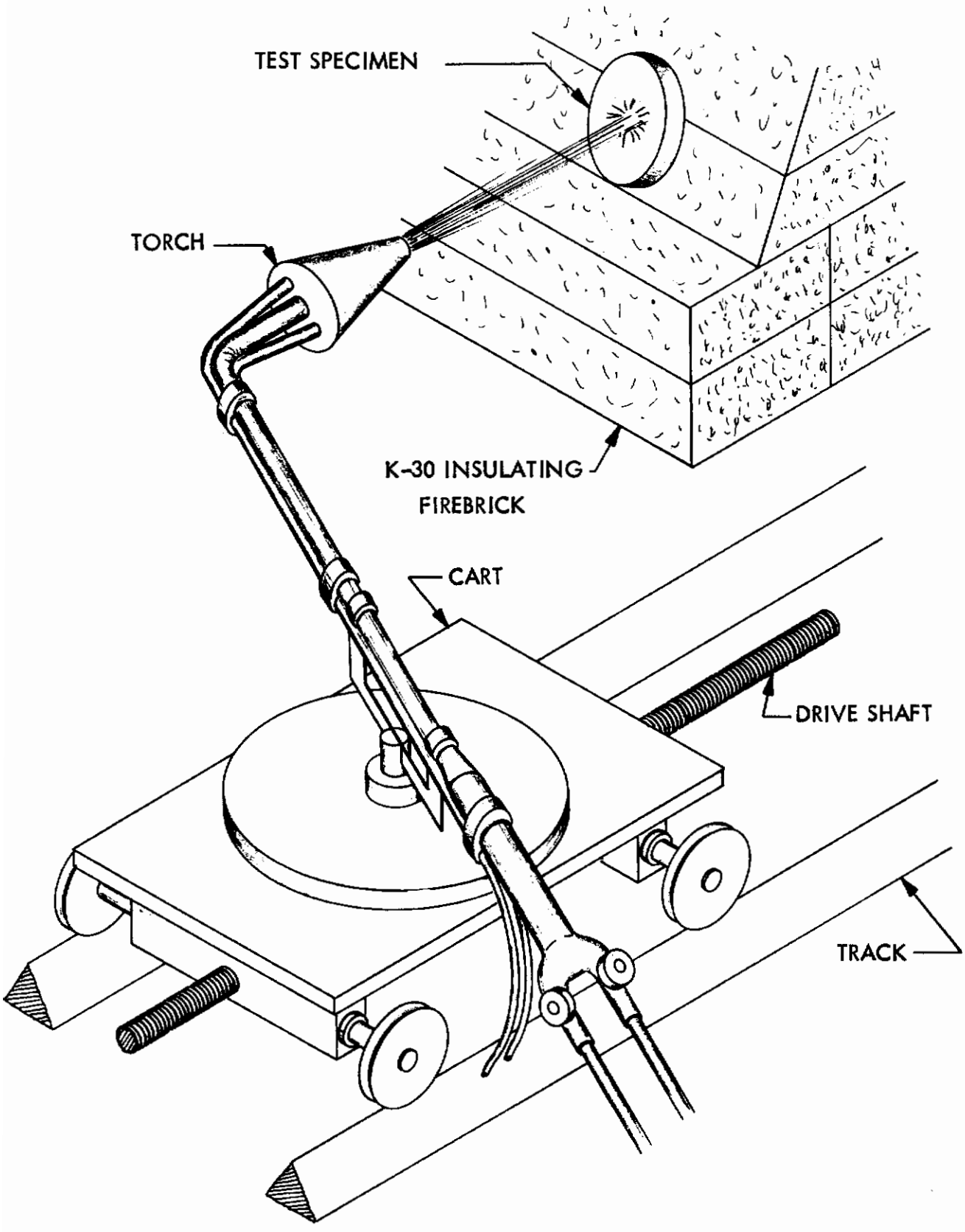

FIGURE 10 SINGLE-TORCH OXYACETYLENE TEST FACILITY

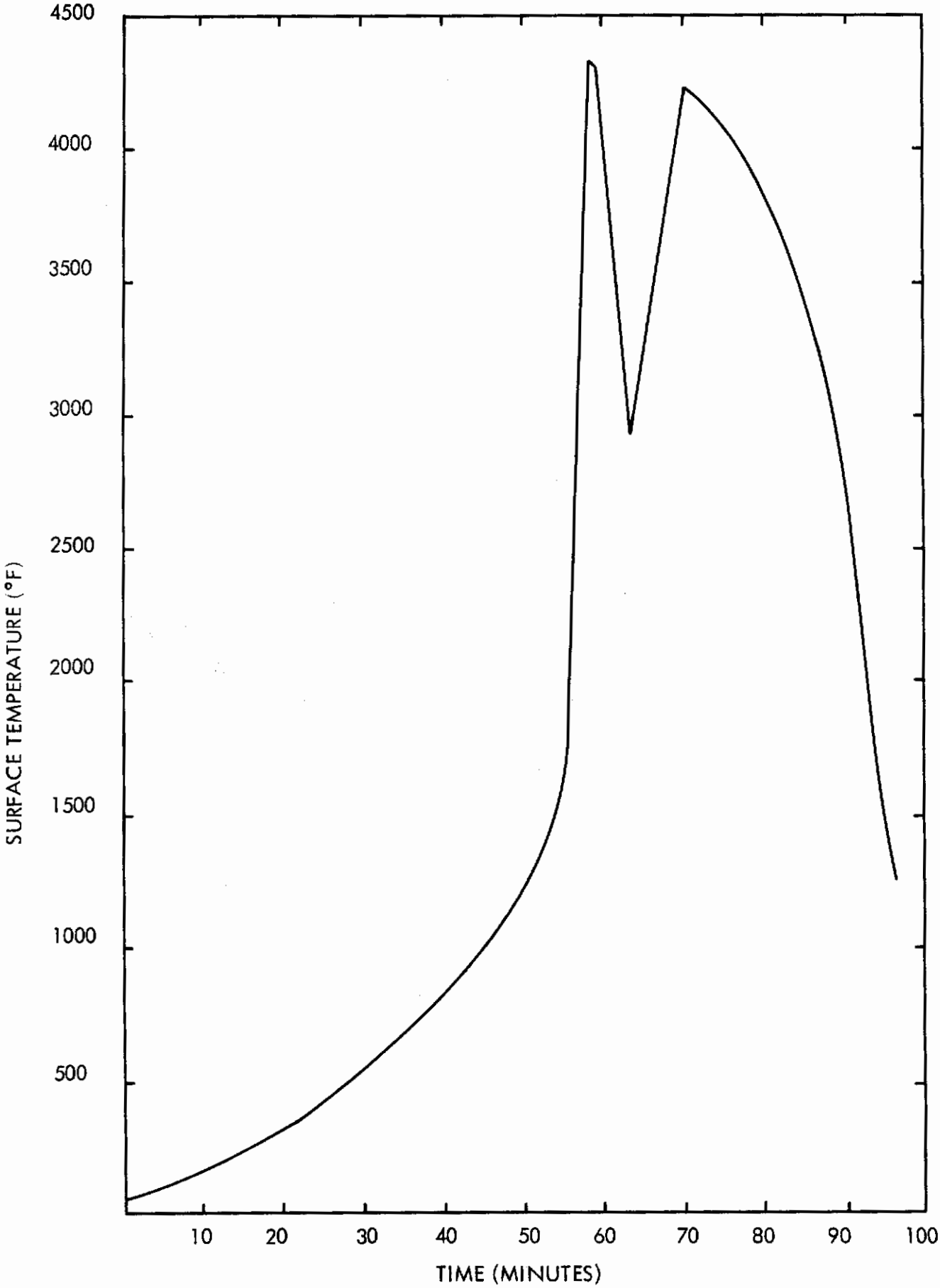

FIGURE 11. TYPICAL NOSE CAP HEATING RATE SIMULATION FOR A GLIDE RE-ENTRY VEHICLE

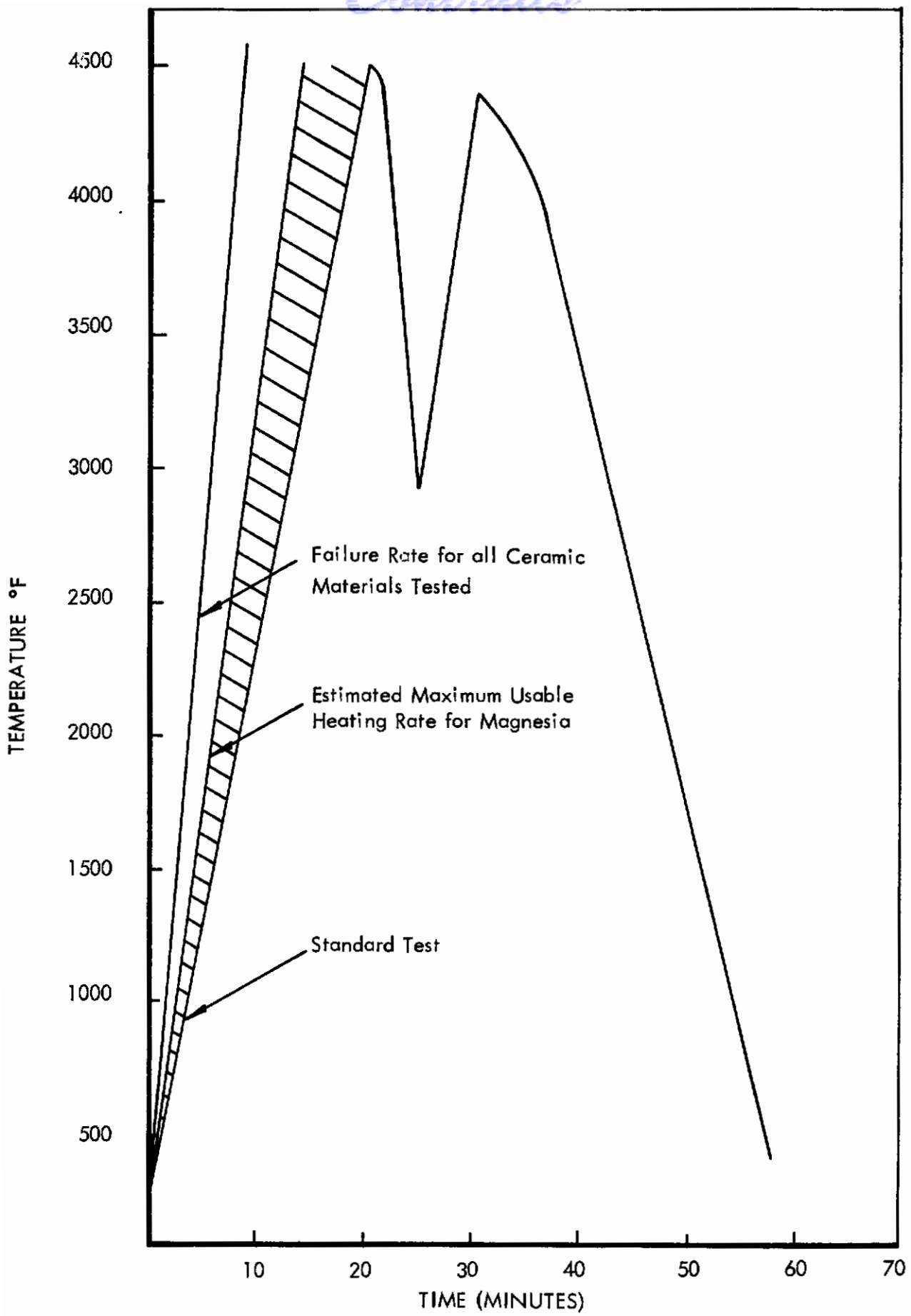

FIGURE 12. HEATING RATES USED FOR EVALUATION OF MATERIAL SYSTEMS

the maximum heating rate that the zirconia body could withstand. Thus, samples able to pass this test successfully were at least equivalent to the zirconia body in thermal shock resistance.

3) Triple Oxyacetylene Torch Test Facility — This test facility differs from the facility shown in Figure 10 in that three torches are used. With the exception of sample sizes, the use of the triple oxyacetylene torch facility is identical with that of the single oxyacetylene torch facility. The samples used in this test were 3-inch diameter disks, 1/2-inch thick. Results from this test were used to establish the feasibility of larger shapes and the effect, if any, of the increased size on thermal shock resistance. Tests to date have not shown the results obtained with this equipment differ appreciably from those obtained with the single torch test facility.

4) Plasma Torch Testing — The plasma torch has proven to be the most versatile of the three test facilities. In addition to the higher heat fluxes produced, monitoring of the operating conditions is relatively simple and the composition of the stabilizing gas may be varied to produce the desired test environment.

The following operating conditions were used with the Metco MB-40, Plasma Flame Unit, based on the manufacturer's recommendations:

Current — 420 amperes
Voltage — 72 volts
Nitrogen — 80 cubic feet per hour
Hydrogen — 7 cubic feet per hour

Disks, 2 inches in diameter and 1/4 inch thick, are placed in a ceramic sample holder and exposed to the plasma as shown in Figure 13. The sample is advanced into the flame gradually to produce the desired surface temperature. The sample is maintained at this point until equilibrium is indicated by constant temperature readings on the surface of the sample. This procedure is repeated in 300°F surface-temperature increments until sample failure occurs.

The following data is recorded in this test:

1) Hot-face surface temperature at each test position as measured by an optical pyrometer;

2) Back-face temperature at each test position measured by a platinum thermocouple;

3) Distance from torch at each position;

4) Temperature at which first indication of melting occurs.

The data is then interpreted to provide information on emittance, thermal conductivity, thermal shock, and maximum-use temperature. These individual procedures are described in the appropriate sections of this report.

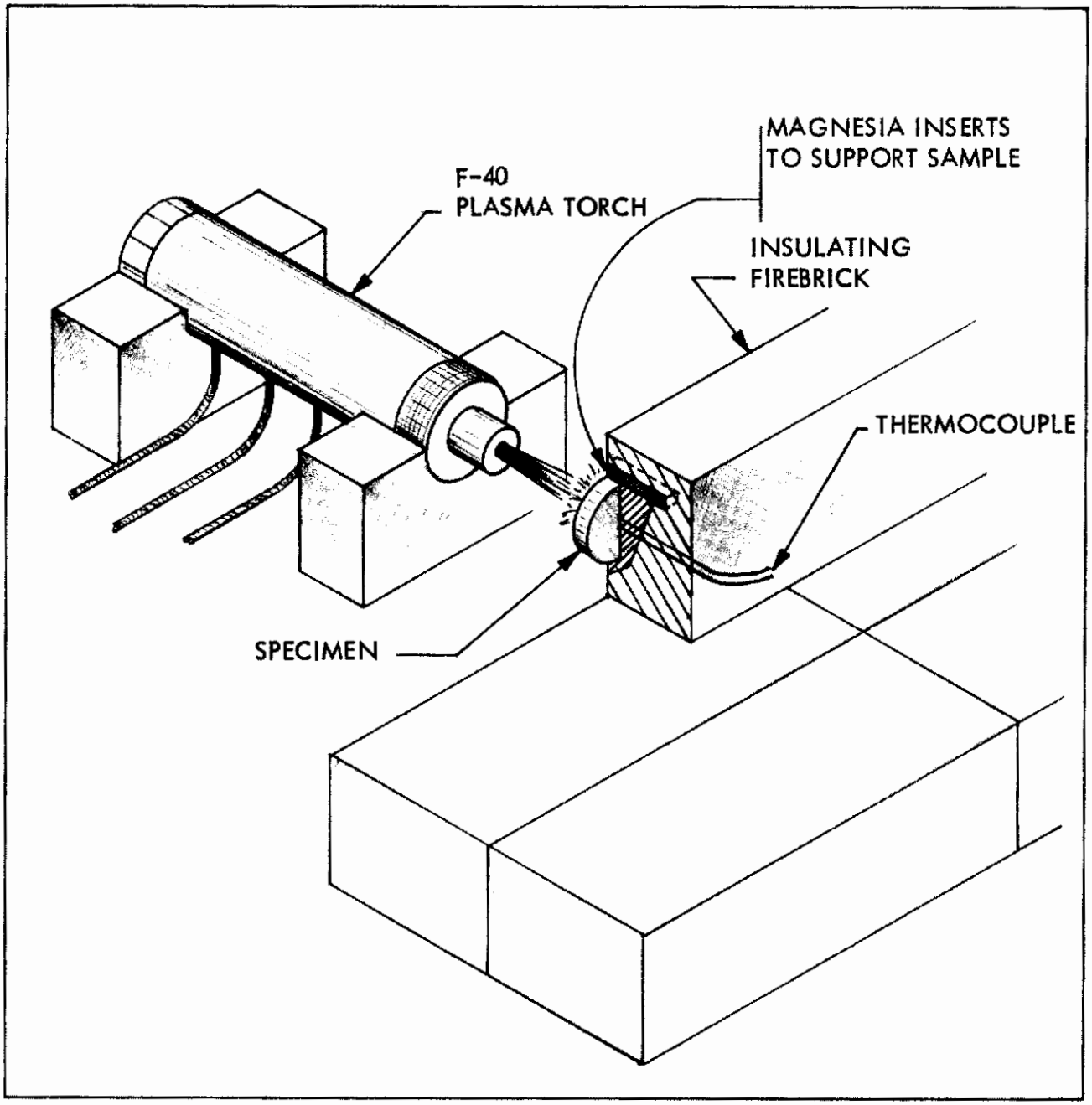

FIGURE 13. PLASMA TORCH SET UP FOR MATERIAL EVALUATION

Component Testing — A leading-edge configuration has been selected for evaluation of relatively large shapes of the material system developed in this program. The size and shape of this component were selected to be compatible with available plasma torch testing facilities such as those at Chicago Midway Laboratories.

The test procedure suggested by Boeing for these samples is as follows:

1) Advance the specimen into the plasma flame at a rate that will achieve a 3000°F surface temperature in 2-1/2 minutes;

2) Continue advancing the specimen to increase the surface temperature 300°F each 2-1/2 minutes until failure of the sample occurs.

This procedure was selected on the basis of a reported 5-minute electrode life for the Chicago Midway plasma torch. The suggested heating rate will result in a 4800°F surface temperature at the end of three electrode changes. This temperature is expected to be the limit of the material systems being tested.

V. DEVELOPMENT OF A MAGNESIA BODY FOR USE IN COMPOSITES

Pressing — The first step taken in the development of a magnesia body was to determine the best method for test sample fabrication. The following fabrication methods were considered: slip casting, hot pressing, and dry pressing. It has been found in previous programs that good thermal shock resistance requires the use of some coarse particles in the ceramic body. Experience has also shown that it is difficult to control the dispersion of coarse particles in a ceramic slip. For these reasons, slip casting was discarded. Magnesia reacts with graphite at relatively low temperatures, which prevented the use of available hot-pressing equipment. Therefore, dry pressing was selected as the most practical means of fabricating the magnesia samples.

Magnorite* (100 F) was used to develop dry-pressing techniques to produce samples that had adequate green strength for handling prior to sintering. These samples were evaluated by visual inspection after removal from the die.

The proper water content was first determined. Samples with 2, 3, 4, 5, 6, and 7 percent water were pressed at 12,000 psi. The samples with 2 and 3 percent water were too dry and broke easily during handling. The samples with 5, 6, and 7 percent water stuck to the die and were, in general, too wet for handling. Four percent was found to be a suitable water content.

To determine the pressure required to form the samples, the water content was held constant at 4 percent and the pressure was varied from 1000 to 20,000 psi. The minimum pressure that would produce samples with sufficient green strength for handling was 12,000 psi. Above 16,000 psi no further improvement was apparent. Most of the test samples were pressed at the latter pressure.

Initial Body Development — The compositions listed in Table 1 were prepared to establish the most promising areas of investigation. Bars, 2 inch by 1/2 inch by 1/2 inch, were pressed at 12,000 psi and sintered 4 hours in air at 2800°F. Evaluation of the materials consisted of visual examination during the fabrication process and a 15-second plasma torch exposure at a heat flux of 400 Btu/ft^2-sec. Of the compositions tested, only compositions D-36 through D-42 showed appreciable thermal shock resistance. This was attributed to the mixture of coarse and fine particles. From these tests it was concluded that control of particle size distribution was the most promising means of improving shock resistance.

Sintering — Magnesia from three sources was evaluated in determining sinterability. The materials were: General Electric fused magnesia, Mallinckrodt reagent grade magnesium oxide, and Norton Magnorite. Samples fabricated from General Electric fused magnesia and Mallinckrodt reagent grade magnesium oxide were not completely mature when sintered at 2800°F. Norton Magnorite sintered completely in 4 hours at 2800°F. In addition, it is readily available in a wide variety of grain sizes.

*Norton Company, Worchester, Massachusetts.

TABLE I PRELIMINARY SAMPLE TESTS

CODE	COMPOSITION	COMMENTS
D - 1	30 F MgO + .5% Nickel Powder	
D - 2	30 F MgO + 1% Nickel Powder	Poor Thermal Shock, Good Green Strength, Good Fired Strength
D - 3	30 F MgO + 2% Nickel Powder	
D - 4	30 F MgO + 4% Nickel Powder	
D - 5	30 F MgO + 8% Nickel Powder	
D - 6	-325 ZrO_2 + .5% Nickel Powder	
D - 7	-325 ZrO_2 + 1% Nickel Powder	Poor Thermal Shock, Good Green strength, Good Fired Strength
D - 8	-325 ZrO_2 + 2% Nickel Powder	
D - 9	-325 ZrO_2 + 4% Nickel Powder	
D - 10	-325 ZrO_2 + 8% Nickel Powder	
D - 11	30 F MgO + .5% Fine ZrO_2	
D - 12	30 F MgO + 1% Fine ZrO_2	
D - 13	30 F MgO + 4% Fine ZrO_2	Poor Thermal Shock, Good Green Strength, Good Fired Strength
D - 14	30 F MgO + 8% Fine ZrO_2	
D - 15	30 F MgO + 16% Fine ZrO_2	
D - 16	30 F MgO + 32% Fine ZrO_2	
D - 17	30 F MgO + 64% Fine ZrO_2	
D - 18	30 F MgO + 1% Sodium Sulfite	Poor Thermal Shock
D - 19	30 F MgO + 2% Sodium Sulfite	

TABLE 1 (Continued)

CODE	COMPOSITION	COMMENTS
D – 20	Not Used	
D – 21	Not Used	
D – 22	30 F MgO + .5% -30, +90 ZrO_2	
D – 23	30 F MgO + 1% -30, +90 ZrO_2	Poor Thermal Shock, Poor Green Strength, Good Fired Strength
D – 24	30 F MgO + 4% -30, +90 ZrO_2	
D – 25	30 F MgO + 8% -30, + 90 ZrO_2	
D – 26	30 F MgO + 16% -30, +90 ZrO_2	
D – 27	30 F MgO + 32% -30, +90 ZrO_2	
D – 28	30 F MgO + 64% -30, +90 ZrO_2	
D – 29	30 F MgO + 1% Napthylene	
D – 30	30 F MgO + 2% Napthylene	
D – 31	30 F MgO + 4% Napthylene	Poor Thermal Shock, Poor Green Strength, Poor Fired Strength
D – 32	30 F MgO + 8% Napthylene	
D – 33	30 F MgO + 16% Napthylene	
D – 34	30 F MgO + 32% Napthylene	
D – 35	30 F MgO + 64% Napthylene	
D – 36	30 F MgO + 2% Reagent MgO	
D – 37	30 F MgO + 4% Reagent MgO	
D – 38	30 F MgO + 8% Reagent MgO	Fair Thermal Shock, Good Green Strength, Good Fired Strength
D – 39	30 F MgO + 16% Reagent MgO	

TABLE 1 (Continued)

CODE	COMPOSITION	COMMENTS
D - 40	30 F MgO + 32% Reagent MgO	
D - 41	30 F MgO + 50% Reagent MgO	
D - 42	30 F MgO + 100% Reagent MgO	
D - 43	30 F MgO + 3% Sodium Sulfite	Poor Thermal Shock, Good Green Strength, Good Fired Strength
D - 44	30 F MgO + 2% Sodium Sulfite	
D - 45	30 F MgO + 1% Sodium Sulfite	
E - 1	30 F MgO + 3% Conc Sodium Sulfite	Poor Thermal Shock Good Fired Strength
E - 2	30 F MgO + 8% -325 ZrO_2	Poor Thermal Shock Good Fired Strength
E - 3	30 F MgO + 8% -30, +90 ZrO_2	Poor Fired Strength
E - 4	30 F MgO + 8% Reagent MgO	Poor Thermal Shock Good Fired Strength
E - 5	1/2 -12 + 24 MgO + 1/2 Kaiser MgO	Very Poor Fired Strength
E - 6	100 F MgO	Poor Thermal Shock Good Fired Strength
E - 7	Not Used	
E - 8	Fused General Electric MgO	Very Poor Fired Strength
E - 9	33 1/3% G. E. MgO 33 1/3% -12 + 24 MgO 33 1/3% Reagent MgO	Very Poor Fired Strength

TABLE 1 (Continued)

CODE	COMPOSITION	COMMENT
E - 10	33 1/3% -12 +24 MgO 33 1/3% 100 F MgO 33 1/3% Reagent MgO	Very Poor Fired Strength
F - 1	G. E. MgO + 6 2/3% $MgSo_4$ +3 1/3% H_2So_4	Very Poor Fired Strength
F - 2	G. E. MgO + 10% $MgSo_4$ + 5% H_2So_4	Very Poor Fired Strength

Norton Magnorite is 96.39 percent MgO with the following impurities as given by the vendor:

	Percent
CaO	1.91
SiO	1.21
Fe_2O_3	0.23
Al_2O_3	0.26

The ease with which bodies fabricated from this grade of magnesia can be sintered is attributed to the presence of these impurities.

A Globar furnace was used to sinter the magnesia samples prepared under this contract. Sintering temperatures from 2200°F to 2800°F were investigated. Samples sintered below 2200°F proved to be extremely nonuniform, and reliable test data could not be obtained from these samples. Completely sintered bodies could be produced between 2200°F and 2800°F by varying the sintering time from 20 hours at 2200°F to 4 hours at 2800°F. The effect of varying the sintering schedule was evaluated by firing samples of F-18 at 2200°F for 20 hours and at 2800°F for 4 hours. The strengths at room and elevated temperatures were compared (Table 4). Generally, the body fired at 2200°F showed a slightly higher strength. The discrepancy at 3600°F is attributed to experimental error. Because samples prepared by either schedule were essentially equivalent, the 2800°F sintering cycle was used for the majority of the specimens to expedite their fabrication.

Additions of nine compounds were investigated for their ability to further improve properties of Magnorite bodies. The compounds tested were as follows.

Lithium nitrate
Lithium chloride
Lithium fluoride
Aluminum nitrate
Chromium nitrate
Ferrous nitrate
Titanium dioxide
Zirconium oxide
Magnesium chloride

Plasma torch tests were used to evaluate the thermal shock resistance of these samples. The results are shown in Table 2. The samples containing additives showed no improvement in thermal shock resistance when compared with samples not containing additives and, in some cases, the use of additives decreased thermal shock resistance.

None of these compounds had any apparent effect on the density of the magnesia bodies. The slight differences reported in Table 2 are attributed to normal experimental error.

TABLE 2

PHYSICAL PROPERTIES OF MAGNESIA BODIES CONTAINING SINTERING AIDS

Code	Additive*	Firing Temp. °F	Density (gms/cc)	Thermal Shock
A - 1	0.5% $LiNO_3$	2800	2.57	Poor
A - 2	0.5% LiF	2800	2.54	Fair
A - 3	0.5% $Al(NO_3)_3 \cdot 9H_2O$	2800	2.55	Poor
A - 4	0.5% $Cr(NO_3)_3 \cdot 9H_2O$	2800	2.56	Poor
A - 5	0.5% $Fe(NO_3)_3 \cdot 9H_2O$	2800	2.56	Poor
A - 6	0.5% TiO_2	2800	2.57	Fair
A - 7	0.5 ZrO_2	2800	2.57	Poor
A - 8	None	2800	2.56	Fair
B - 1	0.5% $LiNO_3$	2600	2.58	Poor
B - 2	0.5% LiF	2600	2.56	Fair
B - 3	0.5% $Al(NO_3)_3 \cdot 9H_2O$	2600	2.56	Poor
B - 4	0.5% $Cr(NO_3)_3 \cdot 9H_2O$	2600	2.56	Poor
B - 5	0.5% $Fe(NO_3)_3 \cdot 9H_2O$	2600	2.56	Poor
B - 6	0.5% TiO_2	2600	2.58	Fair
B - 7	O.5% ZrO_2	2600	2.57	Poor
B - 8	None	2600	2.57	Fair
C - 1	0.5% $LiNO_3$	2200	2.57	Poor
C - 2	0.5% LiF	2200	2.57	Fair

*Remainder of sample 100F Norton Magnorite

TABLE 2 (Continued)

PHYSICAL PROPERTIES OF MAGNESIA BODIES CONTAINING SINTERING AIDS

Code	Additive*	Firing Temp. °F	Density (gms/cc)	Thermal Shock
C - 3	0.5% $Al(NO_3)_3 \cdot 9H_2O$	2200	2.55	Poor
C - 4	0.5% $Cr(NO_3)_3 \cdot 9H_2O$	2200	2.56	Poor
C - 5	0.5% $Fe(NO3)_3 \cdot 9H_2O$	2200	2.56	Poor
C - 6	0.5% TiO_2	2200	2.57	Fair
C - 7	0.5% ZrO_2	2200	2.57	Poor
C - 8	None	2200	2.55	Fair

* Remainder of sample 100F Norton Magnorite

A final series of tests on the effect of sintering aids on strength was conducted, as reported in Table 3. Magnesium chloride and lithium fluoride were used in these tests. A slight increase in strength was evidenced by some of the bodies containing sintering aids. However, these results were not consistent and in large samples containing lithium fluoride the additive tended to migrate to the lower portions of the sample during sintering leading to nonuniform samples.

Since sintering aids did not appreciably improve the properties of the magnesia bodies, and since suitable bodies could be produced more easily without them, the use of sintering aids was discontinued.

Strength — Tests were conducted to determine the effect of particle size distribution on the body as shown in Tables 4 and 5. The effect of particle size on strength is shown in Figure 14. Maximum strength of about 7000 psi occurs at about 50 percent fines. For comparison, a body containing 100 percent fines was tested. This body had a strength of 7057 psi. Since both compositions had equal strength, it was concluded that little gain in strength could be achieved by increasing the percentage of fine particles to more than 50 percent.

The strength of the best thermal shock resistant bodies was less than 7000 psi. Composition F-14, which proved to be the best material for use in composites, has a room-temperature strength of 6327 psi. At higher temperatures this value decreases to a minimum of 231 psi at 3200°F. At 3600°F it has increased to 400 psi. These values are approximately half that of the Mix 23 zirconia, described in Section VIII.

No correlation was found between room-temperature strength and thermal shock resistance for the magnesia bodies. Compositions F-14 and F-18, which were the best bodies tested in thermal shock resistance, had the highest strength at 3600°F. Composition F-7, which had the third highest strength at 3600°F of the magnesia bodies, also had good thermal shock resistance. However, compositions F-6 and F-9, which were the weakest bodies tested at 3600°F (182 psi and 162 psi, respectively), had better thermal shock resistance than the stronger F-10 and F-11 compositions (245 psi and 230 psi, respectively). Generally, the 3600°F strength showed positive correlation.

Thermal Shock Resistance — Thermal shock resistance of magnesia bodies was evaluated by testing in an oxyacetylene torch facility. Figure 11 illustrates the thermal shock schedule used in testing re-entry nose-cap materials. This profile was used for initial thermal shock tests. Both F-14 and F-18 compositions were tested by this schedule with no indication of thermal shock damage. Heating rates were then increased to the values shown in Figure 12 to more fully evaluate these materials.

As previously mentioned, the particle size distribution of a ceramic body is a major factor in controlling thermal shock resistance. Figures 15 and 16 show a series of magnesia samples (1/2 inch by 1/2 inch by 1 inch) that were thermal shocked in a plasma facility. The extent of thermal shock damage ranges from sample

TABLE 3

HIGH TEMPERATURE STRENGTH OF MAGNESIA BODIES CONTAINING SINTERING AIDS

Code	Composition**	Density (gm/cc)	Modulus of Rupture (psi) Room Temperature	2800°F	3200°F	3600°F
G - 1	F - 14 (Standard)	2.64	5528	399	231	401
G - 2	F - 14 + 2% $MgCl_2$	2.67	4905	344	311	257
G - 3	F - 18 (Standard)	2.67	5333	257	284	401
G - 4	F - 18 + 2% $MgCl_2$	2.68	5220	227	270	282
G - 5	F - 14 + 2% LiF	2.65	5640	197	197	563
G - 6	F - 18 + 2% LiF	2.64	4380	170	228	305
*G - 7	F - 18 + 2% LiF	2.67	6177	281	454	407
*G- 8	F - 14 + 2% LiF	2.65	5607	272	200	210

*Sintered at later date

**See Table 4 for identification of F-14 and F-18

TABLE 4

PHYSICAL PROPERTIES OF MAGNESIA BODIES AT HIGH TEMPERATURES

Code	Particle Size ** (Wt. %) -14 +20	-14 +24	-24 +60	-28 +65	-60 +100	-65 +100	-100 +250	-250	-200 +325	-325	Mallinckrodt Reagent Grade	Density (gm/cc)	Thermal Shock Res.	Modulus of Rupture*** 70°F	2800°F	3200°F	3600°F
F-6+	44.0					13.2			30.8+	10.5+	1.5	2.69	Fair	7010	221	242	182
F-7+	45.0			20.0					20.0+	13.5+	1.5	2.54	Good	3242	290	296	328
F-9	44.0					13.2			30.8			2.69	Fair	5070	130	168	162
F-10	50.0					15.0			31.7	3.3		2.70	Very Poor	6076	771	308	245
F-11	41.7					11.7			28.3	11.7	3.3	2.70	Very Poor	6522	293	211	230
F-12		65.0	11.0		9.0		7.0	8.0				2.57	Fair	3623	191	213	240
F-14	44.0					13.2			30.8	10.5	1.5	2.64	Good	6327	399	231	400
F-18*	45.0			20.0					20.0	13.5	1.5	2.69	Good	5907	564	333	242
F-18	45.0			20.0					20.0	13.5	1.5	2.67	Good	5333	257	259	400
F-3	Magnorite (100F)											2.33	Very Poor	7057	149	133	156
F-4	Magnorite MgO (100F) 6% H_2Sa_4 + 3% $MgSO_4$											2.68	Very Poor	3768	738	223	363
F-5	Magnorite MgO (100F) 5% H_2SO_4 + 5% $MgSO_4$											2.66	Very Poor	3197	523	195	170
F-8	Magnorite MgO (100F) 6% H_2PO_4											2.36	Very Poor	4473	558	296	336
F-13	Magnorite MgO (100F) 2% $MgCl_2$											2.40	Poor	8480	255	324	222

*Sintered for 20 hours at 2200°F, in air
**Norton Magnorite except as noted
***Average of three specimens
+Particles -200 ball milled for 18 hours in acetone

TABLE 5

PHYSICAL PROPERTIES OF MAGNESIA BODIES AT ROOM TEMPERATURE

Code	Particle Size* (Wt. %) -14 +20	-20 +28	-28 +65	-28 +65	-65 +100	-65 +200	-100 +200	-200 +325	-325	Mallinckrodt Reagent Grade	Density (gm/cc)	Thermal Shock Res.	Mod. of Rupture ** (psi)
F - 20	41.0				12.2			32.8	11.5	2.5	2.70	Very Poor	6794
F - 21	46.0				14.2			29.8	9.0	1.0	2.69	Poor	6240
F - 22	39.0				11.2			33.8	12.5	3.5	2.70	Very Poor	6993
F - 23	48.0				16.2			27.8	7.0	1.0	2.68	Poor	6050
F - 24	42.0		4.0		11.2		4.0	28.8	8.5	1.5	2.70	Poor	6311
F - 25	43.0			19.0				19.0	15.5	3.5	2.76	Poor	7053
F - 26	41.0			18.0				18.0	17.5	5.5	2.61	Very Poor	5079
F - 27	47.0			21.0				21.0	10.0	1.0	2.66	Poor	5292
F - 28	49.0			22.0				22.0	6.0	1.0	2.73	Fair	5280
F - 29	43.0	2.0		18.0		6.0		18.0	11.5	1.5	2.74	Poor	5864
F - 30	44.7				13.4			31.3	10.6		2.64	Poor	6795
F - 31	44.5			16.6				25.4	12.0	1.5	2.69	Poor	6123
F - 32	44.5				16.6			25.4	12.0	1.5	2.68	Poor	6378

*Norton Magnorite except as noted

**Average of six specimens

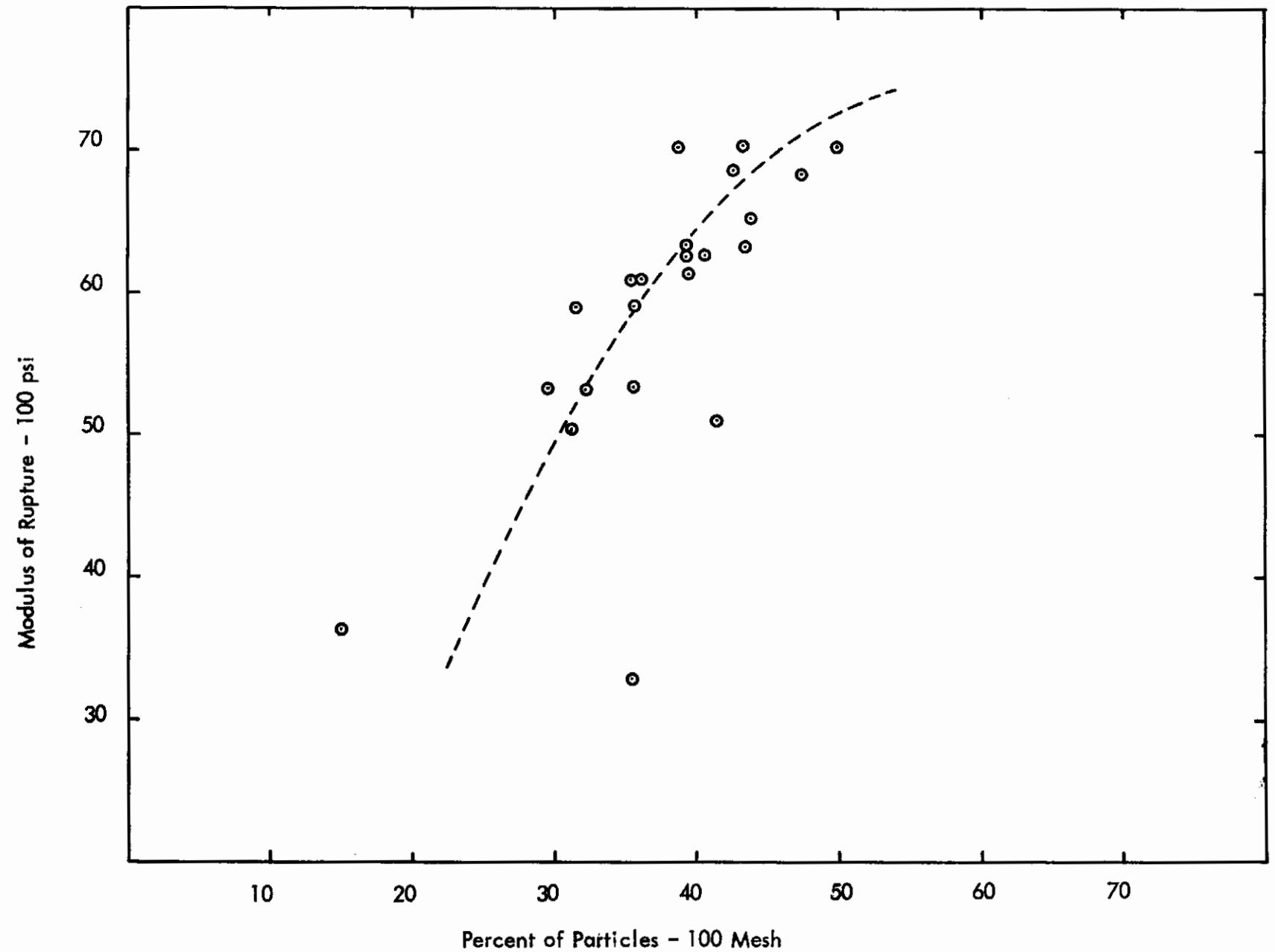

FIGURE 14. STRENGTH OF MAGNESIA BODIES AS A FUNCTION OF PARTICLES SMALLER THAN 100 MESH

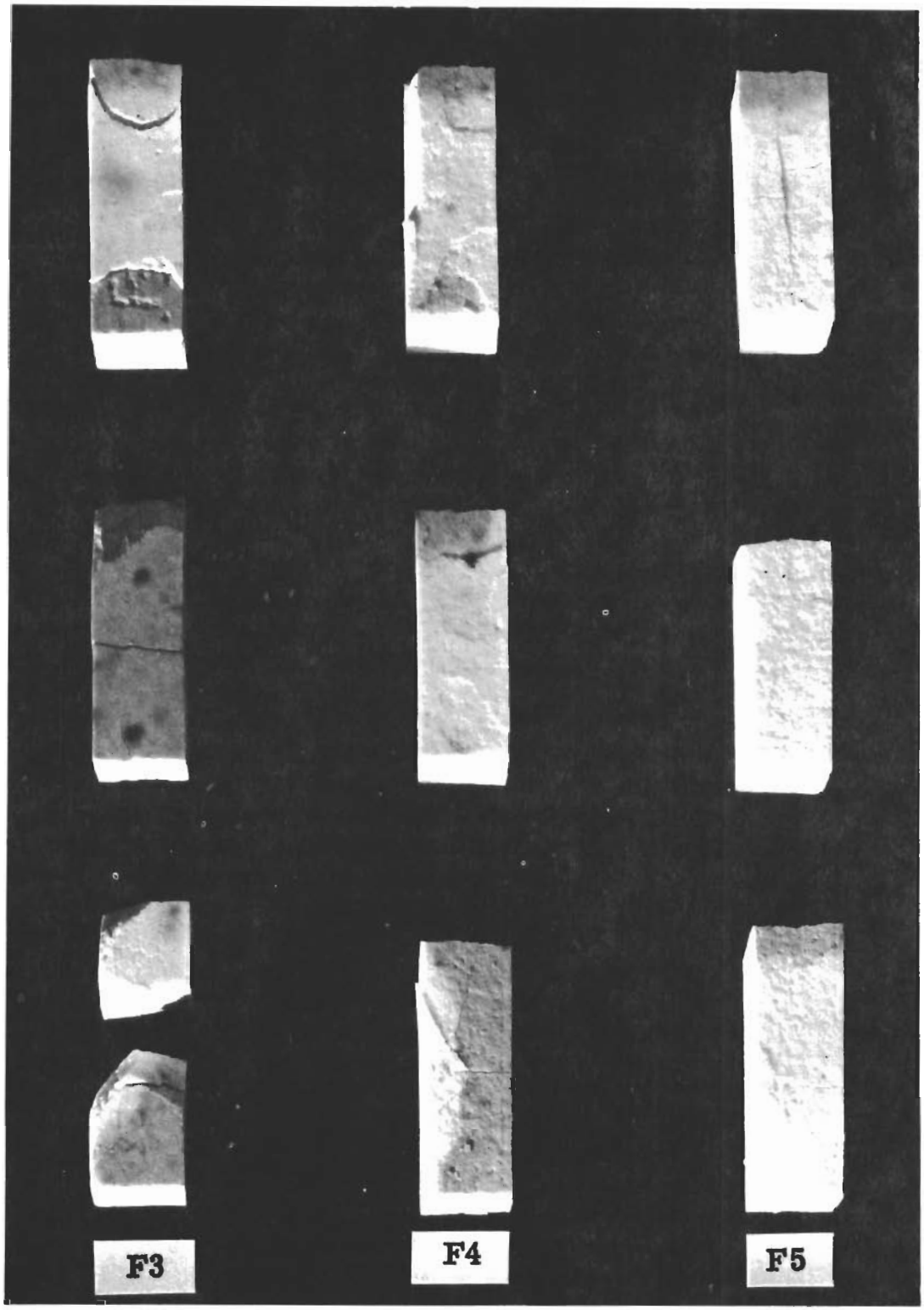

FIGURE 15

MAGNESIA 1/2" x 1/2" x 2" SPECIMENS AFTER THERMAL SHOCK TESTING

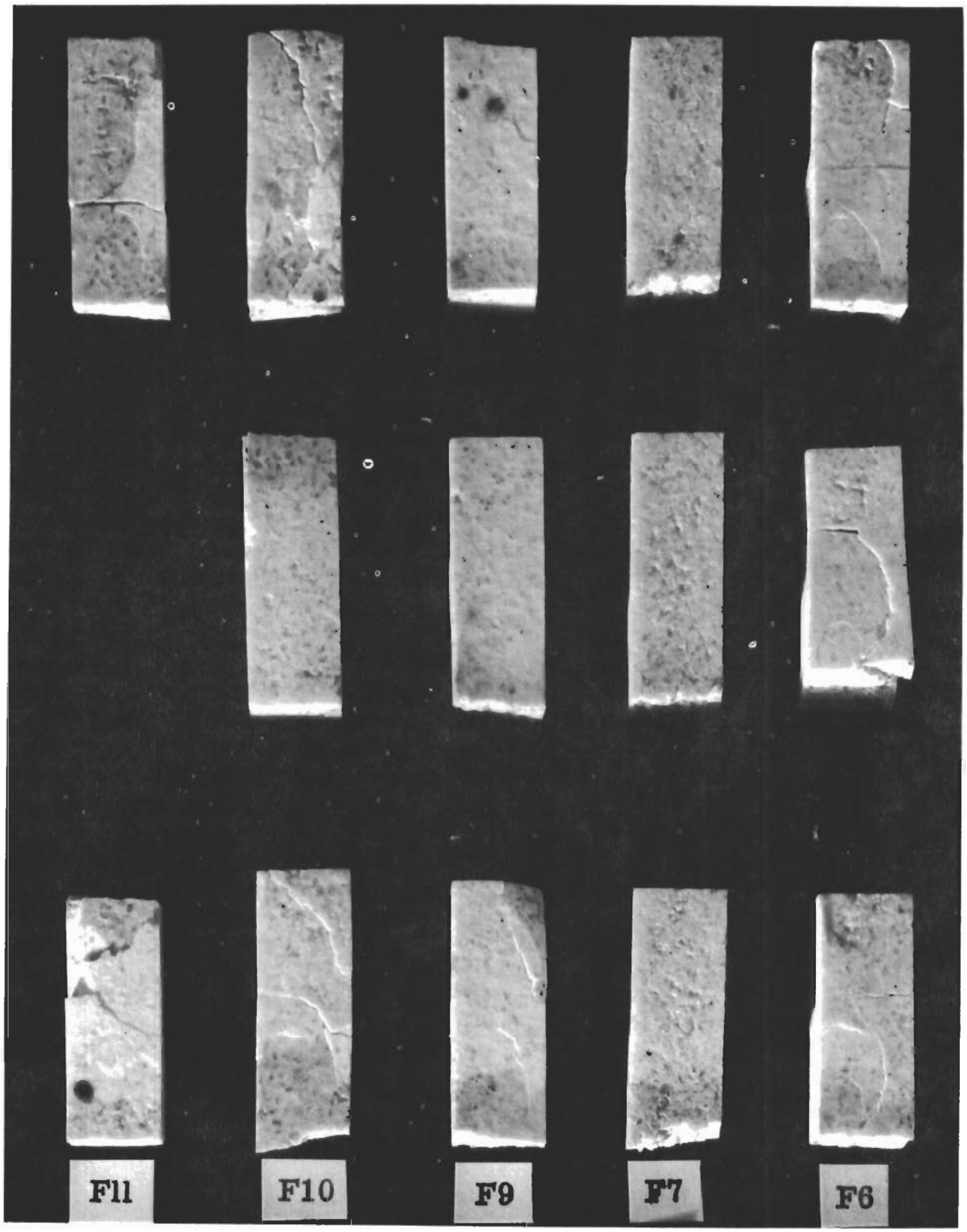

FIGURE 16

MAGNESIA 1/2" x 1/2" x 2" SAMPLES AFTER THERMAL SHOCK TEST

F-3, which failed the moment it was exposed to the torch, to sample F-7, which was unaffected by an exposure of 10 seconds at 4700°F.

Figures 17 through 23 are photographs of 2-inch-diameter and 1/4-inch-thick magnesia samples that were thermal shock tested in the single oxyacetylene torch facility. The single oxyacetylene torch was used to heat the sample surface from room temperature to 4100°F in 2 minutes. This temperature was maintained for 2 minutes. The torch was then removed and the sample permitted to cool. Mix 23 (Figure 17) zirconia had three cracks, formed during heating, that extended through the sample. F-12 (Figure 18) had one severe crack on the back that occurred during cooling.

F-14 (Figure 19) had excellent thermal shock resistance, and only a small hairline crack formed during cooling. F-15 and F-16 (Figures 20 and 21) contained large and small particles with no intermediate sizes. Both had poor thermal shock resistance.

Composition F-17 (Figure 22) contained microcracks produced during fabrication by omitting medium-sized particles (-20 + 100 mesh) and using only coarse and fine particles. The microcracks had no apparent effect on the thermal shock properties. F-18 (Figure 23) showed excellent thermal shock with no signs of cracking.

In the initial tests, Mix F-14 and Mix F-18 were found to have good thermal shock resistance. Thirteen additional compositions were fabricated with systematic variations in particle size distribution as shown in Table 5. All of these samples were inferior to compositions F-14 and F-18 in thermal shock resistance.

Erosion Resistance — The flame erosion of dense magnesia depends on the temperature and velocity of the impinging flame. The erosion observed under the plasma flame was not only more severe, but also of a different type than that produced by the oxyacetylene torch. In an oxyacetylene torch, at 250 Btu/ft^2-sec, the fine particles erode away leaving the coarse particles protruding above the surface. The plasma torch test, at 670 Btu/ft^2-sec, produces an equal erosion rate for all particles. In the former, the loss of material apparently is due to a softening and subsequent erosion of the fine particles. Subjecting the material to higher heat fluxes causes the surface material to vaporize before the heat has penetrated to a sufficient depth to weaken the bond of the surface particles. The low heat-flux erosion is largely controlled by thermal diffusivity and high heat-flux erosion rates by heats of vaporization.

Maximum Use Temperatures — The maximum use temperature can best be stated in terms of heat flux and time. The following data is based on the time required to penetrate a 1/4-inch thickness of magnesia with a plasma torch.

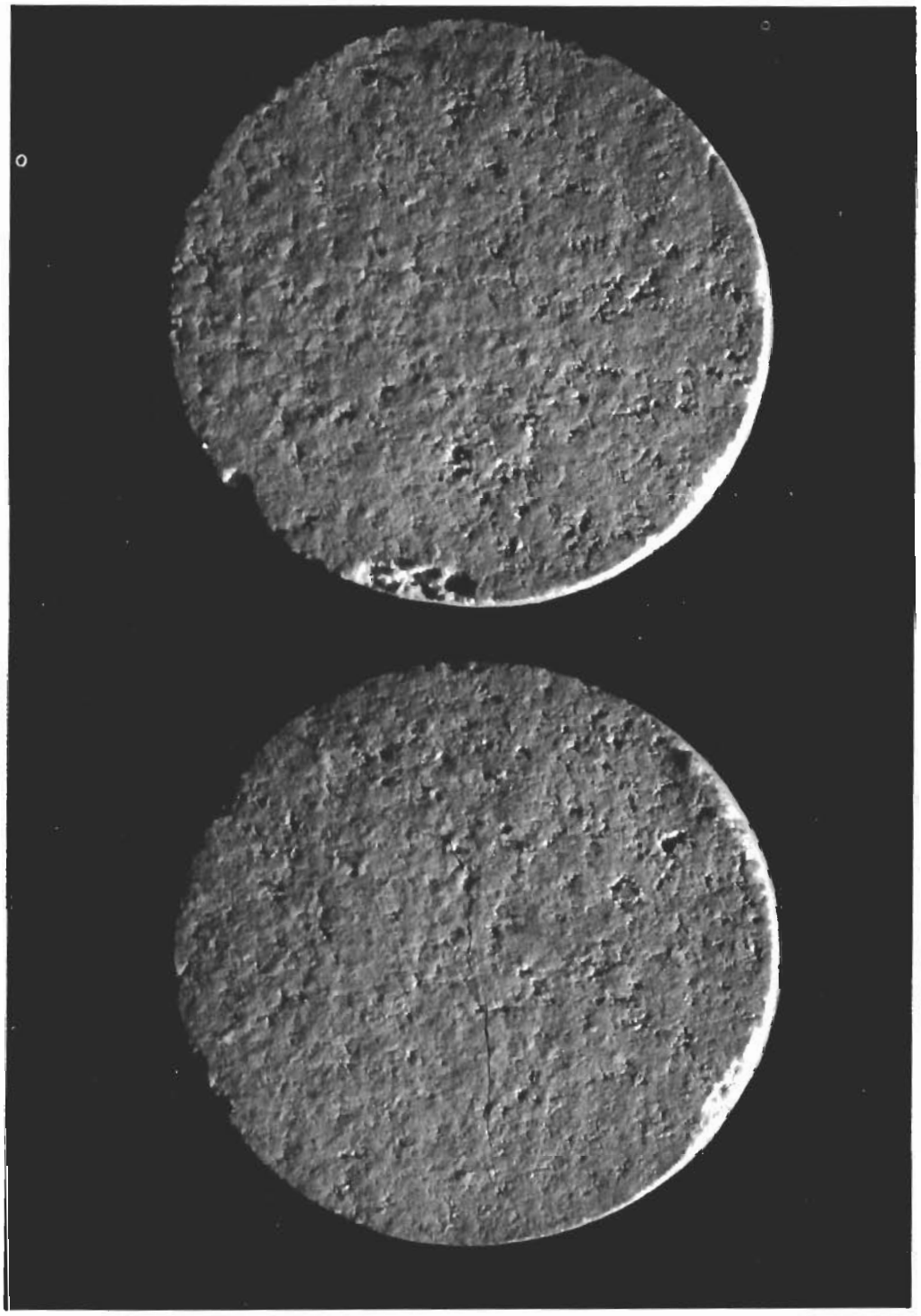

2" DIA. SPEC.

FIGURE 17

THERMAL SHOCK TESTED MIX 23 ZIRCONIA

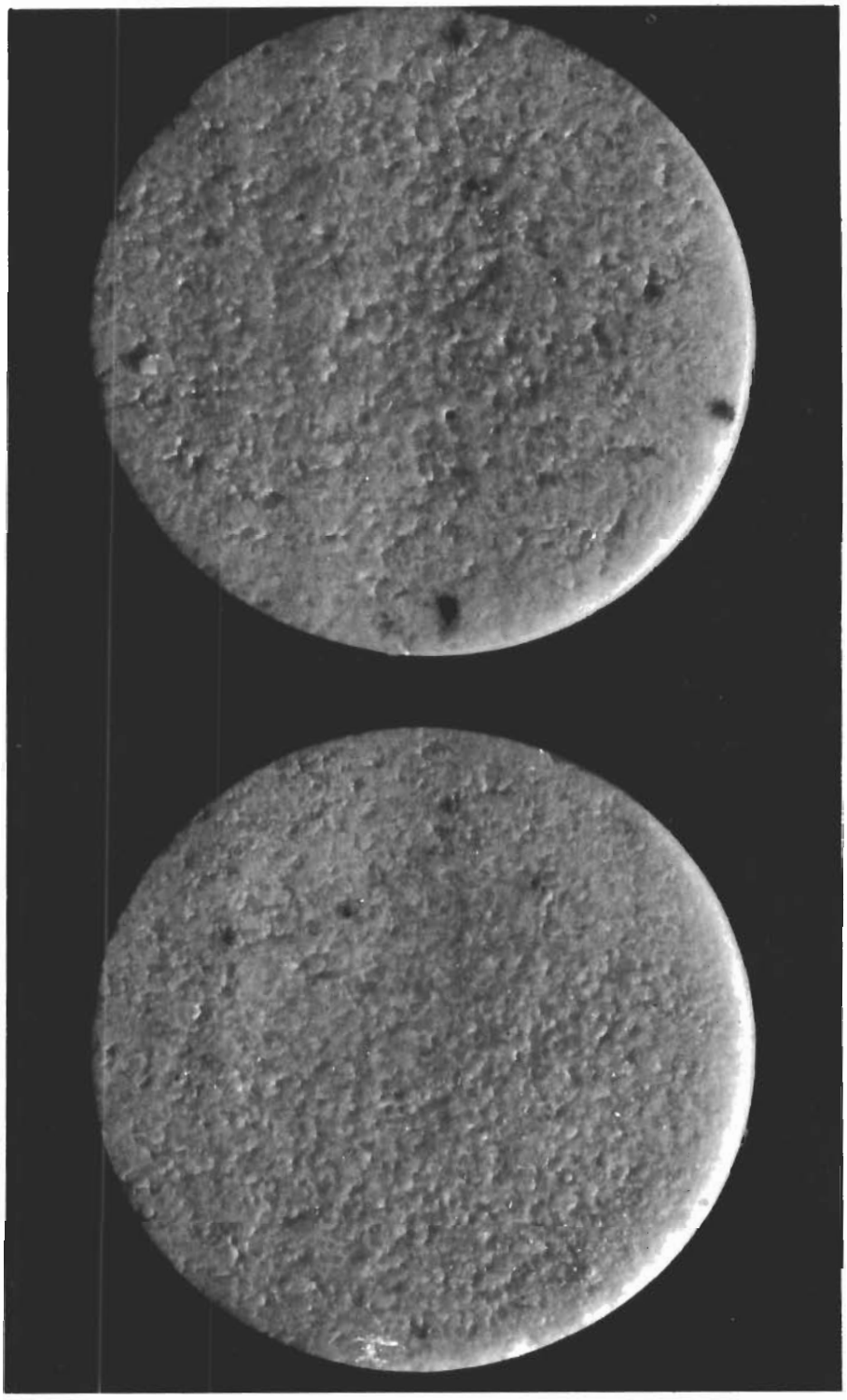

2" DIA. SPEC.

FIGURE 18

THERMAL SHOCK TESTED CONTROLLED PARTICLE SIZE MAGNESIA
COMP. F-12

2" DIA. SPEC.

FIGURE 19

THERMAL SHOCK TESTED CONTROLLED PARTICLE SIZE MAGNESIA
COMP. F-14

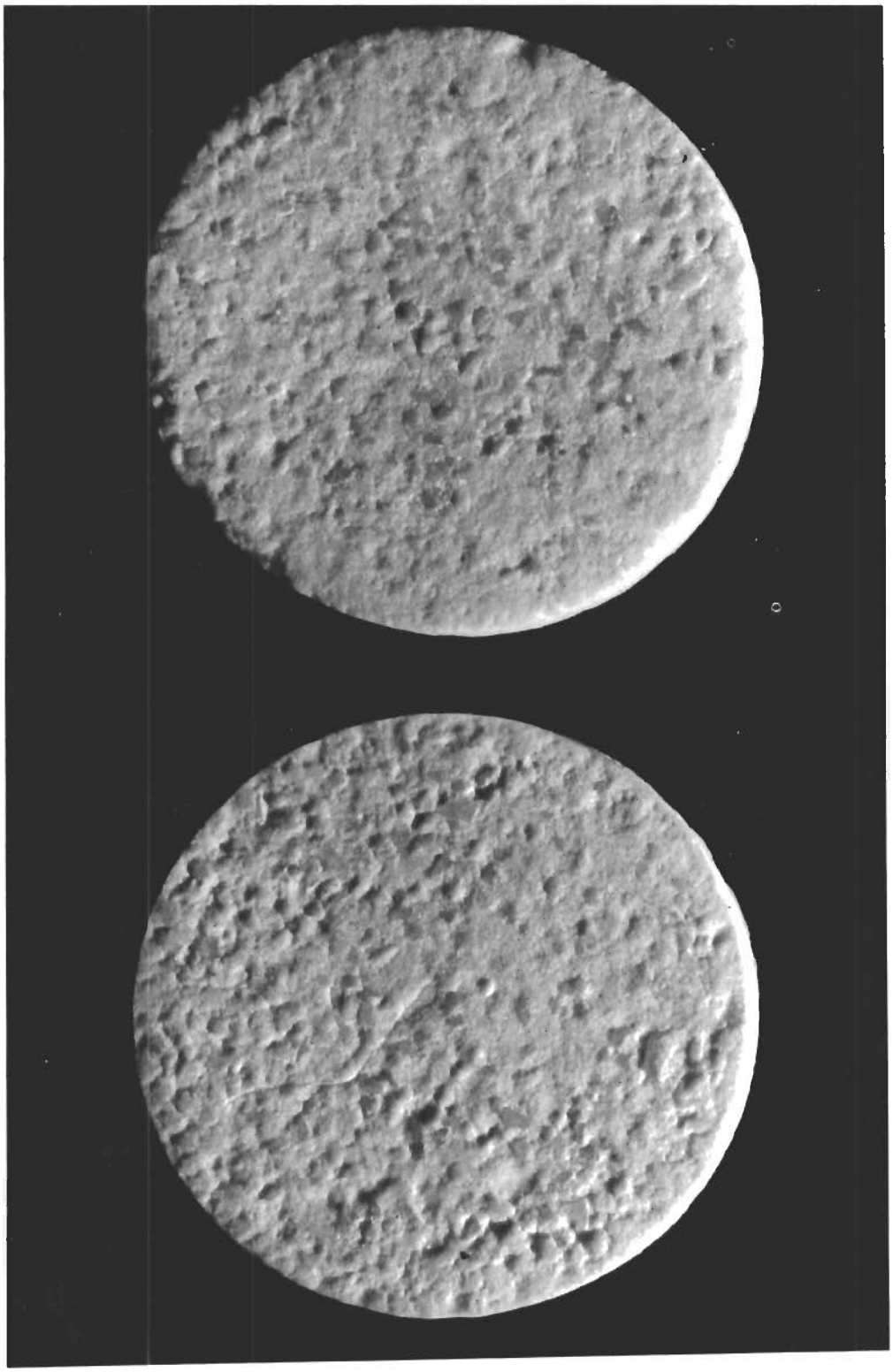

2" DIA. SPEC.

FIGURE 20

THERMAL SHOCK TESTED CONTROLLED PARTICLE SIZE MAGNESIA
COMP. F-20

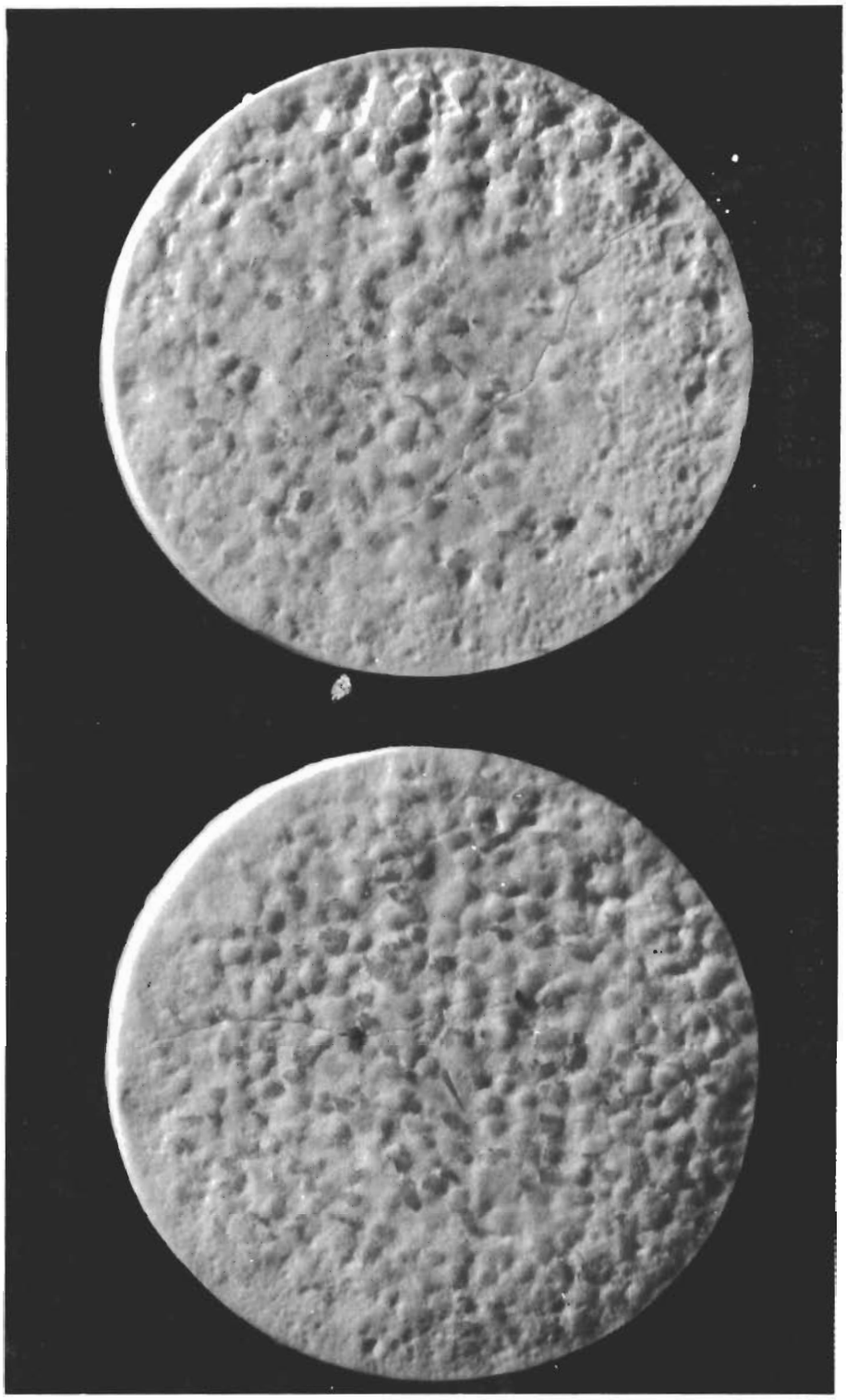

2" DIA. SPEC.

FIGURE 21

THERMAL SHOCK TESTED CONTROLLED PARTICLE SIZE MAGNESIA

COMP.F-16

2" DIA. SPEC.

FIGURE 22

THERMAL SHOCK TESTED CONTROLLED PARTICLE SIZE MAGNESIA

COMP. F-17

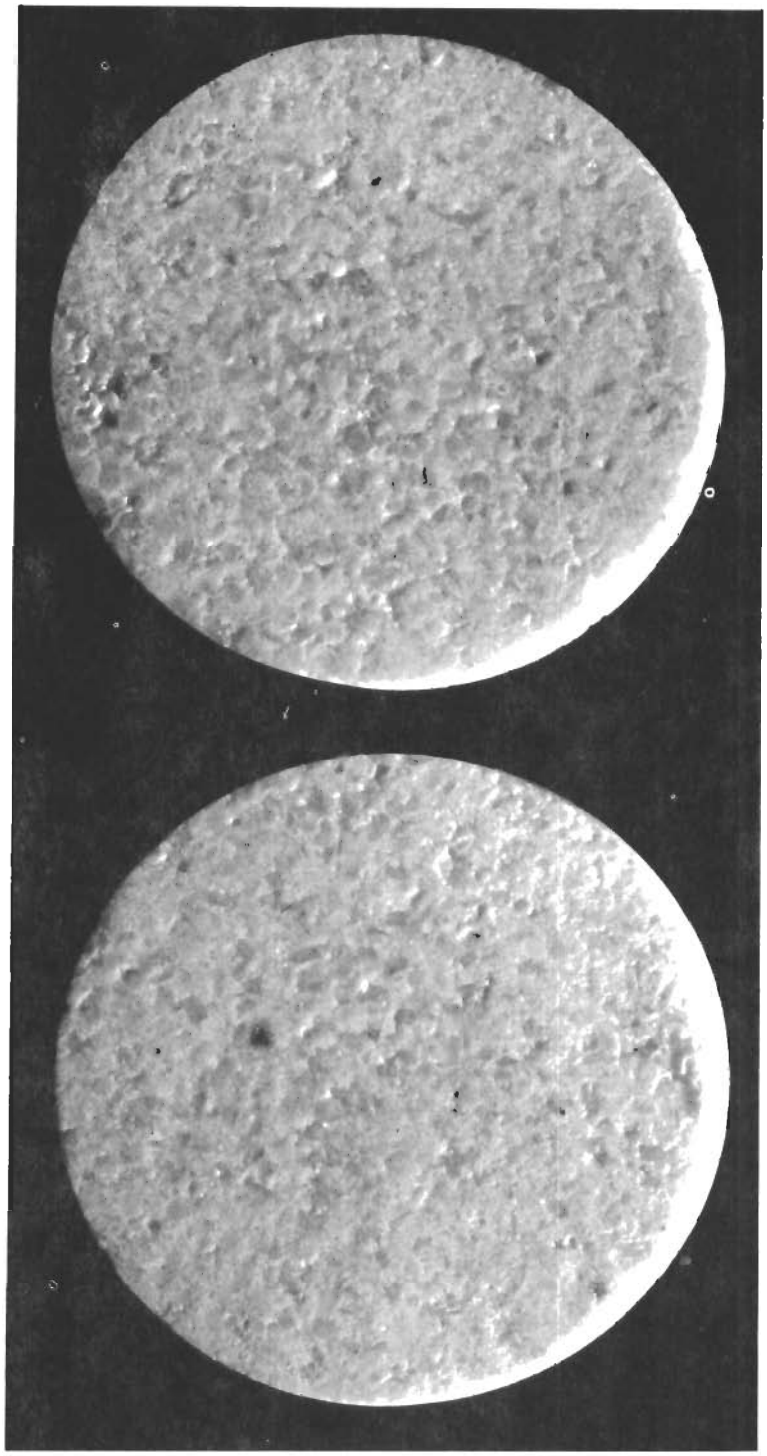

2" DIA. SPEC.

FIGURE 23

THERMAL SHOCK TESTED CONTROLLED PARTICLE SIZE MAGNESIA

COMP. F-18

Apparent Optical Temperature (°F)	Time (min)	Heat Flux Btu/ft^2-sec
4500	30-45	390
4850	5-8	670

Density — The average density for the magnesia body (F-14) submitted to ASD is 2.64 gm/cc or 164.5 lb/cu ft, ± 2 percent.

Thermal Expansion — The average coefficient of thermal expansion for Mix F-14, over a range of 70°F to 1800°F, is 6.16×10^{-6} in/in °F. Figures 24 and 25 are graphs of the thermal expansion of F-18 and F-14, respectively, over this range.

Insulation Properties — While testing magnesia for thermal shock resistance, the apparent optical temperature of the front face and the actual (thermocouple) temperature of the back face were recorded. This data was used to show the thermal gradient in a given thickness of material.

Figures 26 through 29 are graphs showing the hot- and cold-face temperatures of four typical magnesia bodies. The average temperature drop through magnesia was 1130°F. Figure 30 is a graph showing the hot- and cold-face temperatures of a Mix 23 zirconia specimen. The average temperature drop through Mix 23 zirconia was 1301°F.

The effect of oxide additives on the thermal drop and the emittance is discussed in Section VI.

Effect of Additives on the Emittance of Magnesia Bodies — One of the limitations in the use of either magnesia or thoria as a replacement for zirconia is their low emittance. This is illustrated graphically in Figure 31, which depicts the effects of the relative emittance of these materials on surface temperature while subjecting them to equivalent heat fluxes.

The effect of minor additives on emittance was investigated to determine if the emittance of a magnesia body could be increased to a value comparable to that of zirconia. The following compounds were tested as 2 percent additions to the magnesia body.

1) Nickel oxide
2) Chrome oxide
3) Iron oxide
4) Aluminum oxide
5) Cobalt oxide

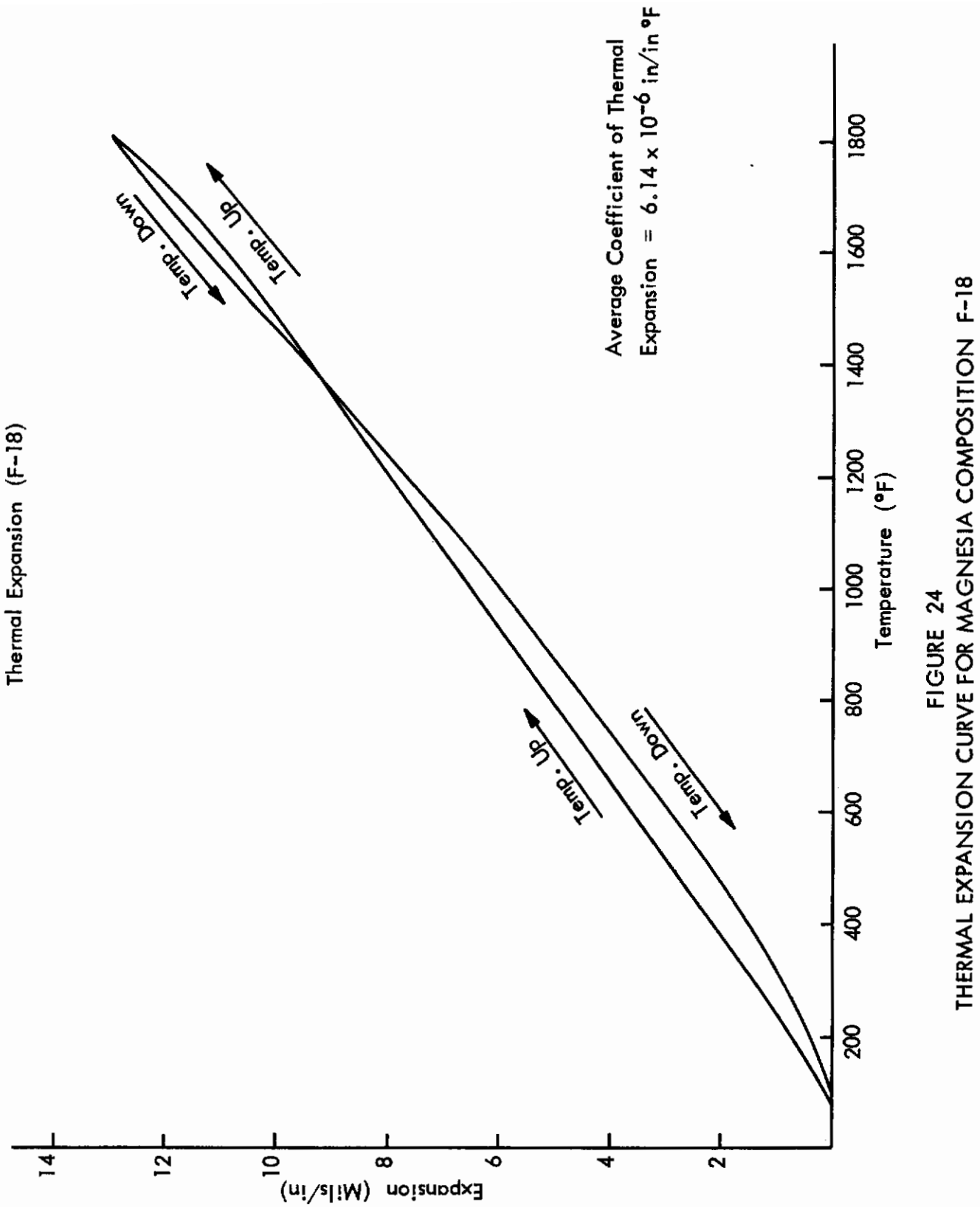

FIGURE 24
THERMAL EXPANSION CURVE FOR MAGNESIA COMPOSITION F-18

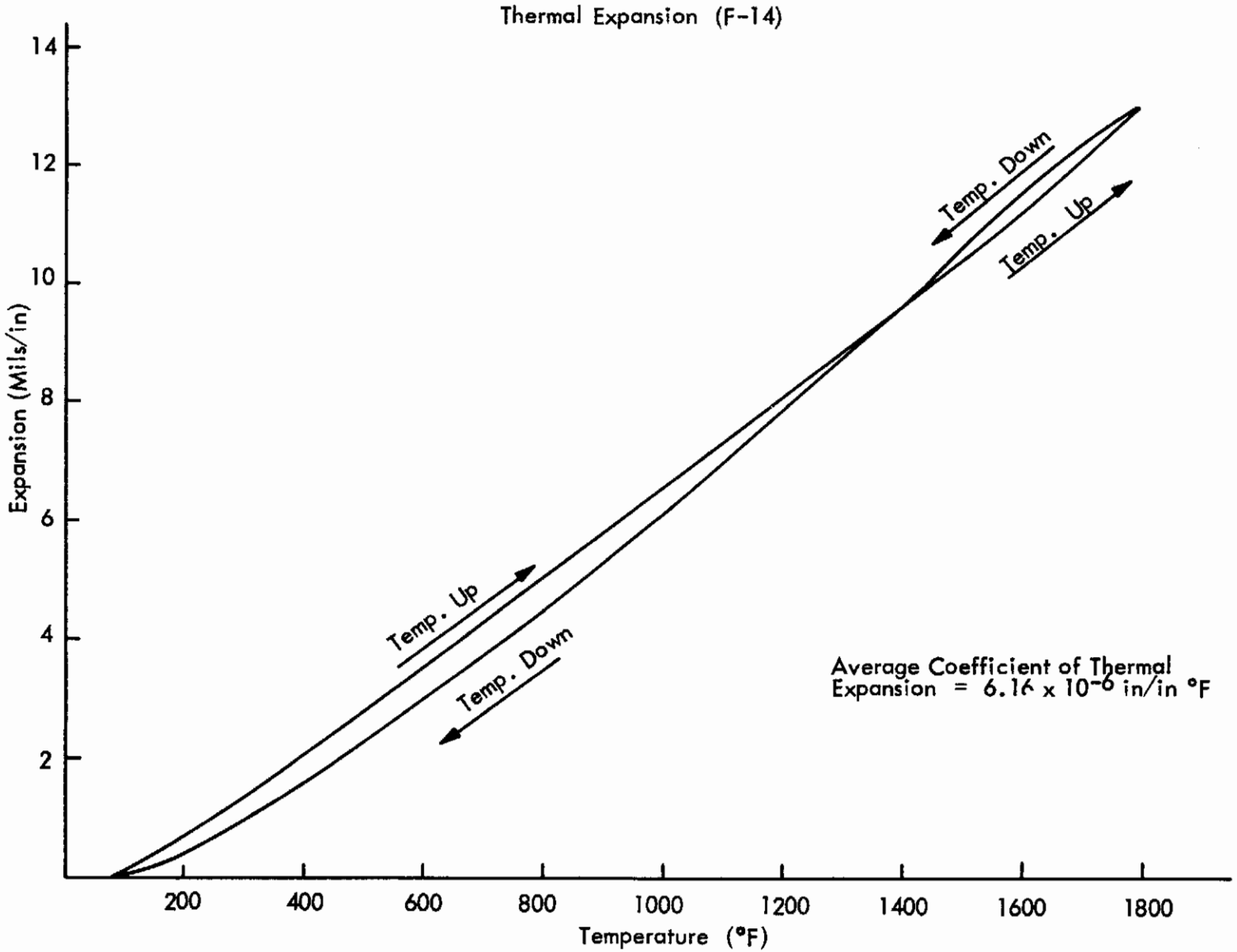

FIGURE 25
THERMAL EXPANSION CURVE FOR MAGNESIA COMPOSITION F-14

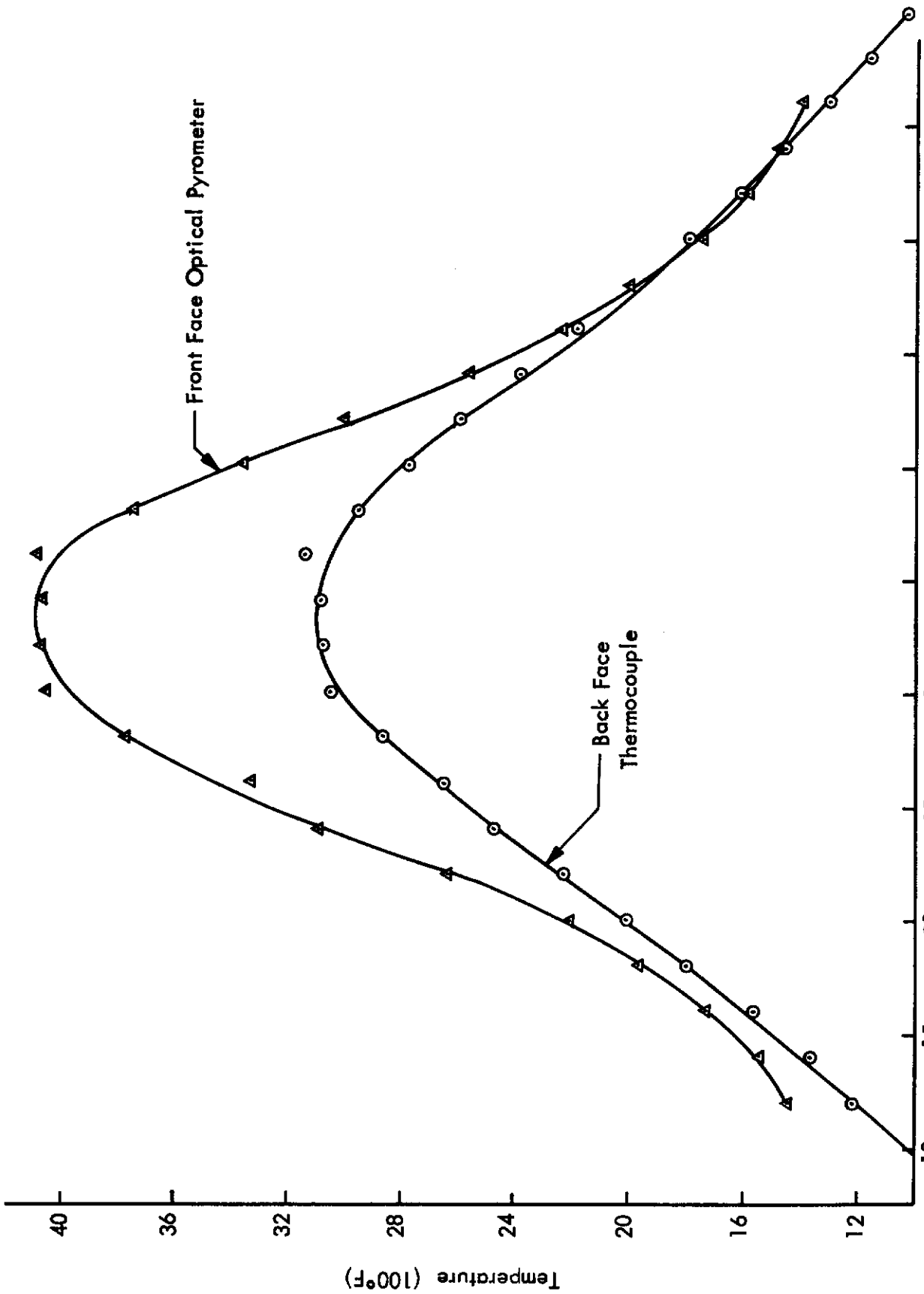

FIGURE 26

HOT AND COLD FACE TEMPERATURES FOR MAGNESIA COMPOSITION F-14 DURING TEST

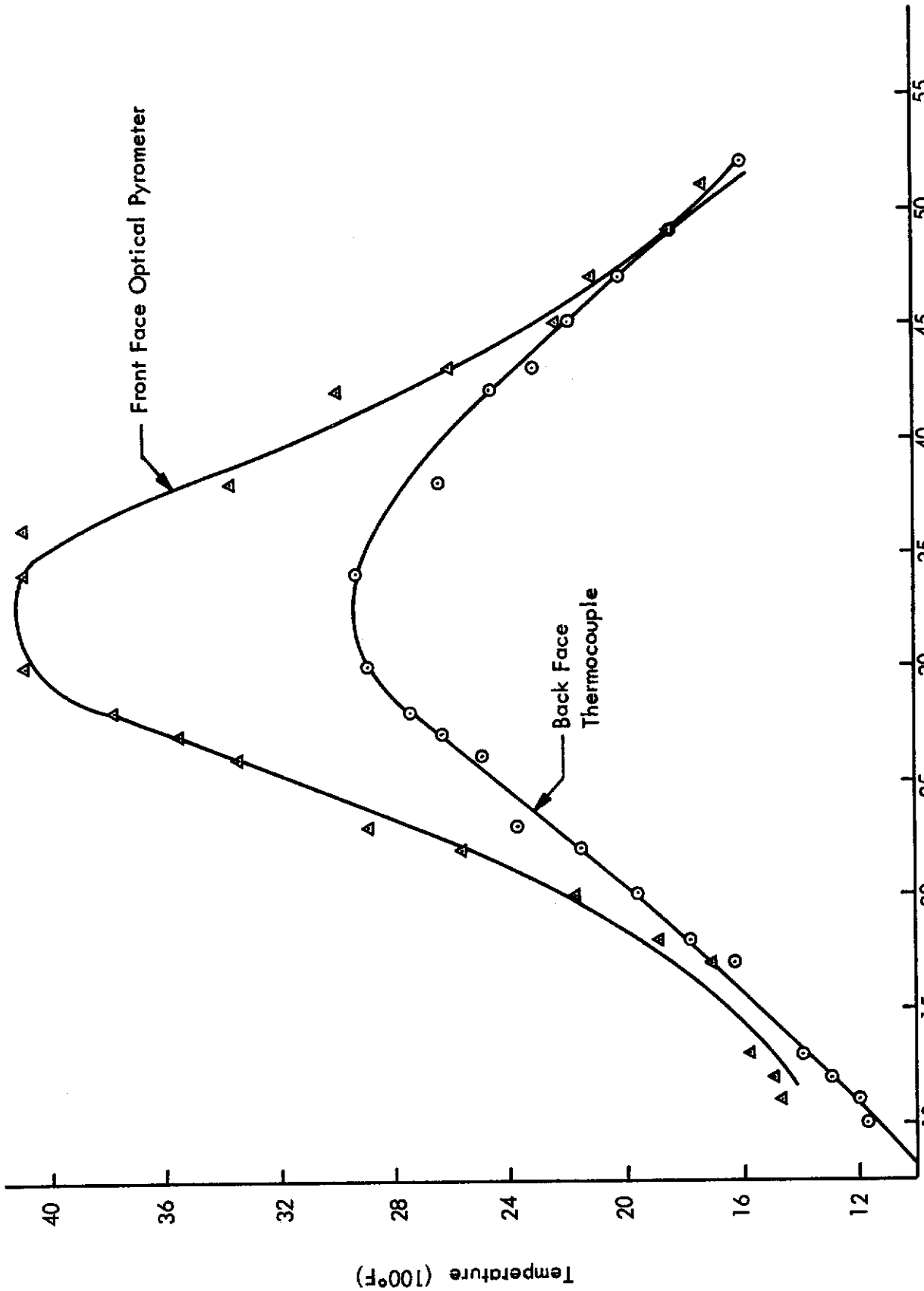

FIGURE 27

HOT AND COLD FACE TEMPERATURES FOR MAGNESIA COMPOSITION F-17 DURING TEST

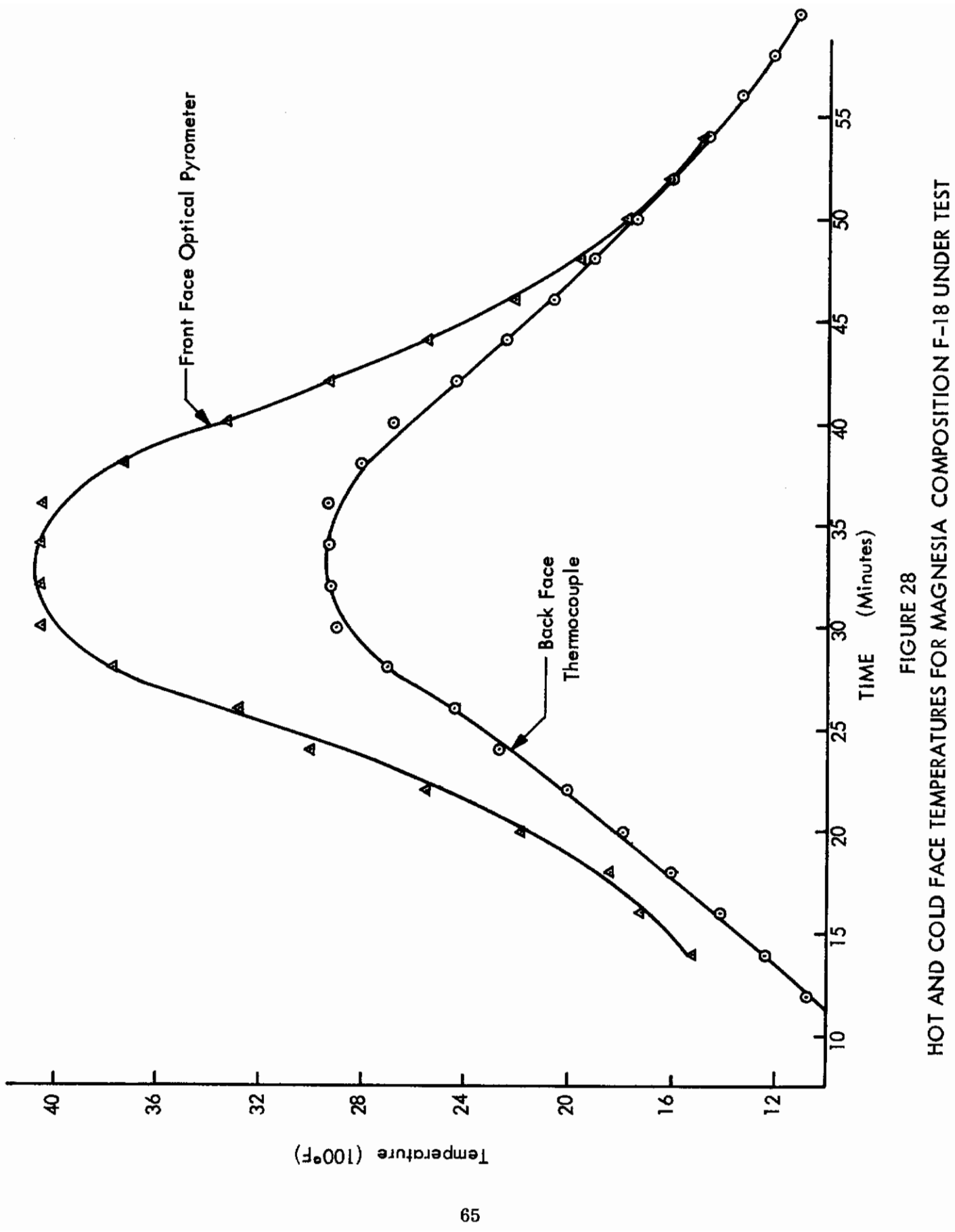

FIGURE 28

HOT AND COLD FACE TEMPERATURES FOR MAGNESIA COMPOSITION F-18 UNDER TEST

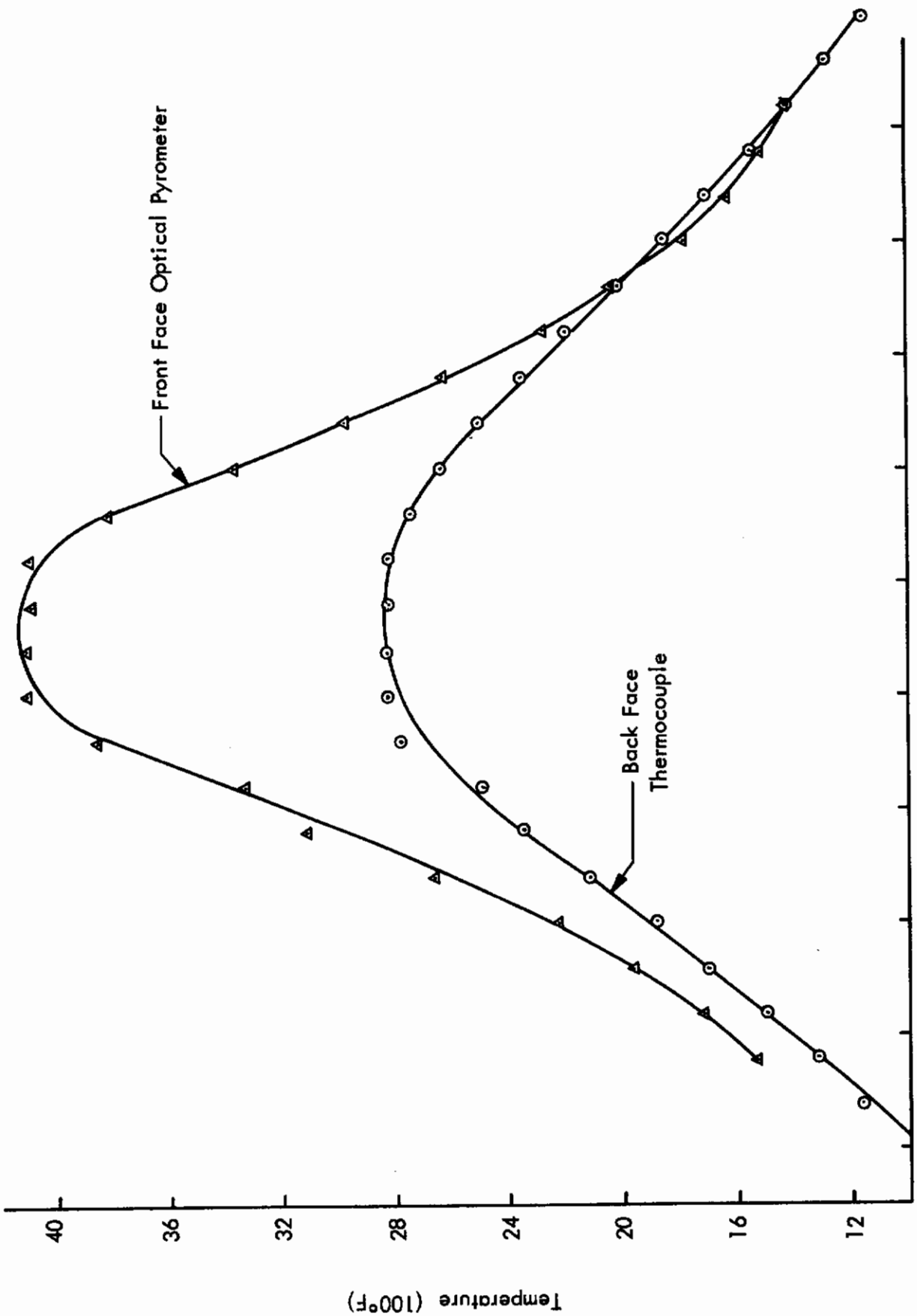

FIGURE 29

HOT AND COLD FACE TEMPERATURES FOR MAGNESIA COMPOSITION F-15 UNDER TEST

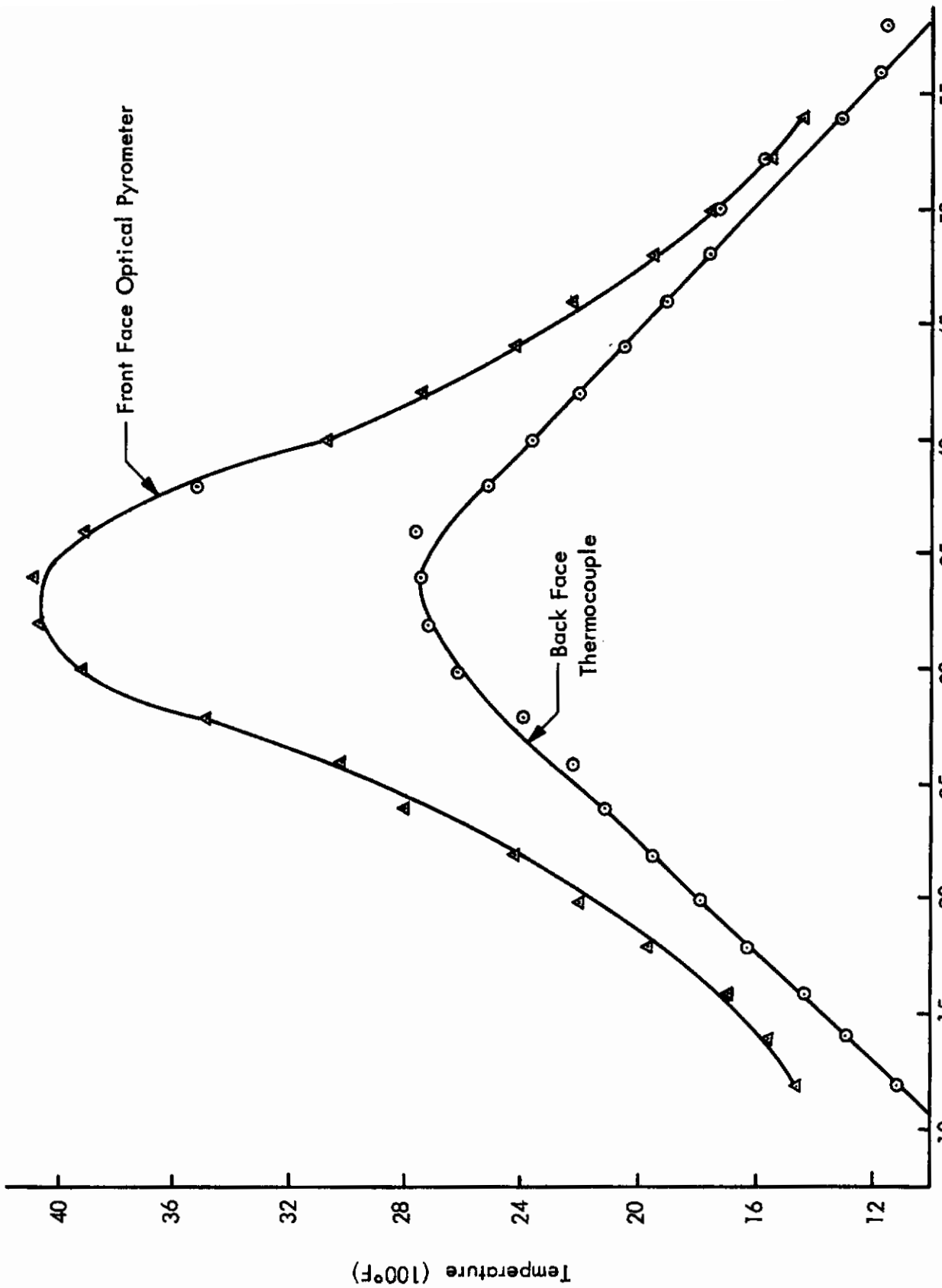

FIGURE 30
HOT AND COLD FACE TEMPERATURES FOR ZIRCONIA UNDER TEST

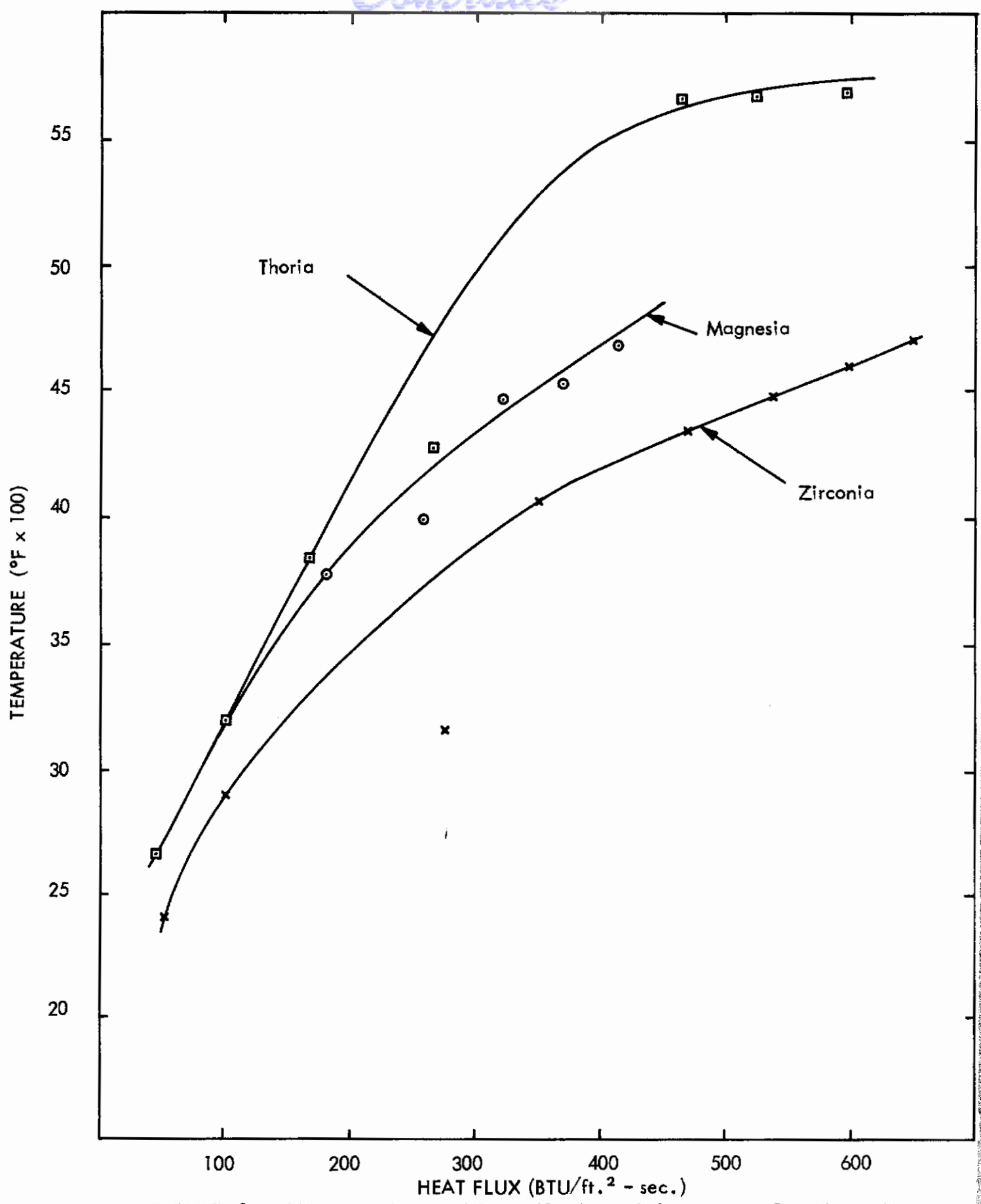

FIGURE 31. EQUILIBRIUM SURFACE TEMPERATURES OBSERVED FOR MAGNESIA, THORIA AND ZIRCONIA BODIES SUBJECTED TO EQUIVALENT HEAT FLUXES

The results of these tests are shown in Figures 32 through 34. Figure 35 shows the appearance of the samples after testing. The first two graphs are a plot of the cold-face temperature of the various 1/4-inch-thick samples versus the cold-wall heat flux on the exposed surface. In these tests, it was assumed that the thermal conductivity of all samples was unaffected by the presence of the additive. On this basis, the temperature of the back surface is an inverse function of emittance.

Cobalt oxide and nickel oxide were found to be the most effective additives for increasing emittance. However, they also tended to flux the magnesia body. Chrome oxide was somewhat less effective in increasing the emittance of the magnesia body, but the specimens prepared with this additive did not show an appreciable decrease in melting point.

Further comparison of the effect of emittance was made. Figure 33 shows the effect of emittance on the optical surface temperature of the chrome-oxide addition. Up to 3600°F, both chrome oxide and nickel oxide are equivalent. Above this temperature the effect of nickel oxide diminishes.

Some attempts were made to calculate the true emittance of the magnesia bodies based on data reported for zirconia. However, this necessitated a grey-body assumption for radiation and that heat transfer to both materials be identical. Because of the cumulative error encountered in applying both assumptions simultaneously, this effort was discontinued.

The appearance of the samples after testing is shown in Figure 35. A zirconia sample shown for comparison is badly eroded. The magnesia samples have been less affected by the test. The samples containing nickel and cobalt oxides are eroded through. In the remaining samples, the erosion was approximately 50 percent of the way through the 1/4-inch sample. This erosion occurred at the end point of the test.

The emittance of composition F-18 was measured in the thermal-radiation test facility. This data is reported in Table 7. Due to problems in radiation shielding, this test was limited to a maximum temperature of 2600°F. At this temperature an emittance of 0.32 was established. Olson and Morris (51) also report that the emmissivity of pure magnesia is 0.32 at 2600°F. However, Bradshaw and Matthews (52) report a considerably lower value of 0.22.

Impact Strength — The impact strength of several magnesia specimens was measured as shown in Table 6. Prior to these tests, F-14 and F-18 appeared to be equivalent. The difference in average impact strength between F-14 (0.32 ft/lb) and F-18 (0.19 ft/lb) was the basis for selecting composition F-14 for submission to ASD as the better of the two compositions.

Chemical Resistance — F-14 magnesia specimens were boiled for 8 hours in concentrated and dilute solutions of the following acids and bases to determine their stability.

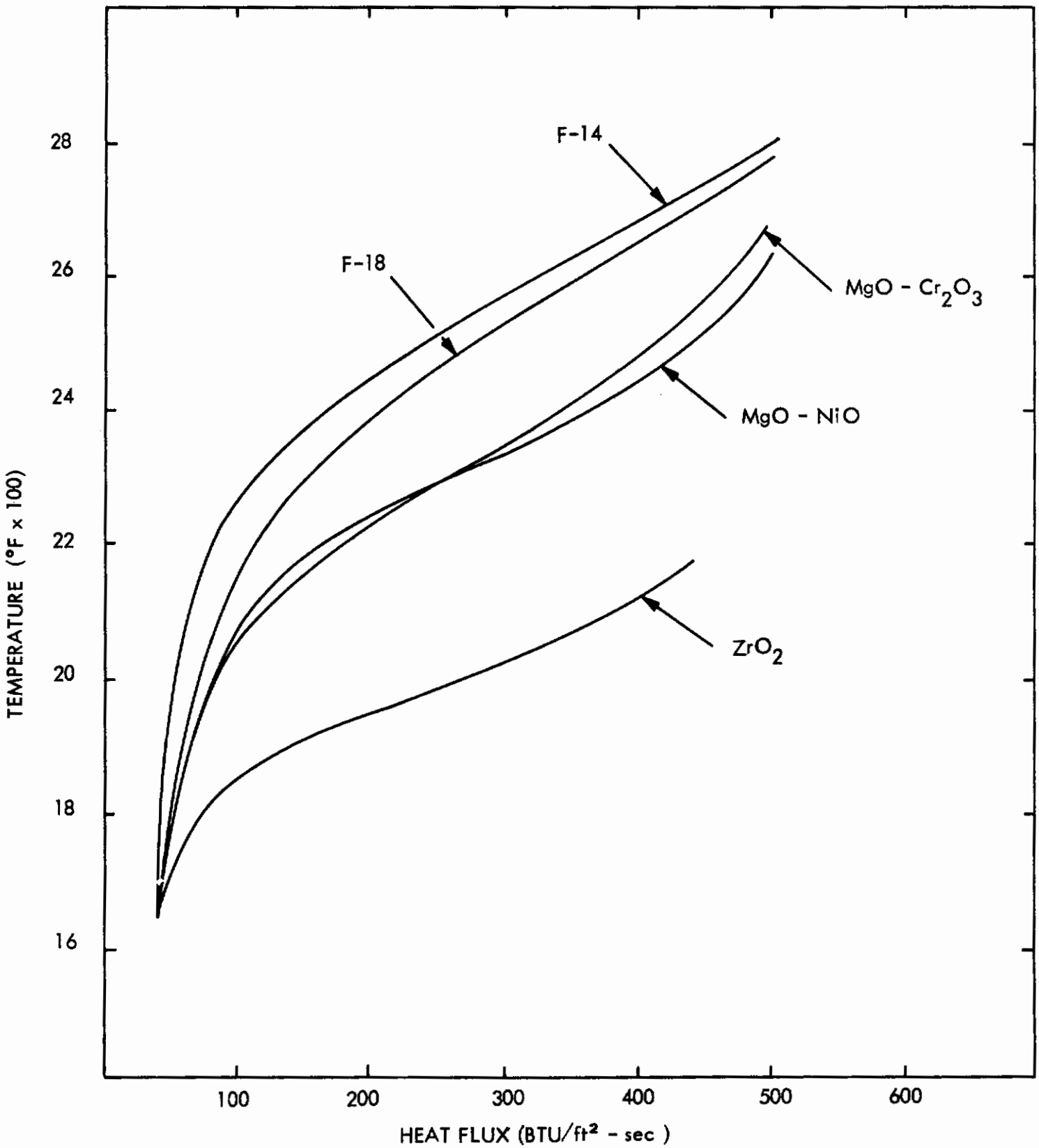

FIGURE 32 COLD FACE TEMPERATURES FOR MAGNESIA AND ZIRCONIA BODIES CONTAINING ADDITIVES EXPOSED TO EQUIVALENT HEAT FLUXES

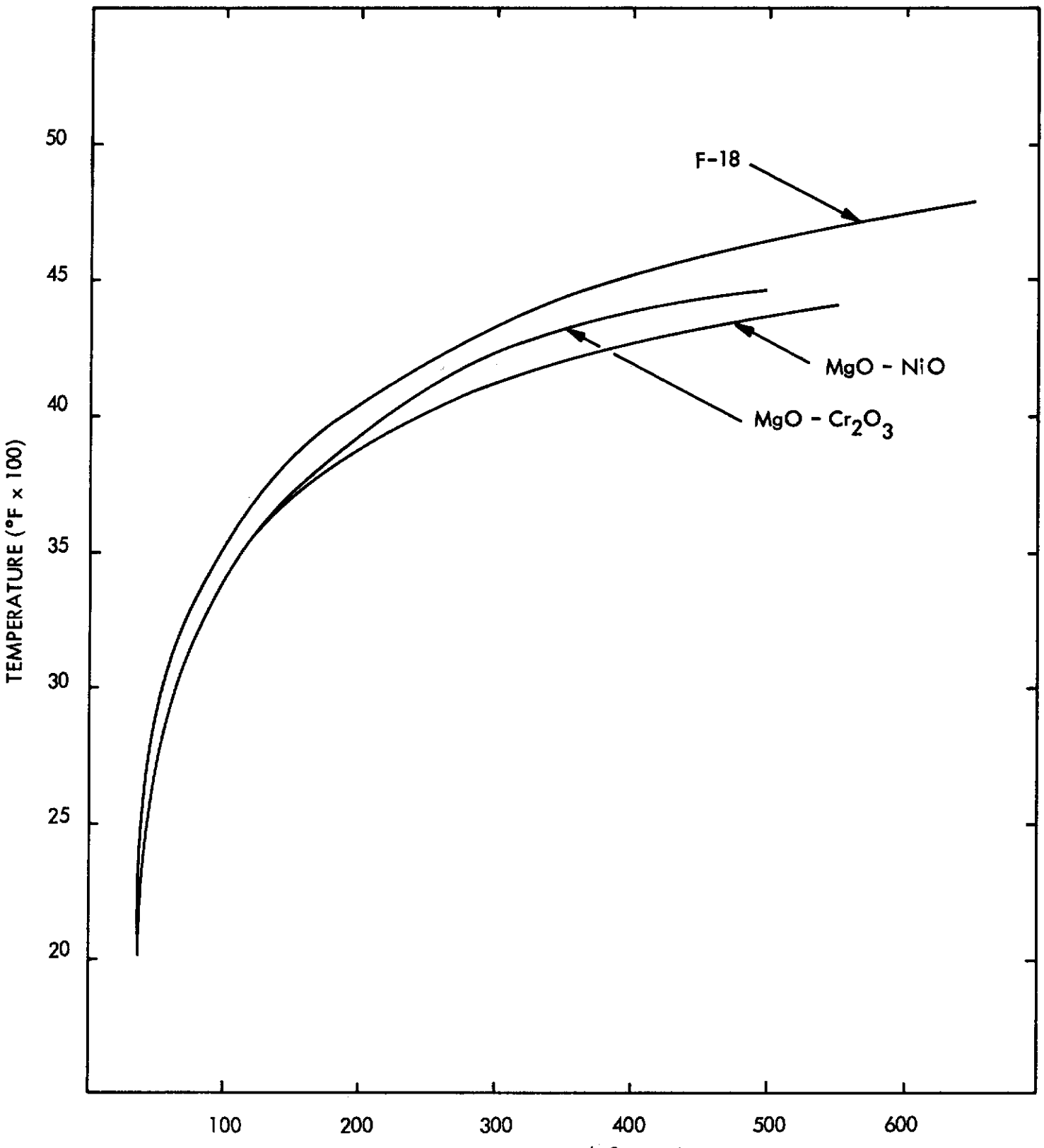

FIGURE 33 OBSERVED SURFACE TEMPERATURES FOR MAGNESIA BODIES EXPOSED TO EQUIVALENT HEAT FLUXES

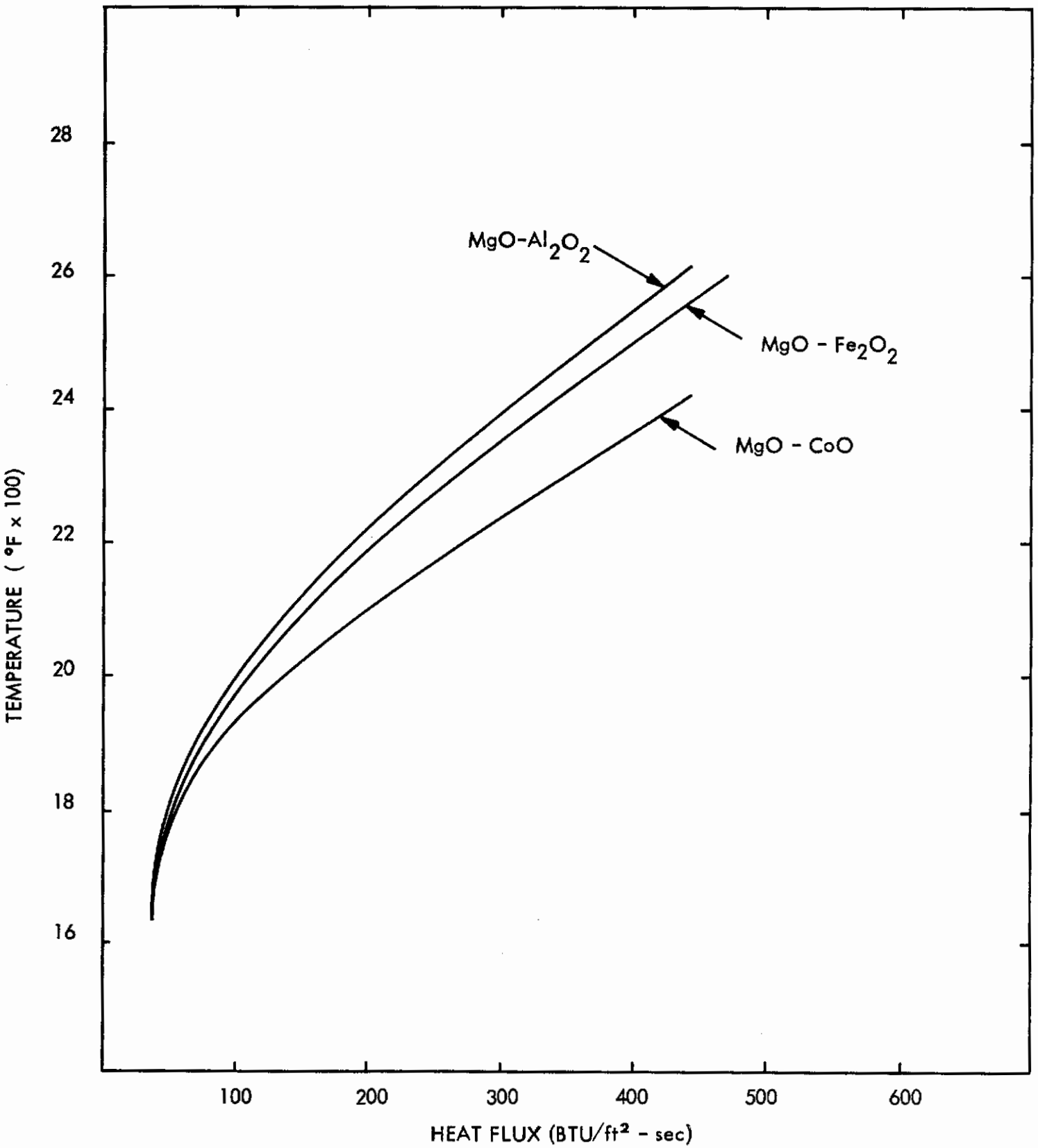

FIGURE 34 COLD FACE TEMPERATURES FOR MAGNESIA BODIES CONTAINING ADDITIVES EXPOSED TO EQUIVALENT HEAT FLUXES

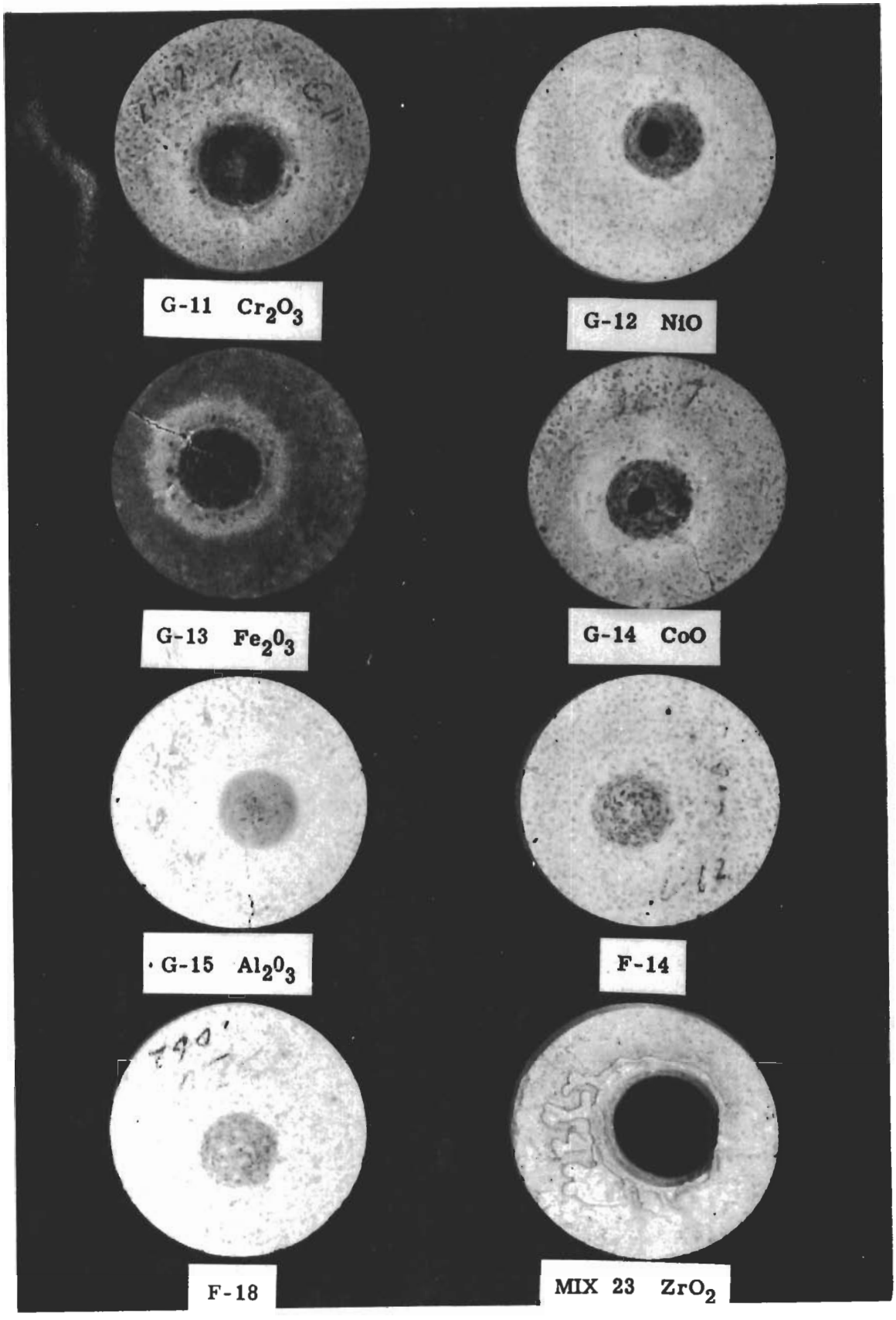

FIGURE 35 TESTING FOR COMPARATIVE EMITTANCE

TABLE 6

IMPACT STRENGTH OF SOME MAGNESIA BODIES

Code	Particle Size (Wt. %) -14 +20	-20 +28	-28 -65	-65 +100	-65 +200	-100 +200	-200 +325	-325	Mallinckrodt Reagent Grade Magnesium Oxide	Impact Strength* (ft-lbs)
F - 14	44.0			13.2			30.8	10.5	1.5	0.32
F - 18	45.0		20.0				20.0	13.5	1.5	0.19
F - 20	41.0			12.2			32.8	11.5	2.5	0.17
F - 21	46.0			14.2			29.8	9.0	1.0	0.27
F - 22	39.0			11.2			33.8	12.5	3.5	0.13
F - 23	58.0			16.2			27.8	7.0	1.0	0.13
F - 24	42			11.2		4.0	28.8	8.5	1.5	0.17
F - 25	43.0		19.0				19.0	15.5	3.5	0.22
F - 26	41.0		18.0				18.0	17.5	5.5	0.20
F - 27	47.0		21.0				21.0	10.0	1.0	0.22
F - 28	49.0		22.0				22.0	6.0	1.0	0.11
F - 29	43.0	2.0	18.0		6.0		18.0	11.5	1.5	0.26
F - 30	44.7			13.4			31.3	10.6		0.23
F - 31	44.5		16.6				25.4	12.0	1.5	0.42
F - 32	44.5			16.6			25.4	12.0	1.5	0.28

*Average of four specimens

TABLE 7

EMITTANCE OF COMPOSITION F - 18 (MAGNESIA)*

Temperature	Emittance
1950°F	0.38
2020°F	0.34
2084°F	0.34
2225°F	0.30
2240°F	0.30
2400°F	0.30
2600°F	0.32

*Measured on thermal radiation test facility
Figure 4

1) Hydrochloric acid
2) Phosphoric acid
3) Nitric acid
4) Sodium hydroxide
5) Ammonium hydroxide

The samples were slightly attacked by hydrochloric acid and phosphoric acid, and severely attacked by sodium hydroxide. The samples disintegrated in sodium hydroxide in less than 4 hours. The other reagents did not appreciably attack the test specimens.

Reaction with Zirconia and Thoria — The formation of eutectic compound limits the contact temperature between magnesia and zirconia or magnesia and thoria. The magnesia-zirconia eutectic temperature is 3600°F, and the magnesia-thoria eutectic temperature is 4000°F.

VI. CERAMIC FOAMS

Ceramic foams were developed for use with metal-ceramic composite structures. These foams are used as an insulating backing to protect the metal supporting structure from heat. To ensure compatibility with the magnesia-based composites, magnesia was selected for development into a ceramic foam. Since successful zirconia foams had previously been produced by chemical blowing and mechanical whipping, these methods were selected for use with magnesia.

Chemical Blowing — For this report, chemically blown foams are defined as those in which the pores in the ceramic body are produced by gas generated through a chemical reaction. A liquid suspension of the ceramic particles is prepared which has sufficient viscosity to retain the gas bubbles and preserve the porous structure until the liquid is removed through evaporation. The foams produced in this manner are closed-cell structures that show low permeability to gases and liquids. They also have relatively large pores in comparison with foams produced by other methods.

The best zirconia foams produced at Boeing by chemical blowing use the reaction between zirconium metal and phosphoric acid to generate the required gas. This combination is particularly satisfactory for zirconia in that the end product is a phosphate-bonded zirconia that does not contain any reaction products that would reduce the refractory properties of the foam.

An attempt was made to apply chemical blowing to magnesia foams. For these tests, compositions were prepared differing from the previously tested zirconia only in that magnesia was used in place of zirconia. The desirability of substituting magnesium for zirconium was considered. However, the proper ratio of liquid to ceramic to metal was known for use with zirconium, and the use of magnesium would have introduced an additional variable in the preliminary tests, which were intended to demonstrate only the feasibility of chemically blown magnesia foams. The following reagents were tested as reactants with the zirconium metal.

1) Hydrochloric acid
2) Hydrogen peroxide
3) Sodium carbonate
4) Phosphoric acid

Because the magnesia reacted vigorously with all of the foaming agents before they could be uniformly dispersed through the magnesia suspension, large, non-uniform cavities were created in the foam. Attempts to dilute the reactants sufficiently to retard the reaction rates gave suspensions that were too fluid to properly entrap the evolved gas. Due to time limitations, the development of chemically blown magnesia foams was discontinued.

Mechanically Whipped Foams — These foams are produced by entrapment of air in a liquid suspension of ceramic powder. The required air bubbles are generated by mechanical agitation (whipping) of the suspension, and surface active agents are added to stabilize the liquid foam. Inorganic binders are also used to provide adequate strength during drying and firing. Previous experience with zirconia had shown Glim* to be effective in controlling foaming action during whipping; hence, it was used for the magnesia foams. Plaster ($CaSO_4 \cdot 1/2H_2O$) was used to produce the required strength for drying and firing. This material was converted to calcium oxide during the firing operation and, in the amounts used, did not appreciably affect either the resistance to hydration or the refractory properties of the magnesia foams.

Whipping Procedure — The effect of variations in whipping speed and time was the first phase of investigation in producing mechanically whipped foams. Magnesia** was substituted for zirconia in a composition previously proven suitable. These samples were prepared using a Sunbeam No. 10 mixer. Three-hundred grams of the dry ingredients were placed in the mixer and agitated for 3 minutes to ensure uniform dispersion. The required amount of liquid was added and the foam whipped at the speeds and for the times shown in Table 8.

Immediately after whipping, the foam was poured into aluminum forms to produce 2-inch by 2-inch by 1-inch samples. The samples were allowed to set approximately 2 hours, at which time the forms were removed. These samples were then air dried for 24 hours and sectioned. Tests of strength and density were conducted after an additional 24-hour drying period. None of these samples were fired, since the objective was to establish the optimum whipping speed and time for foams with a uniform, small-pore size.

Figure 36 illustrates the effect of varying the whipping time on magnesia foams whipped at 780 rpm. The increase in whipping time tends to increase average pore size. This is attributed to the coalescence of the small voids with time.

The samples shown in Figure 37 have been whipped for similar times at 660 rpm. These foams behave in a manner similar to those previously prepared, except that the maximum number of small voids appears at the end of 1 minute rather than 1/2 minute as was the case when the samples were whipped at higher speeds. For samples whipped at 555 rpm (Figure 38) the results were similar, with a whipping time of 4 minutes being required to produce a satisfactory size and distribution of pores.

Attempts to produce foams at lower whipping speeds were unsatisfactory (Figure 39) because the plaster "set up" before adequate foaming action occurred.

---

* 82-1/2 percent alkylphenyl polyglycol ether; B. T. Babbitt, Inc., 386 4th Ave., New York 16, New York.

**Magnorite, 22°F; Norton Company, Worchester, Massachusetts.

TABLE 8

EFFECTS OF WHIPPING SPEED AND TIME ON MAGNESIA FOAMS

Code	Speed (rpm)	Whipping** Time (min)	Unfired Density (gm/cc)	Unfired Compressive Strength (psi)	Comments
M-1	780	0.5	0.8	160.5	Very few pores
M-2	780	1.0	0.81	119.5	Non-uniform pore size
M-3	780	2.0	0.63	64.9	Non-uniform pore size
M-4	780	4.0	0.27		Plaster settled out
M-5	660	0.5	1.15	193.8	Very few pores
M-6	660	1.0	1.02	180.3	Non-uniform pore size
M-7	660	2.0	0.69	96.3	Uniform small pores
M-8	660	4.0	0.43	14.0	Plaster settled out
M-9	555	0.5	1.29	262.2	Insufficient time for foaming
M-10	555	1.0	1.22	237.1	Partially foamed
M-11	555	2.0	1.02	171.3	Non-uniform pore size
M-12	555	4.0	0.73	103.4	Uniform small pores
M-13	430	0.5	1.57	391.5	Speed insufficient to produce foaming
M-14	430	1.0	1.40	458.8	Speed insufficient to produce foaming

TABLE 8 (cont'd)

EFFECTS OF WHIPPING SPEED AND TIME ON MAGNESIA FOAMS*

Code	Speed (rpm)	Whipping** Time (min)	Unfired Density (gm/cc)	Unfired Compressive Strength (psi)	Comments
M-15	430	2.0	1.22	399.4	Speed insufficient to produce foaming
M-16	430	4.0	1.08	190.9	Speed insufficient to produce foaming

*COMPOSITION (All samples air dried for 24 hours)
63.2% -100 mesh fused magnesia (General Electric)
10.1% K-62 Plaster
25.0% Water
1.7% Glim Detergent
**Sunbeam No. 10 Mixmaster

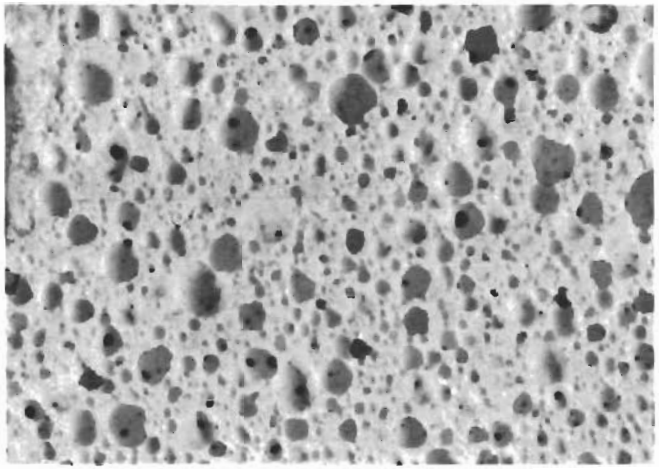

1/2 Minute

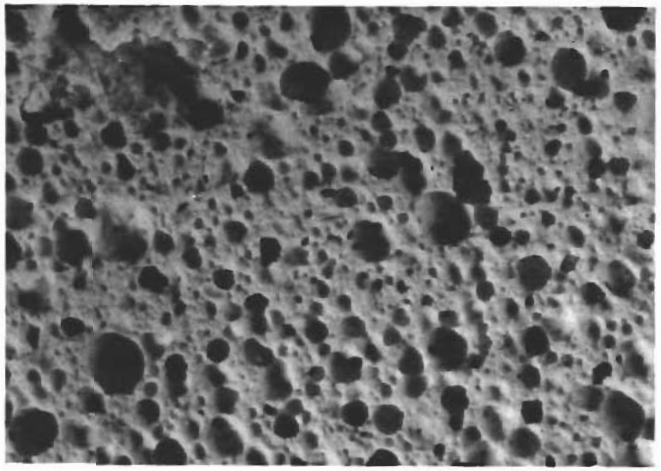

1 Minute

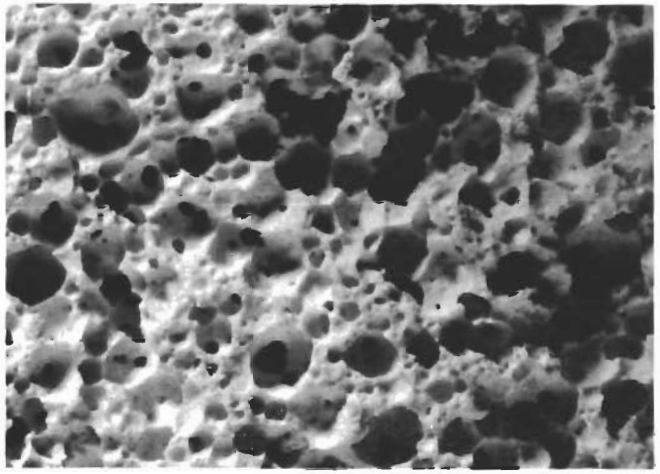

2 Minutes

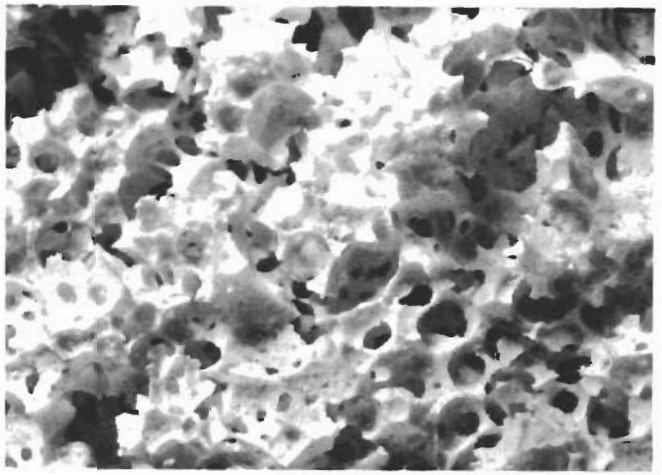

4 Minutes

FIGURE 36 CROSS SECTION OF FOAMS WHIPPED AT 780 RPM - MAGNIFIED 25X

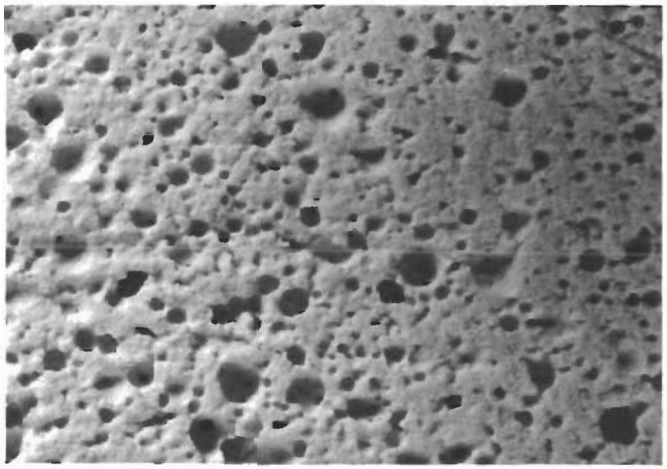

1/2 Minute

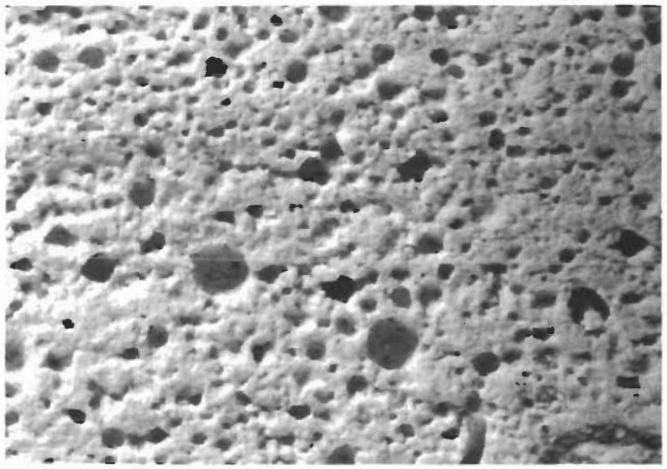

1 Minute

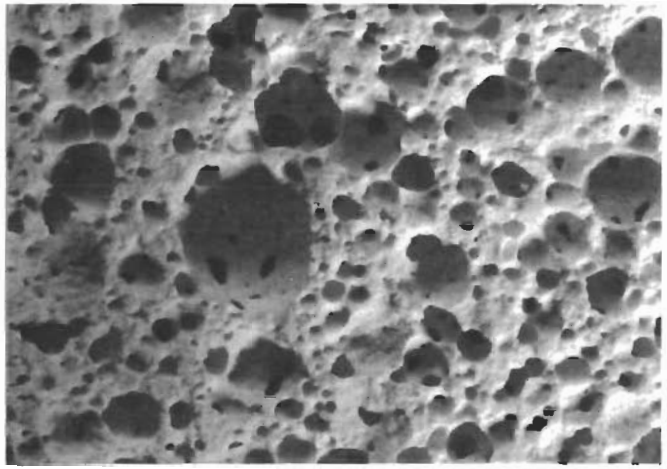

2 Minutes

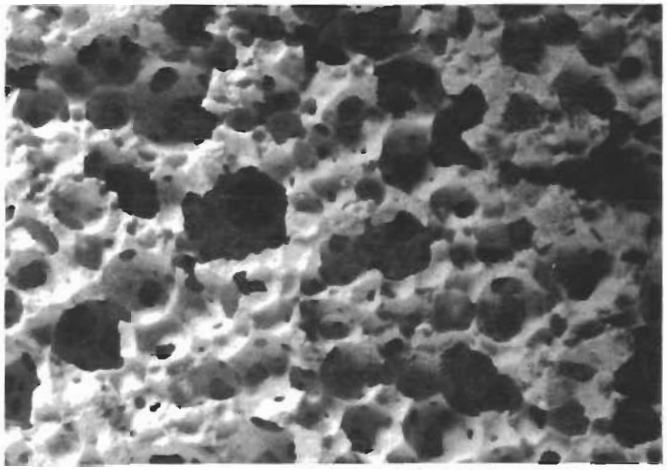

4 Minutes

FIGURE 37 CROSS SECTION OF FOAMS WHIPPED AT 660 RPM - MAGNIFIED 25X

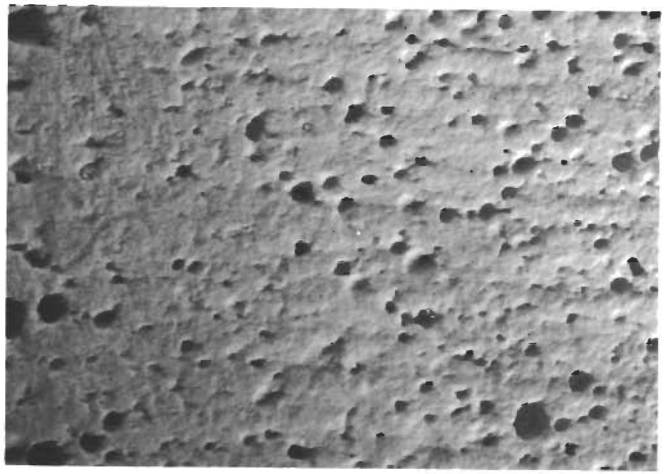

1/2 Minute

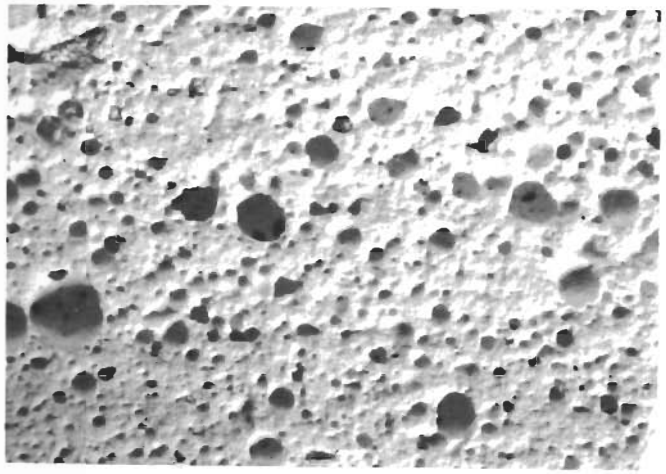

1 Minute

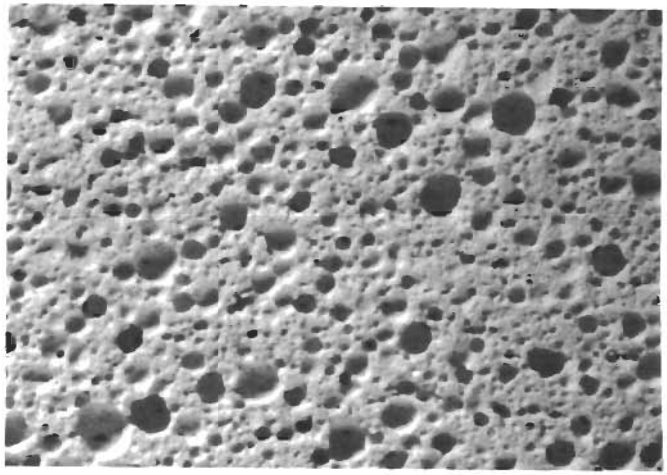

2 Minutes

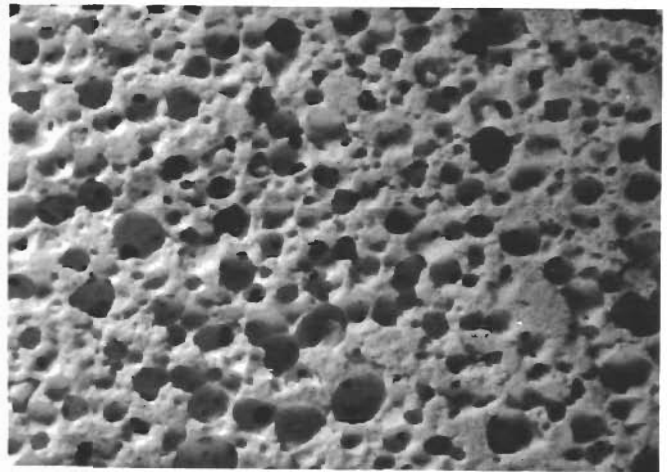

4 Minutes

FIGURE 38 CROSS SECTION OF FOAMS WHIPPED AT 555 RPM - MAGNIFIED 25X

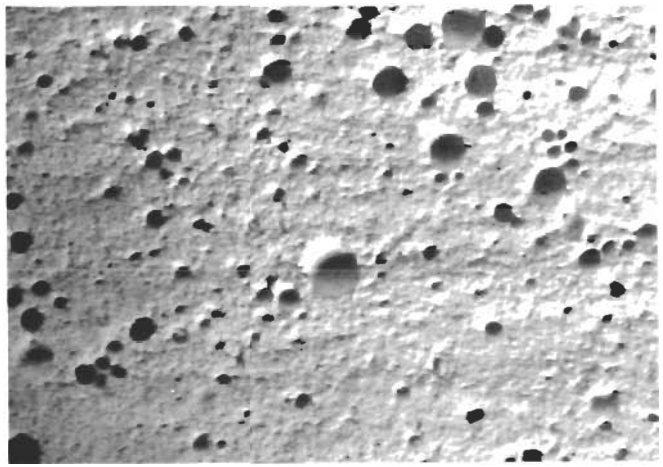

1/2 Minute

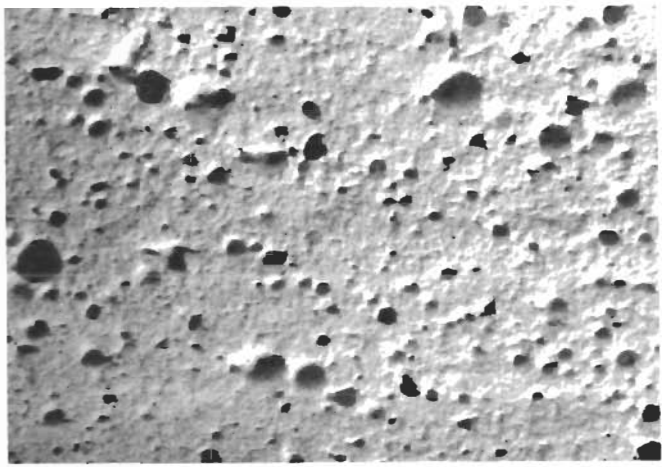

1 Minute

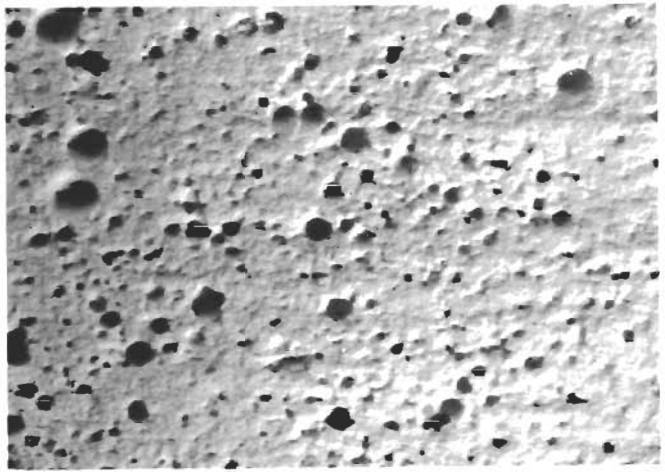

2 Minutes

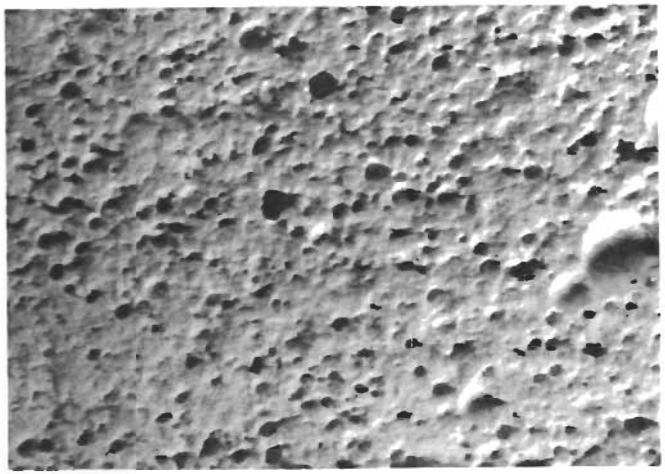

4 Minutes

FIGURE 39 CROSS SECTION OF FOAMS WHIPPED AT 430 RPM - MAGNIFIED 25X

From these tests, compositions M-12 and M-7 were selected for further development. The former being whipped 4 minutes at 555 rpm and the latter for 2 minutes at 660 rpm.

Effect of Liquid Content — The effect of varying the liquid content of the ceramic foam compositions was determined using the whipping speeds and times previously established for compositions M-7 and M-12. The liquid content of compositions was varied from 20.3 percent to 31.2 percent, as shown in Table 9 and Figures 40 through 43.

At 660 rpm, 25-percent water produced a foam with good strength properties and suitable pore size. Less water produced insufficient foaming action; increasing the water content produced materials that were weak and possessed large, nonuniform pores.

At the lower speed (555 rpm), 26.9-percent liquid content produced a comparable material. Generally, it was found that less liquid content was required at the higher whipping speeds and that by varying the liquid content, equivalent foams could be prepared at either speed.

Preparation of Large Foam Samples — For this program, it was necessary that large pieces of foam be prepared. Since the Sunbeam mixer used previously was limited to a maximum sample weight of 300 gms, new samples were prepared using a Hobart Model K5-M mixer and 2660 gram samples. These samples are tabulated in Table 10.

By visual comparison of the samples prior to firing, it was found that composition M-44, containing 27.9-percent water, was essentially the same as the previously prepared M-7 composition in pore size. Since it was intended that these samples would be fired, no additional tests were conducted on the unfired samples.

Sintering of Foam Samples — The samples prepared in the Hobart mixer were sintered at the times and temperatures shown in Table 10. After firing, all of the samples were sectioned and examined visually. These sections were then tested for compressive strength and density. This examination showed that sintering for 6 hours did not produce uniform sintering throughout the material. This was evidenced by a soft core in the center of the sample. Four additional samples were prepared and sintered for 22 hours. This lengthened sintering cycle proved adequate to ensure a uniformly sintered body, but did not appreciably alter the density.

Comparision of samples M-44 and M-52 showed them to have essentially the same density, although the sintering time varied from 6 hours to 22 hours. The density of the other samples varied from a high of 1.8 gms/cc to a low of 0.65 gms/cc. Generally, increasing the water content reduced the density.

TABLE 9

EFFECTS OF LIQUID CONTENT ON MAGNESIA FOAMS

Code*	Speed (rpm)	Whipping*** Time (min)	Liquid** (%)	Unfired Density (gm/cc)	Unfired Compressive Strength (psi)	Comments
M - 17	660	2	20.3	1.25	530.4	No foaming occurred
M - 18	660	2	22.1	1.28	588.0	No foaming occurred
M - 19	660	2	23.8	1.20	348.0	Foaming commenced
M - 20	660	2	25.4	0.95	163.0	Uniform foaming
M - 21	660	2	26.9	0.51	31.2	Uniform foaming
M - 22	660	2	28.4	0.35		Excessive pore size
M - 23	660	2	29.8	0.27		Excessive pore size
M - 24	660	2	31.2	0.25		Excessive pore size
M - 25	555	4	20.3	1.60	475.2	Nofoaming occurred
M - 26	555	4	22.1	1.22	495.6	No foaming occurred
M - 27	555	4	23.8	1.19	306.0	Foaming commenced
M - 28	555	4	25.4	1.05	213.6	Uniform foaming
M - 29	555	4	26.9	0.87	123.6	Uniform foaming
M - 30	555	4	28.4	0.48	26.4	Excessive pore size

TABLE 9 (cont'd)

EFFECTS OF LIQUID CONTENT ON MAGNESIA FOAMS

Code	Speed (rpm)	Whipping*** Time (min)	Liquid** (%)	Unfired Density (gm/cc)	Unfired Compressive Strenght (psi)	Comments
M-31	555	4	29.8	0.31		Excessive pore size
M-32	555	4	31.2	0.33		Excessive pore size

*Solid portion consisted of 300 grams of -100 mesh fused magnesia and 56 grams of K -62 plaster
** 94% water 6% Glim
*** Sunbeam No. 10 Mixmaster

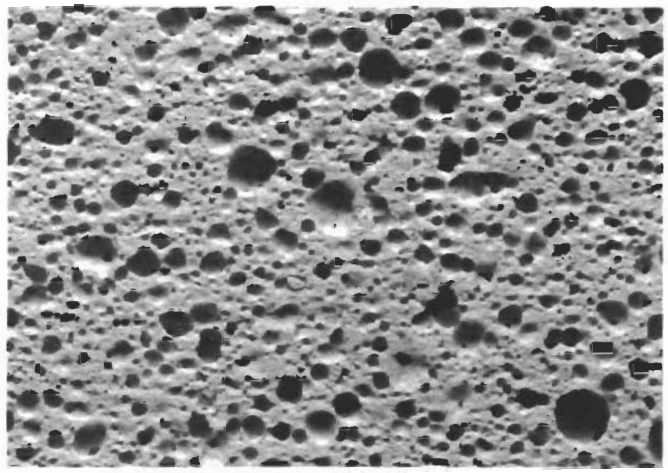

20.3%

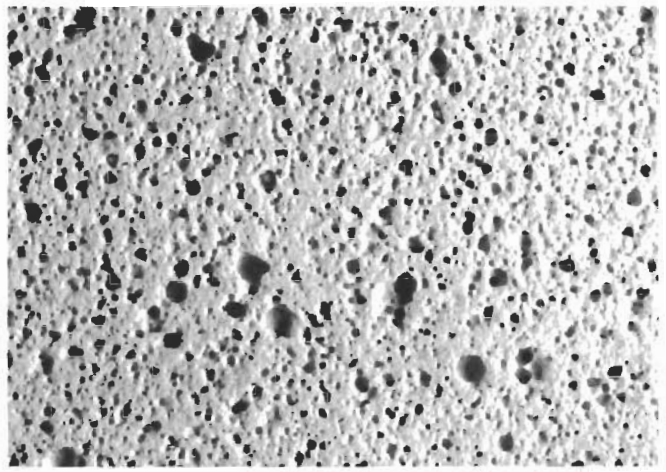

22.1%

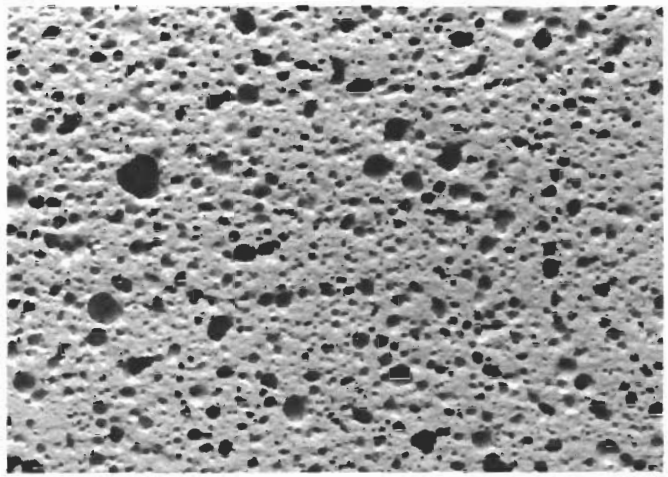

23.8%

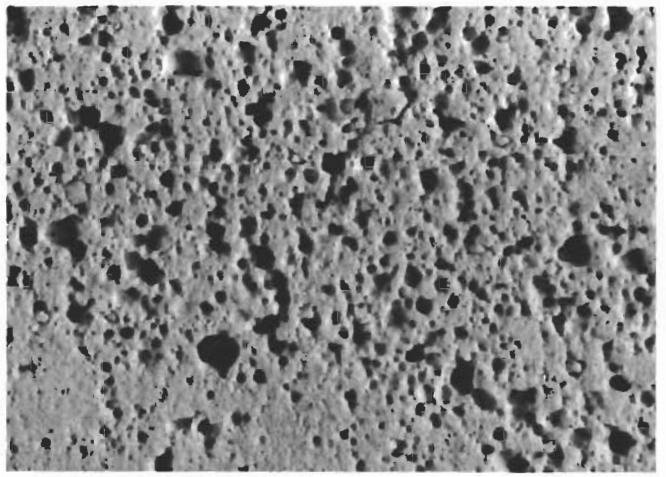

25.4%

FIGURE 40 CROSS SECTION OF FOAMS CONTAINING VARIOUS WATER CONTENTS WHIPPED AT 660 RPM FOR 2 MINUTES - MAGNIFIED 25X

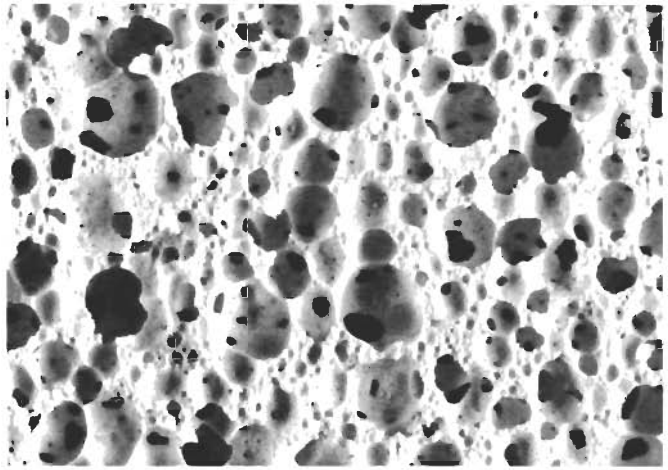

26.9%

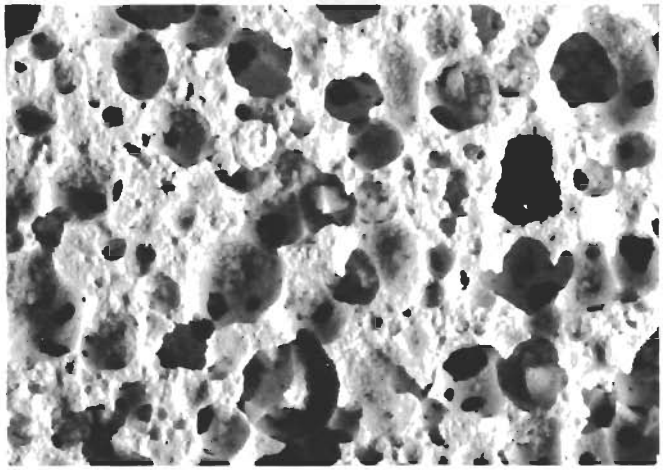

28.4%

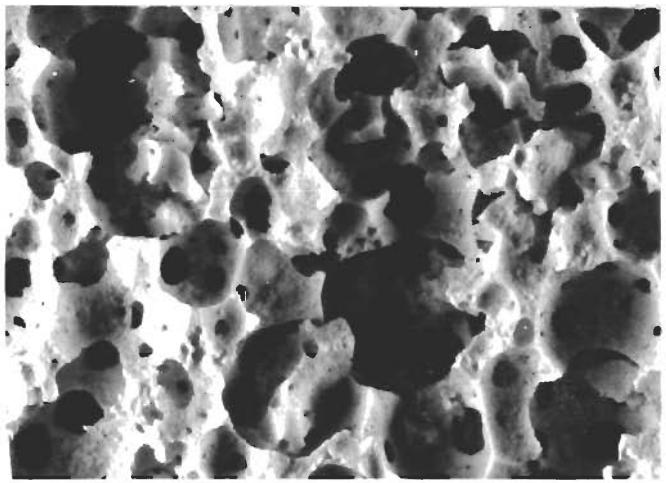

29.8%

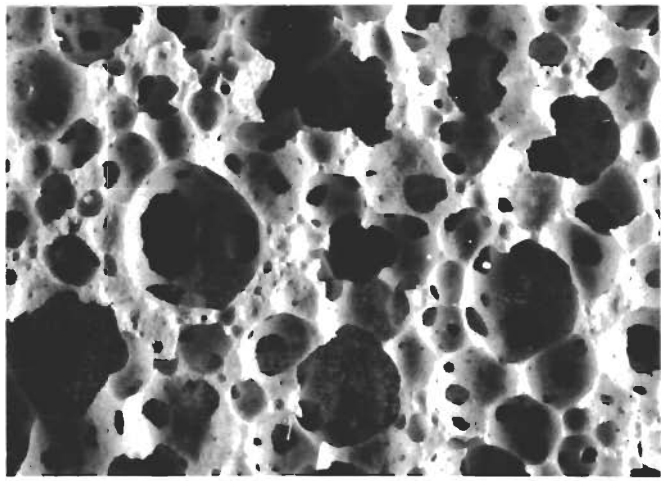

31.2%

FIGURE 41 CROSS SECTION OF FOAMS CONTAINING VARYING LIQUID CONTENT WHIPPED AT 660 RPM FOR 2 MINUTES - MAGNIFIED 25X

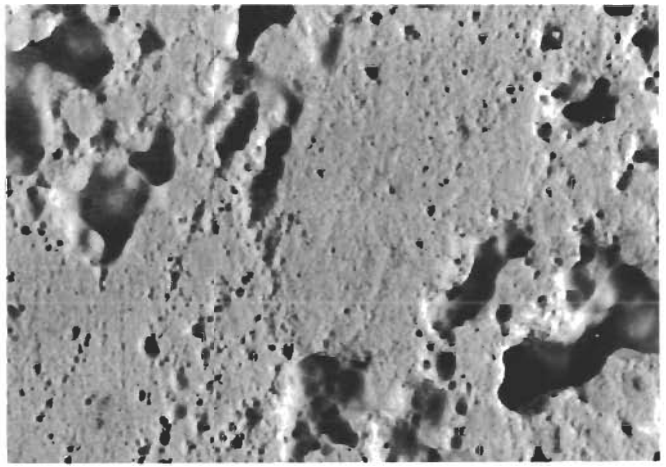

20.3%

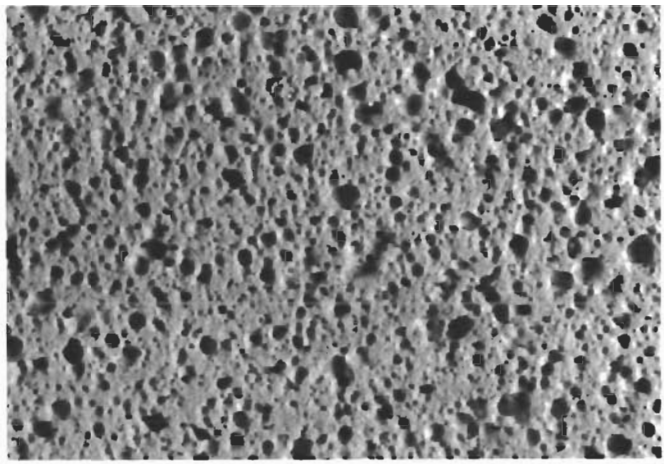

22.1%

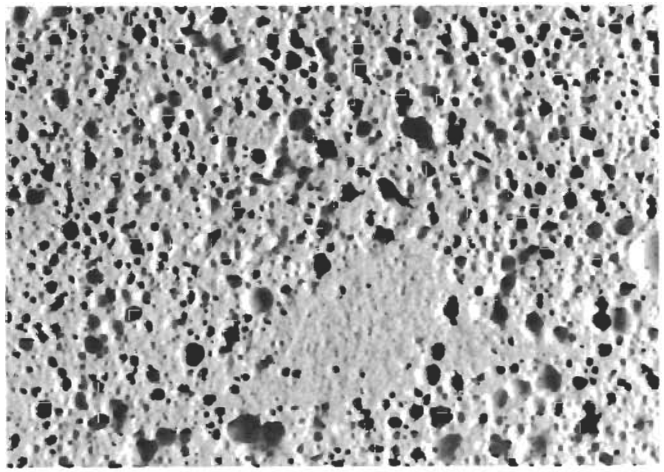

23.8%

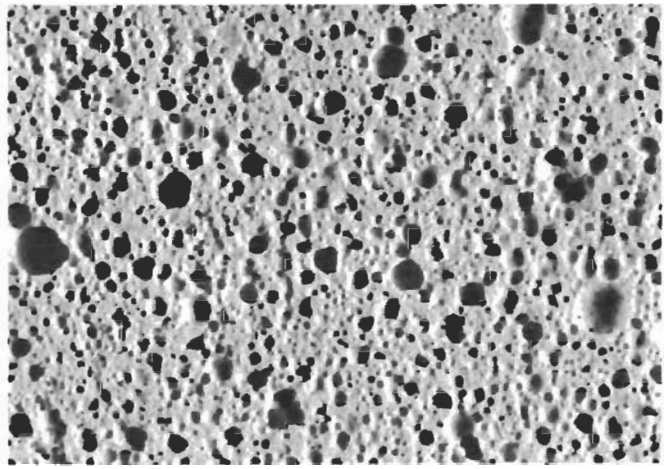

25.4%

FIGURE 42 CROSS SECTION OF FOAMS CONTAINING VARYING WATER CONTENTS WHIPPED AT 555 RPM FOR 4 MINUTES - MAGNIFIED 25X

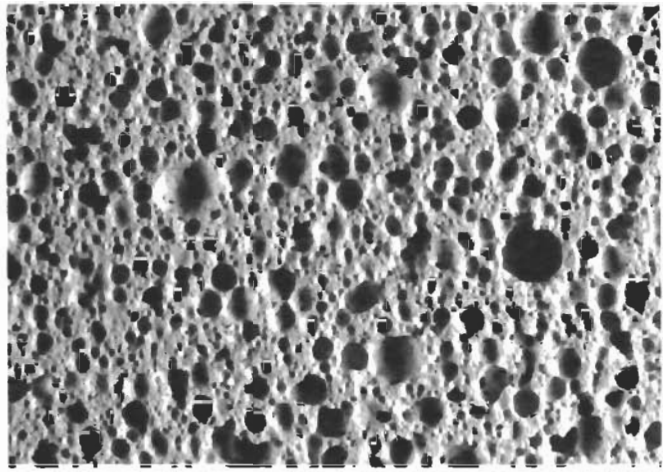

26.9%

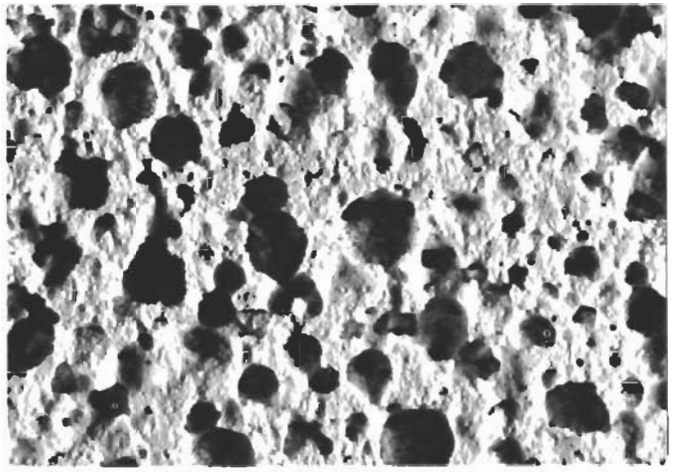

28.4%

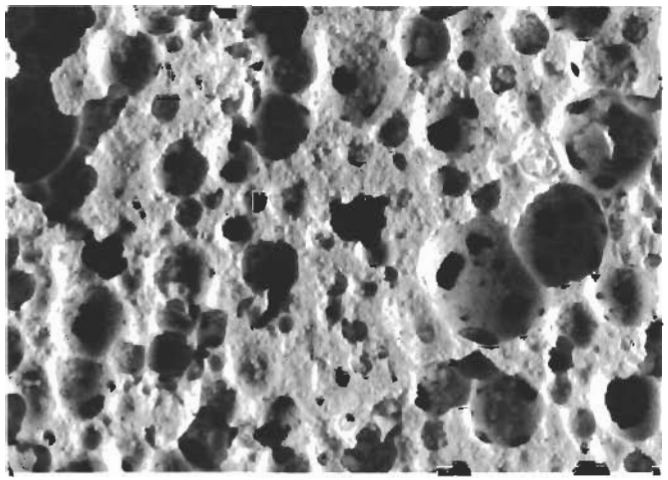

29.8%

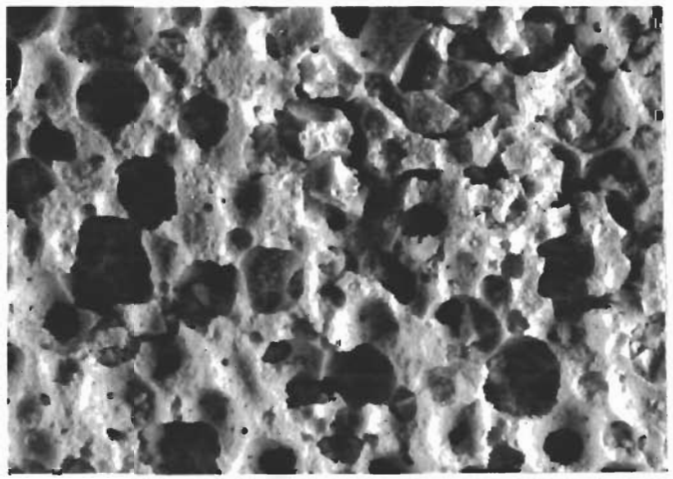

31.2%

FIGURE 43 CROSS SECTION OF FOAMS CONTAINING VARYING WATER CONTENT WHIPPED AT 555 RPM FOR 4 MINUTES MAGNIFIED 25X

TABLE 10

LARGE MAGNESIA FOAM SAMPLES PREPARED AT 640 RPM

Code	Magnesia* (Wt.%)	Plaster** (Wt.%)	Water (Wt.%)	Glim*** (Wt.%)	LiF (Wt.%)	Whipping Time (min)	Sintering Time (hrs)	Cycle Temp. (°F)	Density (gm/cc)	Compressive Strength (psi)	Remarks
M - 33	61.0	10.6	26.4	1.0		2	6	2850	1.80	4800	Insufficient plaster and water content
M - 34	56.4	9.7	32.6	1.3		2	6	2850	0.79	287	Weak Bonding
M - 35	50.7	13.5	33.8	2.0		2	6	2850	0.69	330	Low Magnesia Content
M - 36	47.7	19.0	31.8	1.5		2	6	2850	0.95	1310	Low Magnesia Content
M - 37	51.0	13.5	34.0	1.5		2	6	2850	0.65	278	Non-uniform pore size due to high water content
M - 38	54.9	14.5	29.0	1.6		2	6	2850	0.71	230	Weak bond due to insufficient firing time
M - 39	59.2	15.7	23.5	1.6		2	6	2850	1.18	1560	High density due to insufficient water content
M - 40	54.0	14.4	28.8	1.6	1.2	2	6	2850	0.87	197	Weak bond due to LiF migration
M - 41	53.6	14.3	30.5	1.6		3	6	2850	0.49	250	Weak bond due to high water content
M - 42	53.2	14.1	30.1	1.6	1.0	3	6	2850	0.65	246	Weak bond due to LiF migration
M - 43	57.7	14.5	29.2	1.6		2	6	2850	0.68	730	Uniform foam structure
M - 44	55.7	14.8	27.9	1.6		2	6	2850	0.80	1140	Uniform foam structure
M - 45	56.8	15.1	26.4	1.7		2	6	2850	1.10	1470	High density due to low water and high plaster content
M - 46	59.0	11.7	27.6	1.7		2	6	2850	0.80	990	Uniform foam structure
M - 47	64.3	8.5	25.7	1.5		2	6	2850	0.83	1040	High density due to low water content
M - 48	67.2	8.9	22.4	1.5		2	6	2850	1.26	3600	High density due to low water content
M - 49	55.1	14.7	29.1	1.1		2	22	2850	0.90	1290	High density due to insufficient foaming agent
M - 50	55.0	15.0	29.3	0.7		3	22	2850	1.03	2090	High density due to insufficient foaming agent
M - 51	55.4	14.8	29.5	0.3		3	22	2850	1.09	2040	High density due to insufficient foaming agent
M - 52	55.7	14.7	27.8	1.8		2	22	2850	0.77	650	Best composition evaluated

*Norton Magnorite 220F

**Type K - 62

***A detergent supplied by B. T. Babbitt Inc., 386 4th Avenue, New York 16, New York

Compressive strengths of the samples also varied widely. As previously mentioned, the water content proved to be a controlling factor. The general trend was that an increased water content reduced the strength of the foam. Approximately 700 psi was selected as the optimum compressive strength. Samples with a higher strength were of excessive density, and weaker samples were too friable to be machined to the desired final configuration.

In two of the samples (M-40 and M-42), lithium fluoride was used as a sintering aid. These samples did not show any improvement in sintering because the lithium fluoride tended to migrate through the foam and concentrate at the bottom. This behavior resulted in samples with nonuniform characteristics; consequently, the use of sintering aids was discontinued.

Laminations were observed in some of the samples (Figure 44). These laminations resulted during the transference of the whipped foam from the mixer to the molds. To overcome this problem, a minor variation was introduced in the casting procedure. A 20 mesh screen was placed on top of the molds. This screen served to distribute the foam uniformly throughout the mold and to prevent laminations from occurring in the pouring process. A secondary benefit was achieved in that the screen prevented the entrapment of large air pockets in the pouring operation. This procedure was used for samples M-49 through M-52. Composition M-52 foam was prepared for use in the material systems submitted to the Air Force.

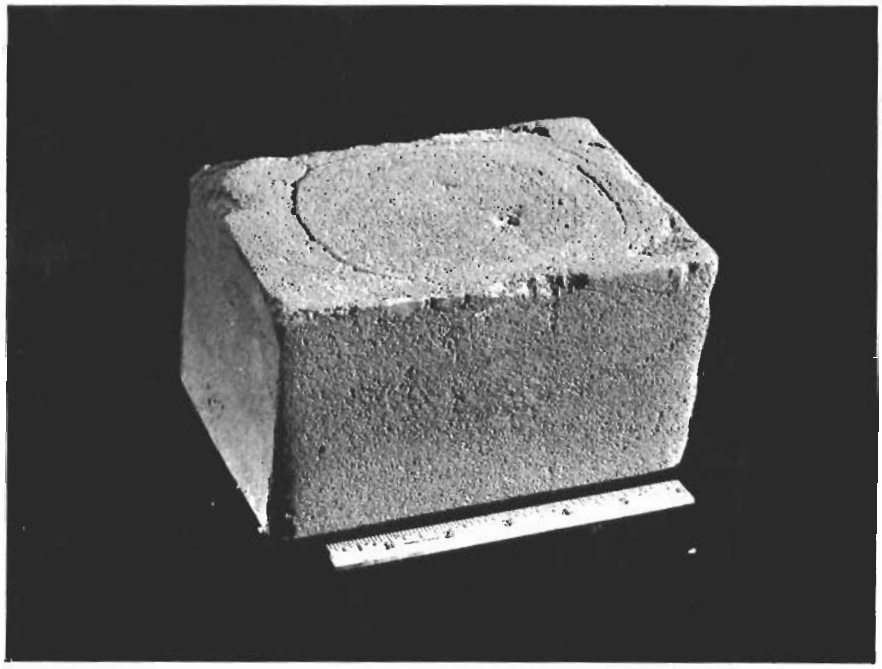

FIGURE 44 MAGNESIA FOAM BLOCK AFTER SINTERING

VII. DEVELOPMENT OF THORIA BODIES FOR USE IN COMPOSITE STRUCTURES

Thoria, the most refractory oxide known, has a melting point above 5500°F. It was expected to have poor thermal shock resistance because of its relatively high thermal expansion and low thermal conductivity. Previous experience with magnesia and zirconia had shown that the thermal shock resistance of ceramic bodies can be improved by careful control of particle-size distribution and the use of a considerable amount of coarse-grained material in the body. Application of this approach required coarse-grained thoria, which was not available commercially.

Therefore, it was found necessary to prefire fine-grained thoria into pellets which could then be crushed to produce the coarse grain. This prefiring operation entailed a temperature of 4160°F. This relatively high temperature produced burner failure in a gas-fired furnace used for sintering. Delay in obtaining and installing a replacement burner prevented accomplishing more work on thoria bodies.

An alternate method of sintering, using an induction furnace, was unsuccessful because a reaction between the graphite furnace lining and the thoria caused the thoria to be converted to thorium carbide.

Preparation of Thoria Grain — The thoria samples in this program were prepared from Linsay Code 115 thoria* powder. This material is a minus 325 mesh, 99-percent pure thoria. Bodies pressed from this material, in the as-received conditions, showed an excessive firing shrinkage and poor thermal shock resistance. To overcome this problem and to produce the required coarse particles, the following procedures were used.

The thoria powder was placed in zirconia crucibles and fired for 12 hours at 2800°F to produce a moderately dense thoria block. This low-temperature (2800°F) prefiring serves to partially densify the thoria powder and to eliminate much of the shrinkage that occurs in the 4160°F sintering operation. As a result, the volume of material to be sintered at 4160°F is considerably reduced with a subsequent saving in furnace life.

The thoria block fired at 2800°F is then crushed to produce a minus 14 mesh particle size and pressed into disks 3-inches in diameter by 1/2-inch-thick. These are fired for 2 hours at 4160°F. Finally, the thoria disks are crushed and screened to produce the following particle size fractions.

*Linsay Chemical Division, West Chicago, Illinois.

-14 + 28 mesh
-28 + 65 mesh
-65 + 100 mesh
-100 + 200 mesh
-200 + 325 mesh
-325 mesh

These size fractions are then used to produce test samples with the desired particle-size distribution.

Preparation of Test Specimens — Table 11 lists the basic compositions that were tested in this program. These specimens were dry pressed at 6300 psi with 4-percent liquid content. After pressing, the samples were dried at 110°F for 24 hours and then sintered at 2800°F for 4 hours. Heating and cooling rates for the sintering cycle were controlled at 215°F/hour. Firing shrinkage of these samples was essentially zero and the density was 9.4 gms/cc.

Evaluation of Thoria Bodies — The thoria compositions developed in this program were tested in the plasma torch for flame erosion resistance and thermal shock resistance using the procedures described for magnesia. Flame erosion resistance is the loss of material due to the combined effects of temperature and gas velocity below the melting point of the sample. These tests showed that the use of sulfuric acid as a binder improved the resistance of the body to flame erosion. This improvement was attributed to an increase in the bonding of the individual grains. However, this increase in erosion resistance was accompanied by a loss of thermal shock resistance. Therefore, the use of sulfuric acid as a binder was discontinued.

The ceramic-bonded specimens were pressed using methyl-cellulose as a binder to provide sufficient strength for handling prior to firing. This method produced a thermal shock resistant body comparable to the zirconia standard when the correct particle-size distribution was used. Composition M-2 was selected for fabrication into leading-edge specimens. The emittance of this body was found to be lower than either the magnesia or zirconia emittance described in Section V.

TABLE 11

COMPOSITION OF THORIA BODIES

Code*	-14 +28	-28 +65	-65 +100	-100 +200	-200 +325	-325	Binder	Erosion Resistance	Thermal Shock Resistance
M - 2	44.7		13.4		31.5	10.6	4% H_2SO_{4**}	Good	Poor
M - 2A	44.7		13.4		31.5	10.6	0.5% Methycell	Fair	Fair
M - 3	45.0	15.0	15.0		15.0	10.0	4% H_2SO_{4**}	Poor	Fair
M - 3A	45.0	15.0	15.0		15.0	10.0	0.5% Methycell	Poor	Fair
M - 4	45.0	5.0	15.0	10.0	15.0	10.0	0.5% Methycell	Fair	Good
M - 5	40.0	7.0	17.0	12.0	12.0	12.0	0.5% Methycell	Very Poor	Very Poor

*All bodies were Lindsay Code 115 Thoria (minimum purity 99%)

**15N Sulfuric Acid

VIII. ZIRCONIA-BASED COMPOSITES

A sulfuric-acid bonded zirconia body has been developed as reported in WADD TR 60-491. This material was further developed in a subsequent program. The effect of additives, bonding techniques, and reinforcing systems on zirconia compositions was studied under these programs. However, in the current program only the physical properties were investigated.

Composition — The zirconia body used in this program has been designated Mix 23. The composition of Mix 23 is as follows:

Percent (by wt)	Material
44.0	-14 +20 mesh stabilized zirconia*
13.2	-65 +100 mesh stabilized zirconia*
30.8	-200 +325 mesh stabilized zirconia*
3.15	Zircoa A**
2.1	Zircoa B**
4.2	Zircoa C**
10.5	Zircoa D**
1.5	Colloidal Zirconia

The binding agent is 1 part water to 3 parts of 15 N sulfuric acid. For dry pressing, 3-1/2 percent (by weight) of this solution is mixed with the dry ingredients. After forming, the body is matured in 4 steps.

1) Dried for 24 hours at 150°F
2) Cured for 24 hours at 800°F
3) Sintered for 4 hours at 2800°F
4) Sintered for 1 hour at 3100°F

Modulus of Rupture — In Figure 2, the modulus of rupture for zirconia Mix 23 is shown graphically as a function of temperature. These are the average of two determinations at each of the following temperatures: 70°F, 1000°F, 2000°F, 2800°F, 3200°F, and 3600°F. The strength of the zirconia body decreases as temperature increases to 2800°F. At this point, the trend is reversed. This is attributed to a sintering action. In addition, a change from brittle to plastic behavior may reduce the effect of stress concentrations due to surface irregularities resulting in an apparent increase in strength.

Thermal Shock Resistance — Zirconia specimens were tested for thermal shock resistance in a triple oxyacetylene torch facility using the schedule shown in

* Norton Company, Worchester, Massachusetts.
** Zirconium Corporation of America, Solon, Ohio.

Figure 12. The zirconia composition withstood these conditions with no evidence of cracking or spalling; increasing the heating rates led to failure from thermal shock.

Erosion Resistance — In an oxyacetylene torch facility with a heat flux of 250 Btu/ft^2-sec, zirconia erodes very slowly. Figure 45 shows four zirconia specimens that were exposed to a plasma torch (670 Btu/ft^2-sec) for 5 seconds. The samples show considerable evidence of melting. In contrast, magnesia samples subjected to the same heat flux show little evidence of molten material, with the loss of material being due to vaporization.

Maximum Use Temperatures — The maximum use temperature for zirconia for short periods is 4600°F as determined by plasma torch testing. This temperature is determined by observation of the point at which appreciable melting occurs.

Density — 4.88 gm/cc or 304 lb/cu.ft.

Temperature Drop through Zirconia — Figure 30 shows time versus temperature plots for the hot and cold face of zirconia specimens. The specimens were tested in an oxyacetylene torch facility with hot-face temperatures being measured optically and cold-face temperatures determined by platinum thermocouples. The average thermal drop through 1/4-inch of zirconia was 1301°F at a hot-face temperature of 4000°F.

Impact Strength — The average strength for six zirconia specimens tested was 0.17 ft-lb. This value can be compared with F-14 magnesia that had an average impact strength of 0.32 ft-lb.

Emittance — In addition to the tests reported in Section V, the emittance of Mix 23 zirconia was measured in two thermal radiation test facilities. A value of 0.50 at 2800°F was obtained. Since the emittance of zirconia varies rapidly with temperature in the 2500°F to 3000°F range, this value may be in error. Data from other sources indicates that the true value of emittance for Mix 23 zirconia lies between 0.6 and 0.7 at 2800°F.

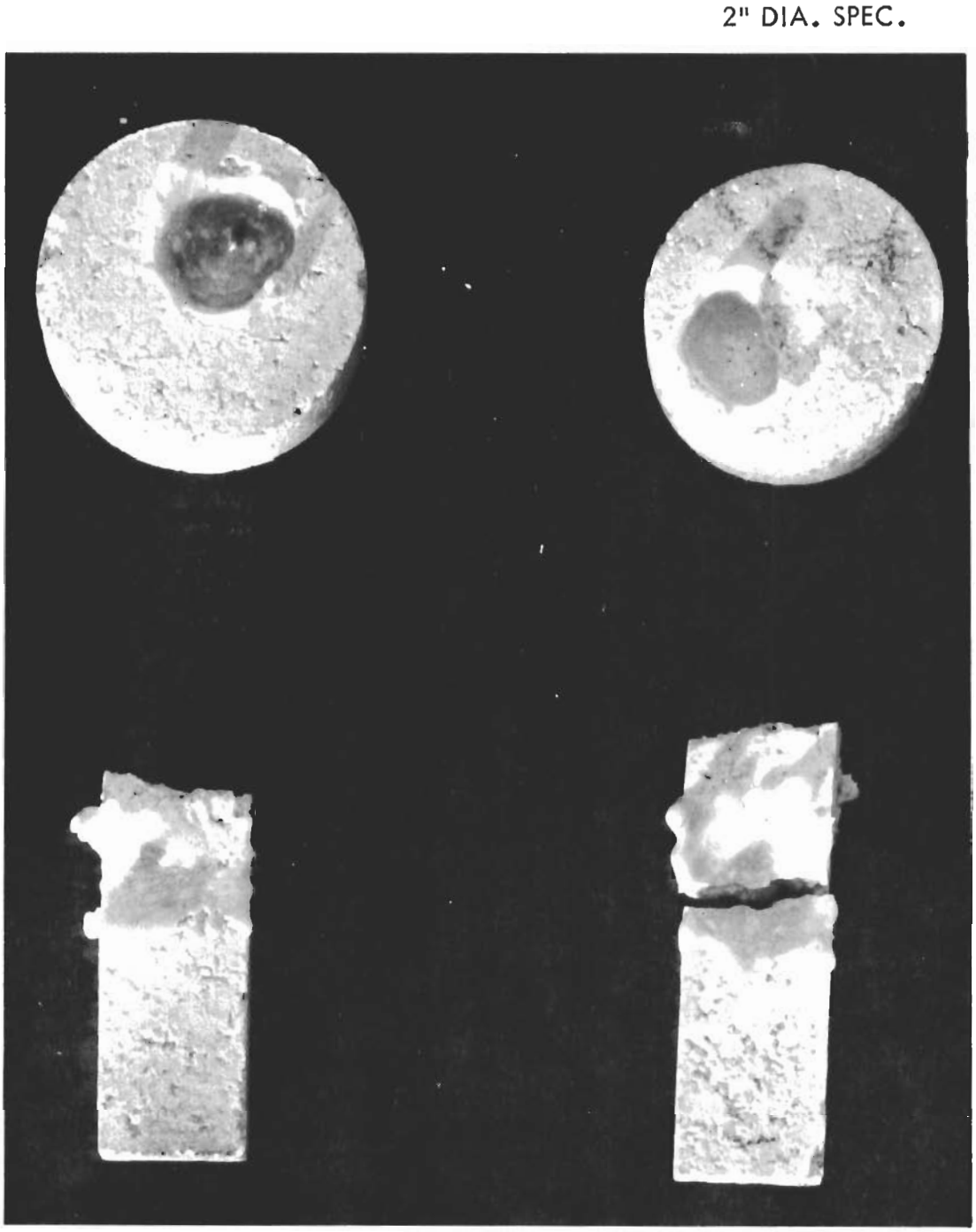

FIGURE 45 ZIRCONIA SAMPLES TESTED ON PLASMA TORCH AT 670 Btu/ft^2-sec

IX. INCORPORATION OF METAL REINFORCEMENT INTO CERAMIC BODIES

Three methods of reinforcement were investigated: metal honeycomb, wires, and flame-sprayed backings.

Metal Honeycomb — Initial tests were conducted using Inconel Stresskin* filled with magnesia. These samples cracked during the sintering operation. Examination of the samples revealed that the honeycomb had been crushed during the pressing operations and that excessive oxidation of the metal honeycomb occurred during sintering. This crushing resulted in stresses that led to the subsequent cracking. A section of this sample is shown in Figure 46.

A modified pressing technique was used to eliminate this problem. After filling, the die was vibrated with an air-operated sander. This vibration ensured uniform fill for the cells in the metal honeycomb, and the buckling was eliminated.

These samples were fired in an argon atmosphere at 2200°F for 4 hours. Figure 47 depicts a sample prepared in this manner. Some oxidation of the metal occurred, but it was not sufficient to appreciably affect the structural integrity of the composite. Additional samples were prepared using conventional Inconel honeycomb. These were readily fabricated using the previously developed methods. A section of a typical sample is shown in Figure 48. The honeycomb cells were uniformly filled and the walls were undistorted. This structure was considered entirely suitable for the present program.

Platinum was too expensive for these tests; thus, Inconel was used for process development and in the samples submitted to the Program Monitor.

Wire Reinforcement — As a preliminary investigation of wire reinforcements, magnesia samples containing tungsten, tantalum, Rene'41, molybdenum, or platinum wires were dry pressed at 12,000 psi and sintered in an argon atmosphere for 20 hours at 2200°F. The samples containing tantalum and tungsten wires cracked during sintering, but those containing Rene'41, molybdenum, and platinum wire did not. The reinforced samples are shown (after sintering) in Figure 49. Cracking of the tantalum sample is clearly evident, with the cracks occurring at each wire location. This cracking was attributed to differential thermal expansion between the two materials.

Investigation of wire reinforcements was limited to these tests. Further tests were not considered desirable since, at this time, it was decided to use only metal honeycomb reinforcements for the composite structures.

---

* A metal-backed honeycomb supplied by John F. Foster Mfg. Company, Costa Mesa, California.

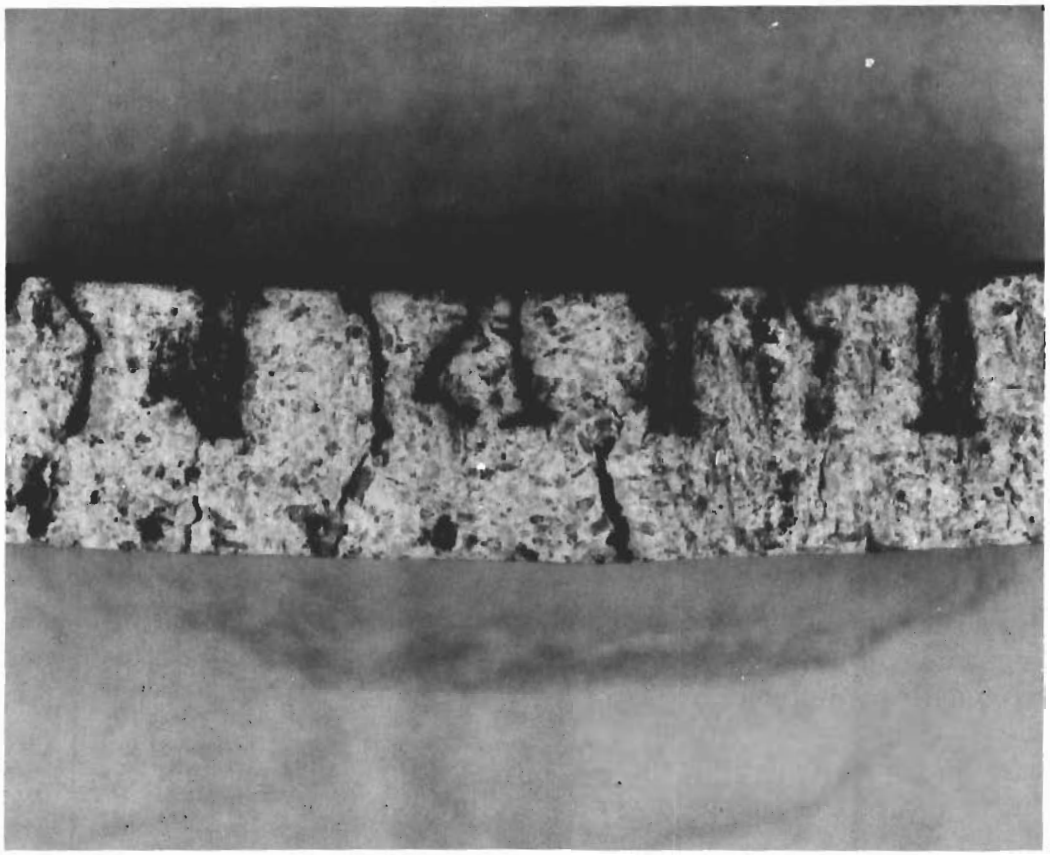

FIGURE 46 CROSS SECTION OF 1/2-in.-THICK MAGNESIA SAMPLE CONTAINING INCONEL "STRESSKIN" REINFORCEMENT AFTER SINTERING IN AIR

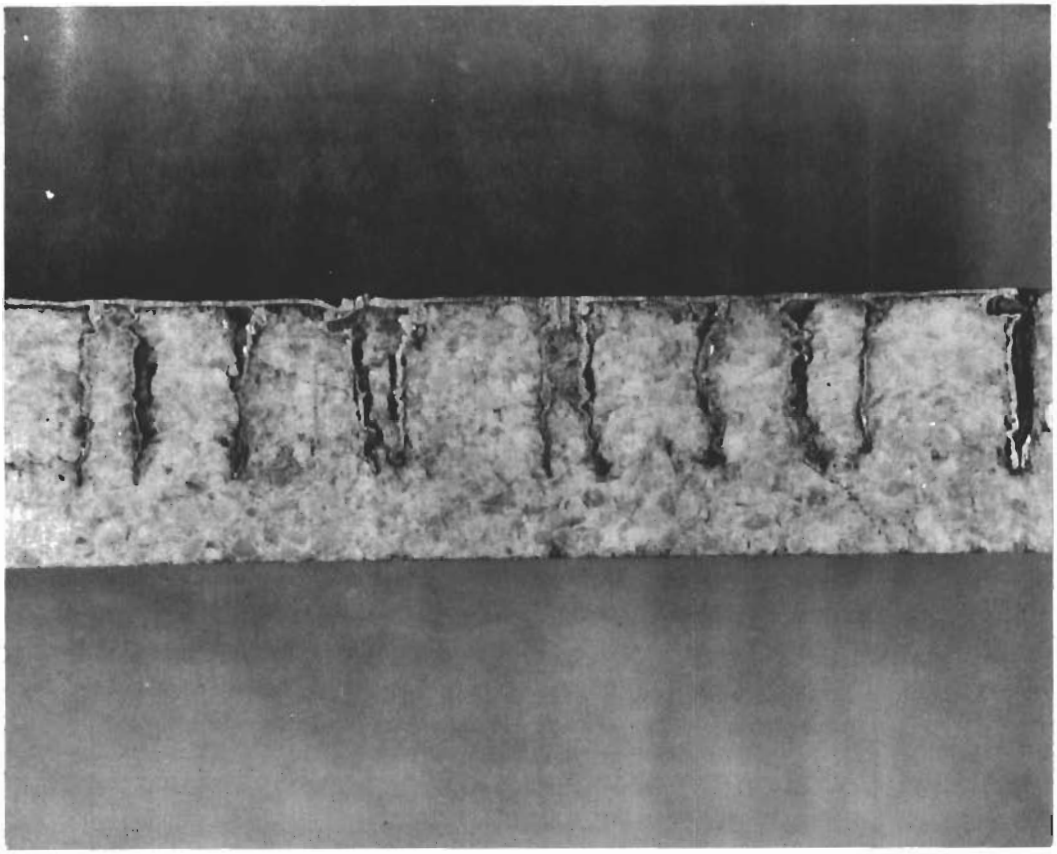

FIGURE 47 CROSS SECTION OF 1/2-in.-THICK MAGNESIA SPECIMEN CONTAINING INCONEL "STRESSKIN" AFTER SINTERING IN ARGON

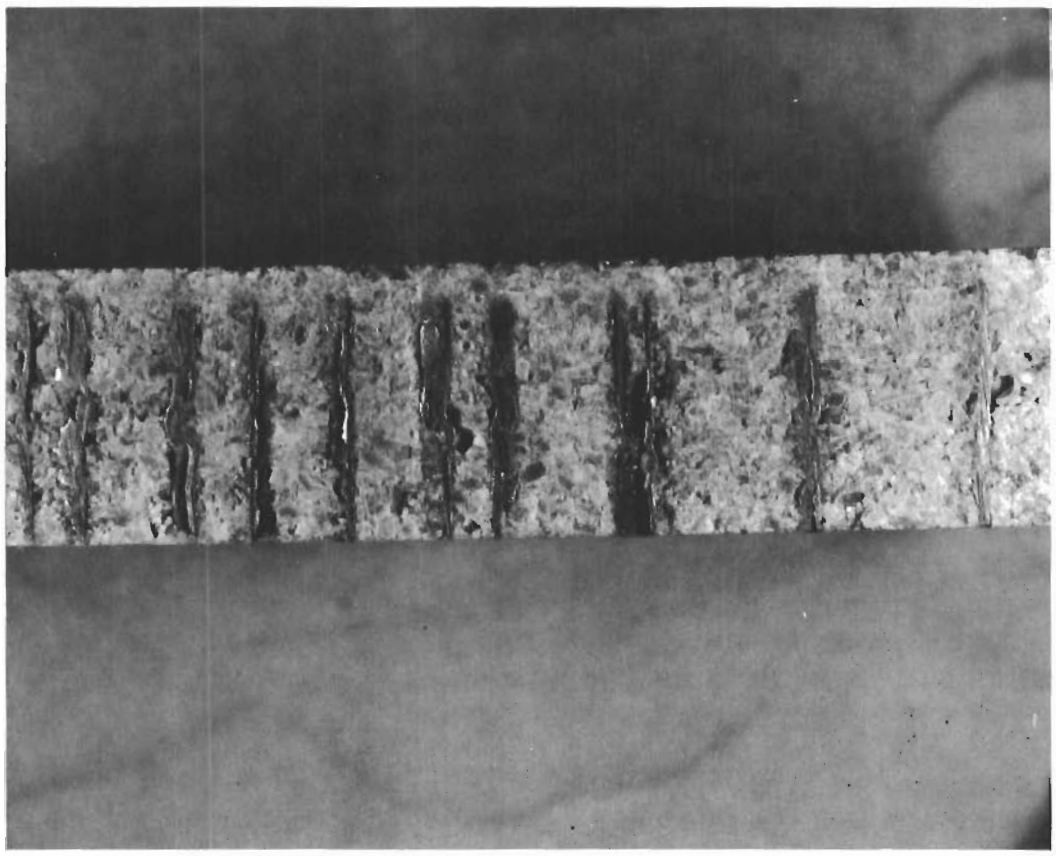

FIGURE 48 CROSS SECTION OF 1/2-in.-THICK MAGNESIA SAMPLE CONTAINING INCONEL HONEYCOMB REINFORCEMENT

MOLYBDENUM WIRE TANTALUM WIRE INCONEL HONEYCOMB

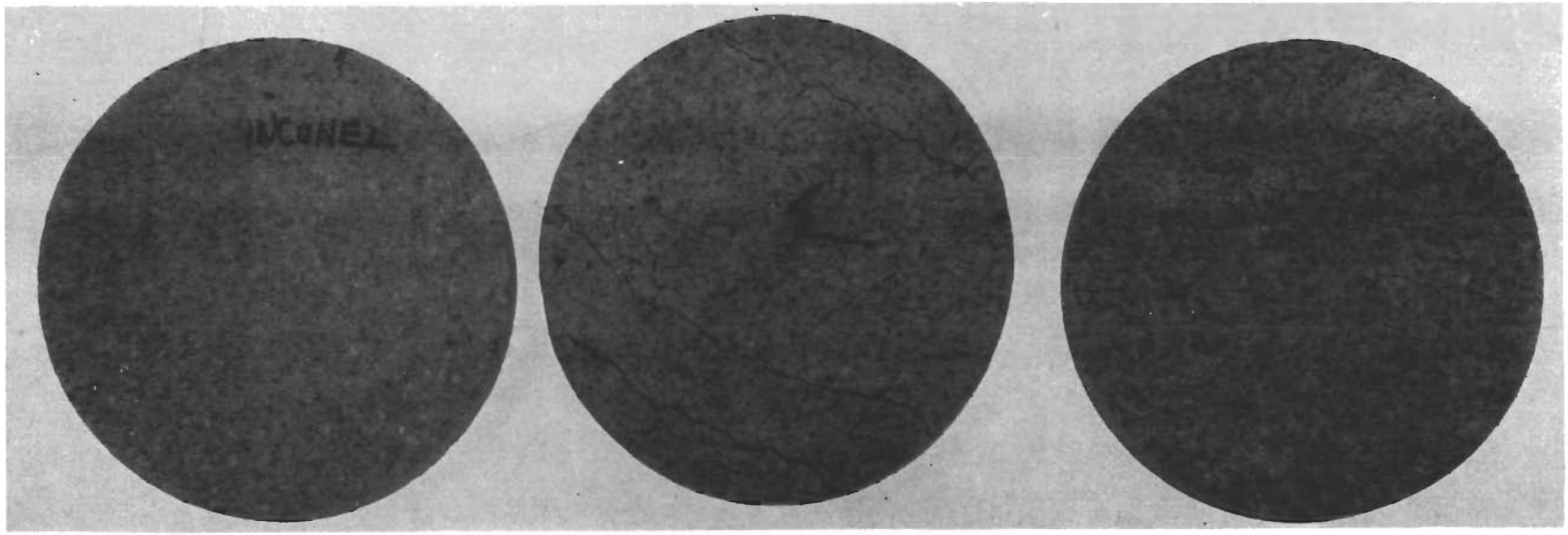

INCONEL HONEYCOMB TUNGSTEN WIRE RENE' 41 WIRE

FIGURE 49 METAL REINFORCED SAMPLES AFTER SINTERING

Flame-Sprayed Backings — The resistance to spalling exhibited by the magnesia body indicated that metal reinforcement might not be required throughout the ceramic phase.

Therefore, coatings of molybdenum, Thermospray 42-C* and Thermospray 41-C**, 0.010 inch thick, were plasma sprayed into the back of 1/2-inch-thick, 2-inch-diameter magnesia disks. These samples were thermal shocked by heating for 2 minutes at a heat flux of 700 Btu/ft^2-sec followed by water quenching. In the molybdenum-backed sample, the magnesia phase cracked normal to the surface, but no spalling occurred and the structure held together. The other two samples delaminated under test. These samples are shown after testing in Figure 50.

This effort was also discontinued because of the decision to use metal honeycomb reinforcements in the final test specimens. The use of a flame-sprayed metal reinforcement on these specimens would require the development of a specialized flame-spray technique that is beyond the scope of the present program.

---

* Metco Thermospray Powder 42-C. A high chrome stainless steel supplied by Metco Inc., Westbury, New York.

** Metco Thermospray Powder 41-C. Similar to Type 316 stainless steel supplied by Metco Inc., Westbury, New York.

THERMOSPRAY 41C

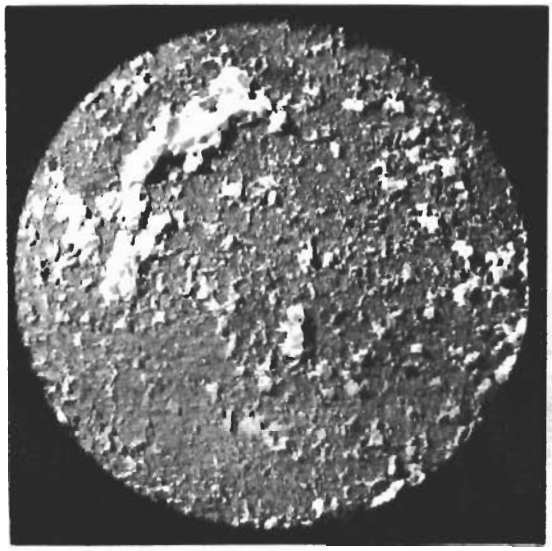

THERMOSPRAY 42C

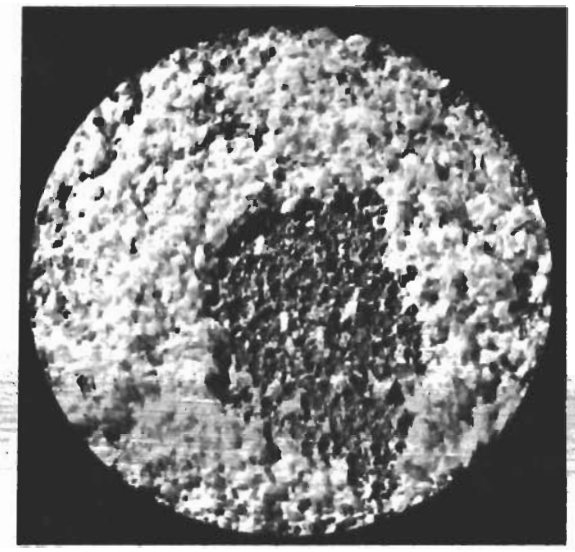

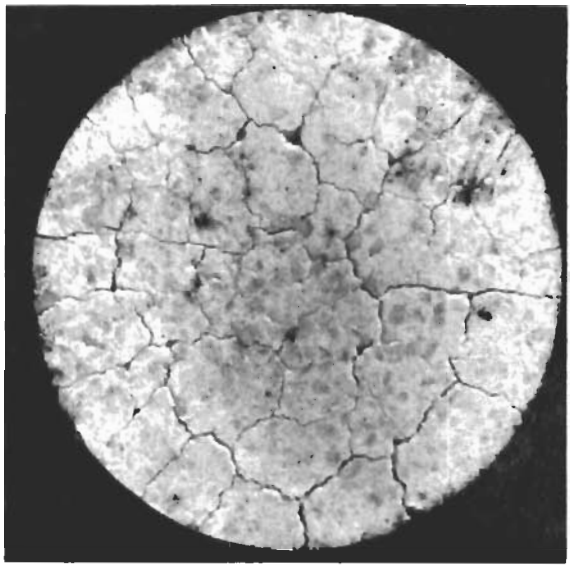

MOLYBOND

2" DIA. SPEC.

FIGURE 50 METAL FLAME SPRAY BACKED MAGNESIA SAMPLES AFTER TESTING

X. COMPARISON OF MATERIAL PROPERTIES

A comparison of the reported properties of magnesia, zirconia, and thoria is tabulated in Table 12. These properties are further compared below. Experimental determinations of these properties are discussed in the sections dealing with the various material systems.

Density — Magnesia is the least dense of the three materials. The bodies produced from this material have a density approximately one-half that of zirconia bodies and one-fourth that of the thoria bodies.

Maximum Use Temperature — Maximum use temperatures of the three materials studied in this program were estimated by observing their behavior when exposed to the plasma torch, as in Figure 31. Maximum use temperature, which was indicated by melting, was determined to be 4600°F for zirconia. (The presence of the 3 to 5 percent of CaO present as a stabilizing agent reduces the 4900°F melting temperature of pure zirconia.) Magnesia is limited to use below 4700°F by fairly severe erosion above this temperature. This loss of material is apparently due to volatilization. Thoria was limited to below 5400°F by erosion above this temperature. The high gas velocity precluded determining whether the erosion was due to melting or volatilization. Literature values of the melting point of thoria vary from 5500°F to 6050°F.

Strength — Magnesia and zirconia bodies have approximately equal strength-to-weight ratios at 3600°F. At room temperature, magnesia is considerably stronger. Strength data was not obtained for thoria.

Thermal Shock Resistance — Thermal shock resistance is difficult to evaluate numerically. Magnesia bodies developed in this program are considerably more resistant to thermal shock than are either the thoria or zirconia bodies. A comparison of the thermal shock properties of the zirconia and thoria bodies shows them to have approximately equivalent resistance.

Thermal Conductivity — Zirconia has the lowest thermal conductivity and magnesia the highest. Thermal conductivity values were not determined experimentally, but when disks 1/4-inch thick were heated by the plasma torch to hot-face temperatures of 4000°F, thermocouples located on the cold face indicated temperatures of 3100°F for magnesia, 2900°F for thoria, and 2800°F for zirconia.

Impact Strength — Impact strength tests show magnesia to have slightly better impact strength than zirconia at room temperature. The average value for magnesia was 0.32 ft/lb, as compared with 0.17 ft/lb for zirconia.

Emittance — Figure 31 represents the effect of emittance on the surface temperature of samples tested on the plasma torch. These curves show that zirconia has the highest emittance, thoria the lowest, and magnesia is roughly midway between. Of the magnesia samples with additives, composition G-11 containing 2-percent chrome oxide proved to be the best. Above 4000°F its apparent emittance was greater than zirconia.

TABLE 12

PROPERTY COMPARISON OF MAGNESIA, THORIA AND ZIRCONIA*

	Melting Point (°F)	Boiling Point (°F)	Density (gms/cc)	Linear Coefficient of Thermal Expansion (x 10^{-7})	Thermal Shock Resistance	Thermal Conductivity Btu/hr-ft^2 (ft/°F) at 2400°F)	Emissivity (Total at 2500°F)	Principle Limitations	Chemical Stability	Principle Advantages
Thoria	5520	8800	9.69	95 (20-1400°C)	Poor	1.3	?	Price Radioactive	Excellent	Chemical Stability and High Melting Point
Magnesia	5070	?	3.58	140 (20-1400°C)	Fair	3.5	0.22	High Vapor Pressure, Hydration	Can be reduced by carbon	Low Density and cost. More refractory than zirconia.
Zirconia	4870	8600	5.56	55 (20-1400°C)	Fair	1.2	0.38	Requires Stabilization to Prevent Phase Change	Moderate	Availability of Currently Developed Compositions and Lowest Thermal Expansion

*Properties of Refractory Materials: Collected data and references, Bradshaw, W. G., and Mathews, C. O., LMSD-2466 Lockheed Aircraft Corporation.

XI. DESIGN AND FABRICATION OF TEST COMPONENTS

The leading-edge segment shown in Figure 51 was selected for evaluating the material systems developed under this program. This component was selected on the basis of ASD recommendations. The size was determined by the capability of available plasma test facilities. It is representative of the possible end-use application that may be found for metal-ceramic composites. The use of a nose-cone shape was considered, but because of its asymmetry and resultant higher thermal stresses, the leading-edge shape was selected for a more complete evaluation of materials.

The design consists of a high density metal-ceramic surface backed by a ceramic foam. The foam serves dual purposes of reducing heat transfer to the substructure and increasing rigidity with minimum additional weight. A detailed description is given below.

1) The leading-edge section is not completely filled with foam. When samples were assembled, a slight change in cement volume occurred during curing. This change was not sufficient to affect the previously prepared flat samples, but when the same methods were applied to the leading-edge section, the test sections fractured. This break occurred along the front center of the leading edge. While this problem could be overcome for fabrication purposes, a similar result could occur during testing. Therefore, a hollow section was adopted to provide room for internal expansion during assembly and test.

2) A back plate of dense magnesia was incorporated to facilitate mounting. Since the foam section was revised, it was no longer feasible to use it as a means of attachment. The back plate was incorporated to provide an anchor point for the attachment stud.

The only variation in fabrication procedures from flat samples is that hydrostatic pressing was used to fabricate the dense outer section. This change was made because the size and shape prevented the use of conventional dies and dry-press procedures.

The die used to fabricate these samples is shown in Figure 52. This die consists of four basic assemblies.

1) The outer case, which supports the die during loading and pressing;

2) The rubber neoprene bag, which prevents penetration of liquid into the sample;

3) The mandrel upon which the part is formed;

4) The cover, which seals the die after filling and maintains proper location of the various components during pressing.

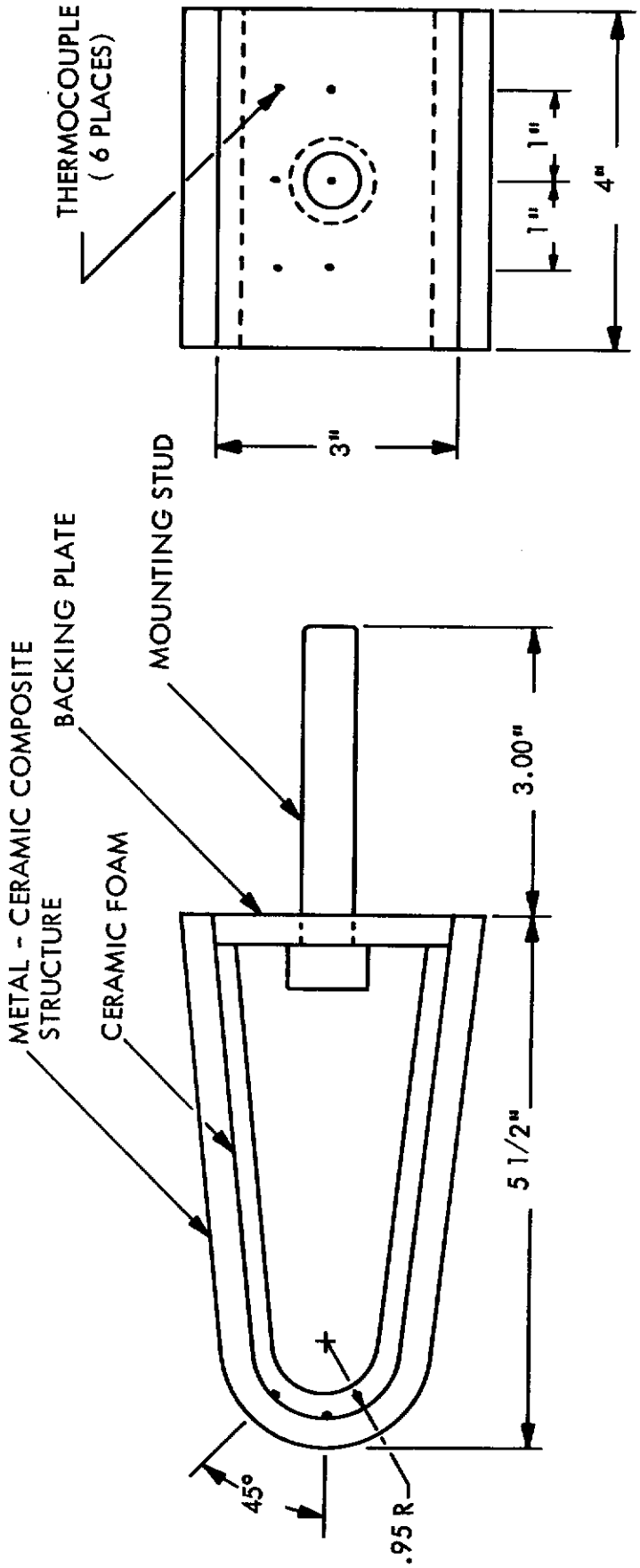

FIGURE 51 LEADING-EDGE TEST COMPONENT CONFIGURATION

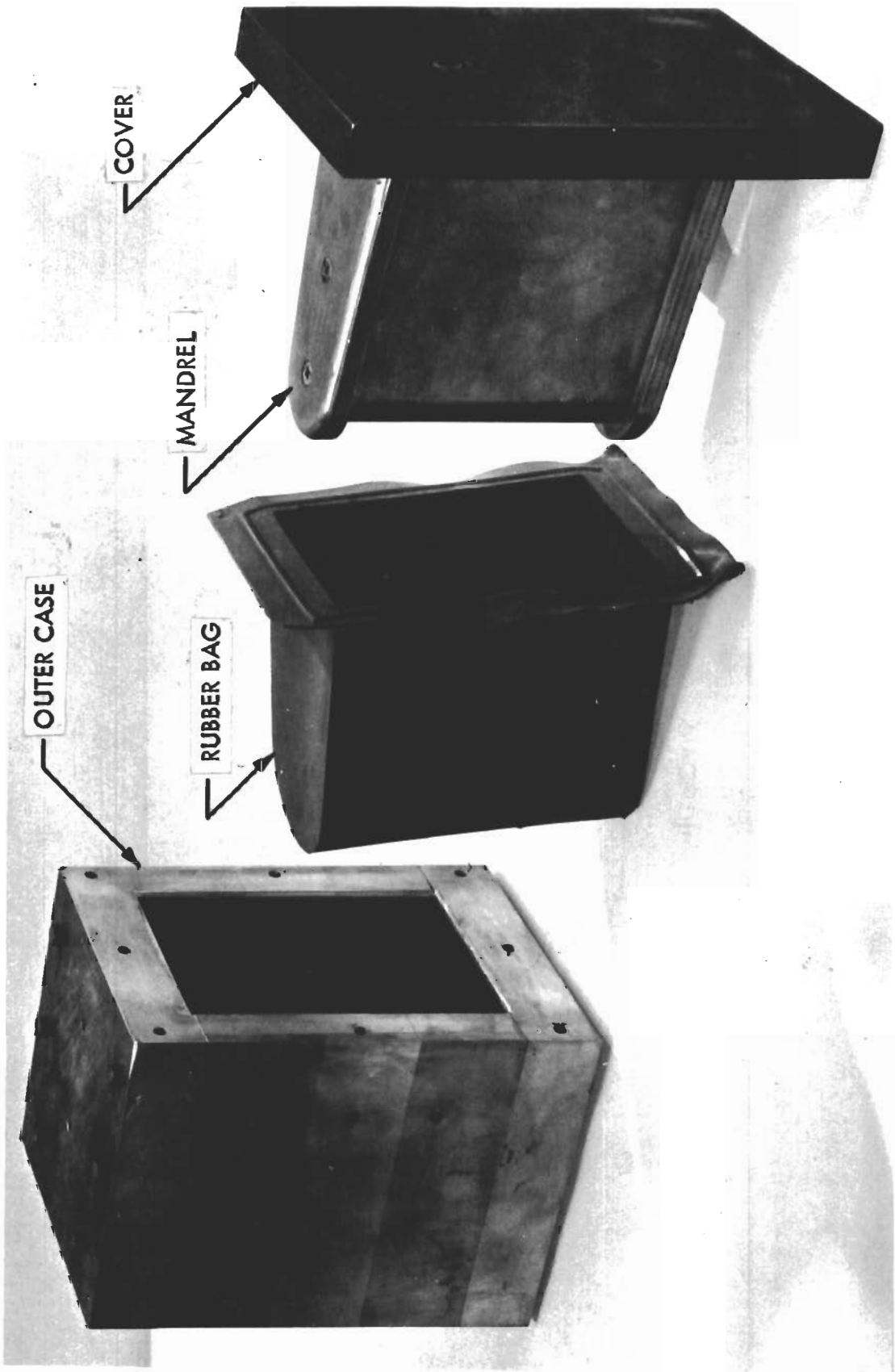

FIGURE 52 HYDROSTATIC DIE FOR FABRICATION OF LEADING-EDGE TEST COMPONENTS

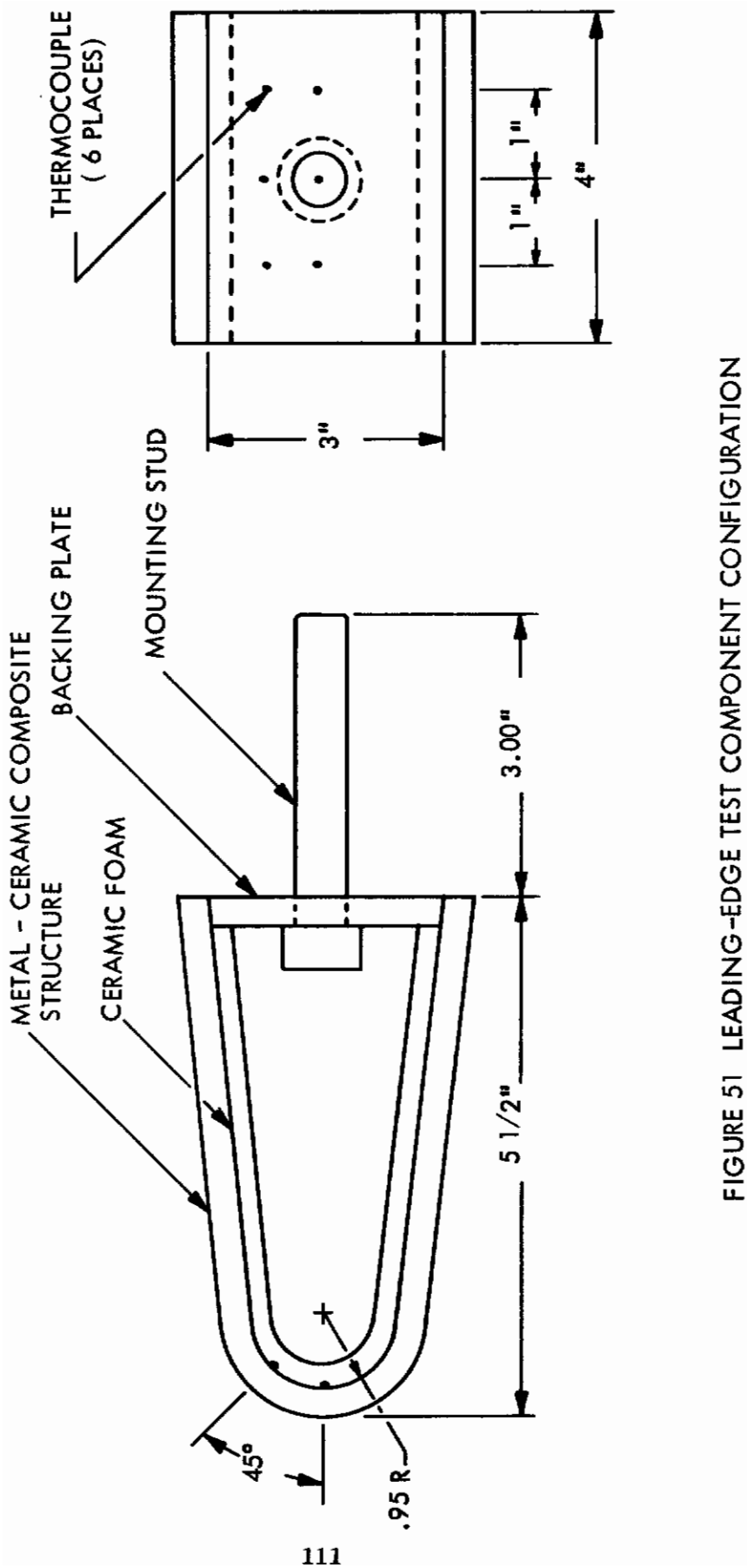

FIGURE 51 LEADING-EDGE TEST COMPONENT CONFIGURATION

In use, the neoprene bag and mandrel are inserted into the case. The latter is supported in its proper location by the two end flanges. The die is loosely filled with the desired ceramic powder and the cover is bolted on.

The assembly is then placed in a hydrostatic pressing facility and the pressure gradually raised to 12,000 psi. The pressure is maintained for 1 minute and then uniformly relieved over a 2-minute period. After pressing, the die is removed from the press and partially disassembled. The pressed part, mandrel, and cover are left intact and dried at 110°F for 16 hours to produce sufficient strength in the sample for handling. The leading-edge section is then removed from the mandrel and dried an additional 24 hours at 150°F. It is then fired according to the schedules described in the appropriate material development section of this report. After firing, the samples are trimmed, ground to final size, and assembled. Semicon* high-temperature cement is used to bond the various parts into a completed test specimen.

Some delays were encountered in this portion of the program due to rupture of the rubber bag during pressing. This resulted from the excess thickness on the flanges used to support the mandrel during filling. These were milled down, thus eliminating the stress on the rubber bag and the resultant failure.

* Semicon of California, 70 Mariposa Avenue, Watsonville, California.

XII. CONCLUSIONS

A magnesia-base composite material has been developed that can withstand the thermal shock and erosion environment to which nose caps and leading edges of re-entry vehicles will be subjected. This material can be used up to 4600°F, above which the erosion rate becomes excessive. The inherently low emittance of magnesia has been increased, through the use of additives, to approximately the same as that of zirconia.

Investigations of the use of sintering aids in magnesia bodies showed them to be ineffective. Materials such as lithium fluoride tend to migrate through large samples producing areas of varying density. None of the sintering aids tested reduced the temperatures required to produce a satisfactory body or improved the thermal shock resistance.

Of the variables investigated, particle-size distribution proved to have the greatest effect on thermal shock resistance. Through control of particle-size distribution, compositions were produced with sufficient thermal shock resistance to withstand heating rates far in excess of those permissible for conventional ceramic bodies. Time did not permit a full evaluation of the effect of the various particle-size distributions, but as a general rule, approximately 40 percent of the material should lie between -14 and +65 mesh.

Attempts to produce a chemically bonded magnesia body yielded samples that had poor thermal shock and erosion resistance.

Thoria compositions were also developed for use in composites. As with magnesia, thoria bodies required a wide range of particle sizes to provide adequate thermal shock resistance. Currently available grades of thoria are not suitable for this purpose; therefore, it is necessary to presinter the thoria powder to obtain the necessary particle sizes. Although thoria is more refractory than either magnesia or zirconia, its high density makes it less suitable for applications below 4800°F where the latter two materials can be used.

Platinum and Inconel are the most satisfactory metals for use as reinforcements in the magnesia and thoria composites. The superalloys tend to embrittle during the sintering of the composite, and refractory metals such as tungsten do not possess sufficient oxidation resistance. For use with thoria, coated tungsten would be desirable. Less refractory metals do not have an adequately high melting point to fully utilize the high-temperature properties of thoria.

XIII. BIBLIOGRAPHY

1. Aves, W. L., "Coating for Re-entry," Metal Progress, V75, N3, pp. 90-4, 189c, 190.

2. Baskin, Y., Arenberg, C. A., and Handwerk, J. J., "Thoria Reinforced by Metal Fibers," Bull. Am. Cer. Soc., 38 (7), pp. 345-48, 1959.

3. Baskin, Y., Greening, T. A., and Kemp, M. D., "Failure Mechanisms of Solid Propellant Rocket Nozzles," Bull. Am. Cer. Soc., 39 (1), pp. 14-17, 1960.

4. Baskin, Y., Handwerk, J. J., Harada, "Some Physical Properties of Metal Fibers," J. Am. Cer. Soc., 43 (9), pp. 489-92.

5. Becker, J. V., "Re-entry from Space," Scientific American, V. 204, No. 1, pp. 49-57.

6. Bell, J. E., and Arnquist, J. L., "Feasibility of Prestressing Ceramics," Boeing Document D2-5344, May 1960.

7. Blocker, E. W., et al., "Development and Evaluation of Insulating Type Ceramic Coatings," WADC Technical Report 59-102, Parts I and II, October 1960.

8. Bradstreet, S. W., "Geometrical Considerations for Composites," Sixth Sagamore Ordnance Material Research Conference, August 1959.

9. Burnett, P. L., Paper presented at the Refractory Composites Working Group Meeting, November 1960.

10. Campbell, I. E., "High Temperature Technology," John Wiley & Sons, New York, 1956.

11. Engle, G. B., and Liggett, L. M., "Graphite — How it Compares with Metals-Ceramics," Materials in Design Engineering, 49 (6), pp. 88-90, 1959.

12. Eubanks, A. G., and Moore, D. G., "Investigation of Aluminum Phosphate Coatings for Thermal Insulation of Airframes," NASA TN D-106, November 1959.

13. Ewing, C. T., et al., "Thermal Properties of Cermets, Metals and Related Materials to 2000°C," NRL Report 5452, ASTIA Document No. 317758. (Confidential)

14. Francis, R. K., and Tinklepaugh, J. R., "Thermal Conductivity in Ceramic-Metal Laminates," J. Am. Cer. Soc., 43 (11), pp. 560-63, 1960.

15. Giles, T. M., Shevlin, T. S., and Everhart, J. O., "Stresses in Polycomponent Solid Ceramics or Cermets," WADC Quarterly Report, Contract AF 33(616)-5515, ASTIA Document No. 230510, September 1959.

16. Harman, C. G., "Non Glassy Ceramics as Fibers," Ceramic Industry, 73 (1), p. 74.

17. "High Temperature — A Tool for the Future," Symposium, Stanford Research Institute, Berkley, California, June 25, 1960.

18. Hoffman, J. A., "Future Possibilities in Fibered Materials," Sixth Sagamore Research Conference, August 1959.

19. Huffman, J. W., Paper presented at the Refractory Composites Working Group Meeting, November 1960.

20. Johnson, R. D., Paper presented at the Refractory Composites Working Group Meeting, November 1960.

21. Koubeck, F. J., et al., "Thermal and Mechanical Properties of Ceramics, Cermets and Metals," Navord Report 6056, February 1958.

22. Leggett, H., and Jaffe, S., "Development of Refractory Composite-Materials Systems for Solid Propellant Rocket Motors," First Quarterly Progress Report, Contract No. DA-04-495-ORD-3068, Hughes Tool Company.

23. Levy, A. V., "Thermal Insulating Ceramic Coatings," Metal Progress, V75, N 3, pp. 86-89.

24. Levy, A. V., "Materials for Uncooled Rocket Nozzles," Metal Progress, 79 (3), pp. 81-82, 1961.

25. Levy, A. V., Locke, S. R., and Leggett, H., "Composite Ceramic-Metal Systems," Astronautics, Vol. 6, No. 4, p. 27, April 1961.

26. Long, J. V., Paper presented at the Refractory Composites Working Group Meeting, November 1960.

27. Long, J. V., "Refractory Coatings for High Temperature Protection," Metal Progress, 79 (3), pp. 114-20, March 1961.

28. Lynch, Quirck, and Duckworth, "Investigation of Ceramic Materials in a Laboratory Rocket Motor," Bull. Am. Cer. Soc., 37 (10), pp. 443-45, 1958.

29. McGee, S. W., "An Investigation of Metal-Ceramic Composites for High Temperature Applications," Armour Research Foundation Report 2175-1, ASTIA Document No. 217445, April 1959.

30. Morden, J. F. C., "Metallic Fibers," Metal Industry, 96 (25), pp. 495-99, June 17, 1960.

31. Nelson, R. A., et al., "Water Stabilized Arc Tests on Nonmetallic Materials," Electrochemical Society Journal, V. 106, N. 4, pp. 317-21.

32. Pearl, H. A., et al., "Refractory Inorganic Materials for Structural Applications," WADC Technical Report No. 59-432, Parts I and II, July 1960.

33. "Preview of Space Metals," Metal Progress, V. 74, N. 4, pp. 96-113.

34. Raynes, B. C., "Studies of the Reinforcement of Metals with Ultra High Strength Fibers," Bureau of Naval Weapons Bimonthly Report No. 2, Contract NOw61-0207-c, March 1961.

35. Schmidt, F., Paper presented at the Refractory Composites Working Group Meeting, November 1960.

36. Sheriden, W. R., "Use of Refractory Ceramics in Rocket Engines," Bull. Am. Cer. Soc., 37 (2), pp. 91-94, 1958.

37. Sklarew, S., "Reinforced Refractory Ceramic Coatings," Sixth Sagamore Ordnance Materials Research Conference, August 1959.

38. Smith, W. E., and Davies, C. F., Summary Report, Contract Nord 18887, ASTIA Document No. 317215. (Confidential)

39. Schwarzkopf, P., and Kieffer, R., "Refractory Hard Metals," The Macmillan Co., 1953.

40. Roller, D., "Summary of Second High-Temperature Inorganic Coatings Working Group Meeting," WADC Technical Report 59-415, June 1959.

41. Shanley, F. R., Knapp, W. J., and Needham, R. A., "Prestressed Ceramic Structures," WADC Technical Report 54-75, Parts I and II, ASTIA Document No. 80124, 1955.

42. Stejskal, L. M., et al., "Development of Reinforced Ceramic Material Systems," WADD Technical Report 60-491, May 1960.

43. Stowell, E. Z., and Tien-Shih Liu, "Parametric Studies of Metal Fiber Reinforced Ceramic Composite Materials," Bu. of Naval Weapons Bimonthly Report No. 5, Contract NOas60-6077-c, ASTIA Document No. 247327, November 1960.

44. Strauss, E. R., Paper presented at the Refractory Composites Working Group Meeting, November 1960.

45. Tinklepaugh, J. R., "Cermets," Reinhold, New York, 1960.

46. Tinklepaugh, J. R., et al., "Metal Fiber Reinforced Ceramics," WADC Technical Report 58-452, Parts I, II, and III.

47. Walton, J. D., "Present and Future Problem Areas for High Temperature Inorganic Coatings," Ceramic Bulletin, 40 (3), pp. 136-41, 1961.

48. Warshaw, S. J., "Prestressed Ceramics," Bull. Am. Cer. Soc., 36 (1), January 1957.

49. Vogan, J. W., "Thermal Protective Surfaces for Structural Plastics," WADD Technical Report 60-110, Parts I and II.

50. Semochylben, M., and Harwood, J. J., "Refractory Metals and Alloys," Interscience, p. 561, New York, 1961.

51. Olson, O. H., and Morris, J. C., "Determination of Emissivity and Reflectivity Data on Aircraft Structural Materials," WADC TR 56-322, Part III.

52. Bradshaw, W. G., and Matthews, C. O., "Properties of Refractory Materials: Collected Data and References," Lockheed Aircraft Corporation, Sunnyvale, California, 1959.